Semi-Parametric Seasonal Unit Root Tests*

Tomás del Barrio Castro[a], Paulo M.M. Rodrigues[b] and A.M. Robert Taylor[c]

[a] Department of Applied Economics, University of the Balearic Islands

[b] Banco de Portugal and NOVA School of Business and Economics

[c] University of Essex

Abstract

We extend the $\mathcal{M}$ class of unit root tests introduced by Stock (1999), Perron and Ng (1996) and Ng and Perron (2001) to the seasonal case, thereby developing semi-parametric alternatives to the regression-based augmented seasonal unit root tests of Hylleberg *et al.* (1990). The success of this class of unit root tests to deliver good finite sample size control even in the most problematic (near-cancellation) case where the shocks contain a strong negative moving average component is shown to carry over to the seasonal case as is the superior size/power trade-off offered by these tests relative to other available tests.

Keywords: Seasonal unit roots, weak dependence, long run variance, demodulated process.
JEL: C12, C22.

1 Introduction

Augmented Dickey-Fuller [ADF] unit root tests are known to suffer significant size distortions when a near-cancellation region caused by a strong negative moving average behaviour is present in the driving shocks. Although increasing the augmentation lag length can mitigate these distortions, a finite sample trade-off occurs with power under the alternative also decreased the greater the lag length used. In discussing ADF tests, Haldrup and Jansson (2006, p.267) argue that "... practitioners ought to abandon the use of these tests..." in favour of the $\mathcal{M}$ tests because of "... the excellent size properties and 'nearly' optimal power properties" of the latter. The $\mathcal{M}$ class of tests, proposed in Stock (1999) and further developed by Perron and Ng (1996) and Ng and Perron (2001), account for weak dependence in the shocks via a non-parametric estimate of the long run variance, rather than parametric lag augmentation. Ng and Perron (2001) show that $\mathcal{M}$ tests based on autoregressive spectral density [ASD] estimators implemented with a modified Akaike information criterion [MAIC] to select the lag length perform particularly well even in the presence of strong negative moving average components.

*We are grateful to the Editor, Peter Phillips, the Co-Editor, Michael Jansson and two anonymous referees for their helpful and constructive comments. Tomás del Barrio Castro acknowledges financial support from projects ECO2011-23934 and ECO2014-58991-C3-3-R. Correspondence to: Robert Taylor, Essex Business School, University of Essex, Wivenhoe Park, Colchester, CO4 3SQ, United Kingdom. Email: rtaylor@essex.ac.uk.

Hylleberg *et al.* (1990) [HEGY] propose a seasonal generalisation of the ADF unit root test allowing the practitioner to test for unit root behaviour at each of the zero and seasonal frequencies. The HEGY tests, like ADF tests, use parametric lag augmentation, to account for weak dependence in the shocks. However, it has been known since the seminal work of Box and Jenkins (1976) that seasonal time series often display significant negative moving average behaviour at the seasonal lag effecting near cancellation regions at both the zero and seasonal frequencies. ARMA behaviour can also be a manifestation of neglected periodic autoregressive behaviour (see, for example, Ghysels and Osborn, 2001, Ch.6). The robustness of seasonal unit root tests to moving average behaviour is therefore a matter of significant practical relevance and simulation evidence suggests that, like the ADF tests, the HEGY tests can be badly oversized in the presence of negative moving averages; see, for example, del Barrio Castro *et al.* (2016).

Motivated by these issues and the success of the non-seasonal $\mathcal{M}$ tests, our purpose is to develop a new class of semi-parametric seasonal unit root tests based on the $\mathcal{M}$ testing approach. In the case of tests at the harmonic seasonal frequencies we show that this requires the use of methods based on demodulated processes. The seasonal $\mathcal{M}$-type tests proposed are based on statistics which correct for weak dependence in the shocks using seasonal long run variance estimates, either sum-of-covariances-based or ASD-based, of the spectrum at the zero and seasonal frequencies. Our analysis explicitly allows for the presence of $ARMA$ shocks. We demonstrate that the limiting distributions of our proposed $\mathcal{M}$ statistics are pivotal under both the null hypothesis and under near-integrated alternatives. Where ASD estimators are used, a seasonal analogue of the MAIC criterion of Ng and Perron (2001), developed in del Barrio Castro *et al.* (2016), can be used to select the lag length, and consistent with the non-seasonal case, we find in a simulation study that the resulting $\mathcal{M}$ tests can deliver significant improvements over augmented HEGY tests.

The remainder of the paper is organised as follows. Section 2 reviews the seasonal model and the seasonal unit root testing framework. Section 3 outlines our proposed class of seasonal $\mathcal{M}$ unit root tests while section 4 details their large sample properties. Section 5 presents a Monte Carlo comparison of the finite sample properties of the HEGY and seasonal $\mathcal{M}$ tests. Section 6 concludes. Supporting material can be found in a Supplementary Appendix available at Cambridge Journals Online (journals.cambridge.org/ect).

2 The Seasonal Unit Root Framework

2.1 The Seasonal Model

Consider the univariate seasonal time-series process $\{y_{Sn+s}\}$, observed with constant seasonal periodicity, S, $S \in \{1, 2, ...\}$, which satisfies the following data generating process [DGP]

$$y_{Sn+s} = x_{Sn+s} + \mu_{Sn+s} \tag{2.1a}$$

$$\alpha(L)x_{Sn+s} = u_{Sn+s},\ s = 1 - S, ..., 0,\ \ n = 1, 2, \ldots, N \tag{2.1b}$$

where μ_{Sn+s} is a purely deterministic component, further details on which are given below, and $\alpha(z) := 1 - \sum_{j=1}^{S} \alpha_j^* z^j$, is an $AR(S)$ polynomial in the conventional lag operator, L. In what

follows we define the total sample size to be $T := SN$ and the number of harmonic seasonal frequencies to be $S^* := \lfloor (S-1)/2 \rfloor$, where $\lfloor . \rfloor$ denotes the integer part of its argument.

We assume that $\{u_{Sn+s}\}$ in (2.1b) satisfies the following conditions:

Assumption 1: The error term u_{Sn+s} in (2.1b) follows the linear process $u_{Sn+s} = \psi(L)\varepsilon_{Sn+s}$, where ε_{Sn+s} is $IID(0, \sigma_\varepsilon^2)$ with finite fourth order moments and where $\psi(z) := 1 + \sum_{j=1}^{\infty} \psi_j z^j$ satisfies: (i) $\psi(\exp\{\pm \mathrm{i} 2\pi k/S\}) \neq 0$, $k = 0, \ldots, \lfloor S/2 \rfloor$; and (ii) $\sum_{j=1}^{\infty} j|\psi_j| < \infty$.

Assumption 1 ensures that the spectral density function of u_{Sn+s} is bounded, and that it is strictly positive at both the zero and seasonal spectral frequencies, $\omega_k := 2\pi k/S$, $k = 0, ..., \lfloor S/2 \rfloor$. Under Assumption 1 the long run variance of u_{Sn+s} may be defined as $\lambda_0^2 := \sigma_\varepsilon^2 \psi(1)^2 = \gamma_0 + 2\sum_{j=1}^{\infty} \gamma_j$, where $\gamma_j := E(u_{Sn+s}u_{Sn+s-j})$, $j = 0, 1, ...$ Notice that $\lambda_0^2 = 2\pi f_u(0)$, where $f_u(\omega)$ denotes the spectrum of $\{u_{Sn+s}\}$. Analogous quantities can be defined at the Nyquist, $\omega_{S/2} = \pi$, frequency, where S is even, as $\lambda_{S/2}^2 := \sigma_\varepsilon^2 \psi(-1)^2 = \gamma_0 + 2\sum_{j=1}^{\infty} \cos[\pi j]\gamma_j$, and at the seasonal harmonic frequencies, $(\omega_k, 2\pi - \omega_k)$, as $\lambda_k^2 := \sigma_\varepsilon^2(a_k^2 + b_k^2) = \gamma_0 + 2\sum_{j=1}^{\infty} \cos[\omega_k j]\gamma_j$, $k = 1, ..., S^*$, where $a_k := \mathcal{I}m(\psi[\exp(\mathrm{i}\omega_k)])$ and $b_k := \mathcal{R}e(\psi[\exp(\mathrm{i}\omega_k)])$, $k = 1, ..., S^*$, with $\mathcal{R}e(\cdot)$ and $\mathcal{I}m(\cdot)$ denoting the real and imaginary parts of their arguments, respectively. Notice that $\lambda_{S/2}^2 = 2\pi f_u(\pi)$ and $\lambda_k^2 = 2\pi f_u(2\pi k/S)$, $k = 1, ..., S^*$.

For the deterministic component in (2.1a), $\mu_{Sn+s} := \delta' z_{Sn+s,\xi}$, we consider three empirically relevant cases ($\xi = 1, 2, 3$). Here and in what follows, it is understood that terms relating to frequency π are to be omitted when S is odd and that where reference is made to the Nyquist frequency this is understood only to apply where S is even.

Case 1: Zero and seasonal frequency intercepts: $z_{Sn+s,1} := [1, \cos(2\pi(Sn+s)/S), \sin(2\pi(Sn+s)/S), ..., \cos(2\pi S^*(Sn+s)/S), \sin(2\pi S^*(Sn+s)/S), (-1)^{Sn+s}]'$.

Case 2: Zero and seasonal frequency intercepts, zero frequency trend: $z_{Sn+s,2} := [z'_{Sn+s,1}, Sn+s]'$.

Case 3: Zero and seasonal frequency intercepts and trends: $z_{Sn+s,3} := [z'_{Sn+s,1}, (Sn+s)z'_{Sn+s,1}]'$.

Following Elliot, Rothenberg and Stock (1996), Rodrigues and Taylor (2007) and Jansson and Nielsen (2011), the initial conditions, $x_{1-S}, ..., x_0$, are taken to be of $o_p(T^{1/2})$. Relaxing this will not alter the limiting null distributions of the test statistics we outline in this paper due to their exact similarity with respect to the initial conditions; see Smith *et al.* (2009).

2.2 The Seasonal Unit Root Hypotheses

The Sth order polynomial $\alpha(L)$ in (2.1b) can be factorised at the zero and seasonal spectral frequencies, ω_k, $k = 0, \ldots, \lfloor S/2 \rfloor$, so that $\alpha(L) = \prod_{k=0}^{\lfloor S/2 \rfloor} \omega_k(L)$, where $\omega_0(L) := (1 - \alpha_0 L)$ associates the parameter α_0 with the zero frequency ($\omega_0 = 0$), $\omega_k(L) := \{1 - 2[\alpha_k \cos(\omega_k) - \beta_k \sin(\omega_k)]L + (\alpha_k^2 + \beta_k^2)L^2\}$ corresponds to the conjugate (harmonic) seasonal frequencies $(\omega_k, 2\pi - \omega_k)$, with the associated parameters α_k and β_k, $k = 1, \ldots, S^*$, and $\omega_{S/2}(L) := \left(1 + \alpha_{S/2} L\right)$ which associates the $\alpha_{S/2}$ parameter with the Nyquist frequency ($\omega_{S/2} = \pi$).

Our interest centers on testing the $(\lfloor S/2 \rfloor + 1)$ unit root null hypotheses,

$$H_{0,0} : \alpha_0 = 1, \qquad H_{0,S/2} : \alpha_{S/2} = 1, \qquad H_{0,k} : \alpha_k = 1, \quad \beta_k = 0, \quad k = 1, \ldots, S^* \tag{2.2}$$

such that $H_{0,0}$ corresponds to a unit root at the zero frequency, while $H_{0,S/2}$ yields a unit root at the Nyquist frequency, and finally $H_{0,k}$, $k = 1, \ldots, S^*$, yields a pair of complex conjugate unit roots at the harmonic seasonal frequencies $(\omega_k, 2\pi - \omega_k)$. Asymptotic power will be considered under the corresponding local alternatives hypotheses; i.e.,

$$\begin{aligned} H_{1,c_j} &: \alpha_j = \exp\left(\tfrac{c_j}{T}\right) \cong \left(1 + \tfrac{c_j}{T}\right), \qquad j = 0, S/2, \\ H_{1,c_k} &: \alpha_k = \exp\left(\tfrac{c_k}{T}\right) \cong \left(1 + \tfrac{c_k}{T}\right) \cap \beta_k = 0, \quad k = 1, \ldots, S^* \end{aligned} \tag{2.3}$$

where c_k, $k = 0, \ldots, \lfloor S/2 \rfloor$ are fixed constants. Under H_{1,c_k} the process $\{y_{Sn+s}\}$ admits either a single root $(k = 0, S/2)$ or a pair of complex conjugate roots $(k = 1, \ldots, S^*)$ with modulus in the neighbourhood of unity at frequency ω_k. These roots are stable for $c_k < 0$ and explosive for $c_k > 0$. Notice that H_{1,c_k} reduces to $H_{0,k}$ where $c_k = 0$, $k = 0, \ldots, \lfloor S/2 \rfloor$. In what follows, let $\mathbf{c} := (c_0, c_1, ..., c_{\lfloor S/2 \rfloor})'$ be the $(\lfloor S/2 \rfloor + 1)$-vector of non-centrality parameters and denote the lag polynomial $\alpha(L)$ under $H_{1,\mathbf{c}} := \cap_{k=0}^{\lfloor S/2 \rfloor} H_{1,c_k}$ as $\Delta_{\mathbf{c}} := 1 - \sum_{j=1}^{S} \alpha_j^{\mathbf{c}} L^j$.

2.3 Seasonal Unit Root Test Regressions

We conclude this section by briefly outlining the regression-based HEGY approach to testing for seasonal unit roots in $\alpha(L)$. A number of objects defined in so doing will also be needed for the subsequent development of our $\mathcal{M}$ seasonal unit root tests in section 3.

First the data are de-trended to give exact invariance to the parameters characterising μ_{Sn+s} in (2.1a); this step will also be required for the seasonal $\mathcal{M}$ tests. To that end, we define the de-trended data series generically as $y^{\xi}_{Sn+s} := y_{Sn+s} - \hat{\delta}' z_{Sn+s,\xi}$ where $\xi = 1$, 2 and 3 corresponds to the deterministic kernels defined in Cases 1, 2 and 3 above. For OLS de-trending, $\hat{\delta}$ is the OLS estimator from regressing y_{Sn+s} onto $z_{Sn+s,\xi}$, while, as in Rodrigues and Taylor (2007), for local GLS de-trending $\hat{\delta}$ obtains from the OLS regression of $\mathbf{y_c}$ on $\mathbf{z_{c,\xi}}$, where

$$\begin{aligned} \mathbf{y_c} &:= (y_{1-S}, y_{2-S} - \alpha_1^{\mathbf{c}} y_{1-S}, y_{3-S} - \alpha_1^{\mathbf{c}} y_{2-S} - \alpha_2^{\mathbf{c}} y_{1-S}, ..., y_0 - \alpha_1^{\mathbf{c}} y_{-1} - \cdots - \alpha_S^{\mathbf{c}} y_{1-S}, \Delta_{\mathbf{c}} y_1, ... \Delta_{\mathbf{c}} y_T)' \\ \mathbf{z_{c,\xi}} &:= (z_{1-S,\xi}, z_{2-S,\xi} - \alpha_1^{\mathbf{c}} z_{1-S,\xi}, z_{3-S,\xi} - \alpha_1^{\mathbf{c}} z_{2-S,\xi} - \alpha_2^{\mathbf{c}} z_{1-S,\xi}, ..., z_{0,\xi} - \alpha_1^{\mathbf{c}} z_{1,\xi} - \cdots \\ &\qquad - \alpha_S^{\mathbf{c}} z_{1-S,\xi}, \Delta_{\mathbf{c}} z_{1,\xi}, ..., \Delta_{\mathbf{c}} z_{T,\xi})' \end{aligned}$$

for $\mathbf{c} = \bar{\mathbf{c}} := (\bar{c}_0, \bar{c}_1, ..., \bar{c}_{\lfloor S/2 \rfloor})'$. The local GLS de-trending parameters, $\bar{c}_k$, $k = 0, ..., \lfloor S/2 \rfloor$, are determined by the significance level that the seasonal unit root tests are to be run at and the de-trending scheme employed; see Rodrigues and Taylor (2007, p.556). For example, under Case 1 for tests run at the 5% level, $\bar{c}_0 = \bar{c}_{S/2} = -7$ and $\bar{c}_k = -3.75$, $k = 1, ..., S^*$. The resulting de-trended series satisfies $\alpha(L) y^{\xi}_{Sn+s} = u^{\xi}_{Sn+s}$ with $u^{\xi}_{Sn+s} := \psi(L) \varepsilon^{\xi}_{Sn+s}$, where u^{ξ}_{Sn+s} and ε^{ξ}_{Sn+s} are the correspondingly de-trended versions of u_{Sn+s} and ε_{Sn+s}, respectively.

The HEGY approach then consists of taking an expansion around the zero and seasonal frequency unit roots $\exp(\pm \mathrm{i}2\pi k/S)$, $k = 0, ..., \lfloor S/2 \rfloor$ to obtain the *augmented* HEGY regression:

$$\Delta_S y^{\xi}_{Sn+s} = \sum_{k=0}^{\lfloor S/2 \rfloor} \pi_k y^{\xi}_{k,Sn+s-1} + \sum_{j=1}^{S^*} \pi^*_j y^{*\xi}_{j,Sn+s-1} + \sum_{j=1}^{p^*} \phi^*_j \Delta_S y^{\xi}_{Sn+s-j} + u^{\xi}_{Sn+s,p^*} \tag{2.4}$$

where $\Delta_S := 1 - L^S$, $y^{\xi}_{k,Sn+s} := \sum_{i=0}^{S-1} \cos[(i+1)\omega_k] y^{\xi}_{Sn+s-i}$, $k = 0, ..., \lfloor S/2 \rfloor$, and, $y^{*\xi}_{j,Sn+s-1} := -\sum_{i=0}^{S-1} \sin[(i+1)\omega_j] y^{\xi}_{Sn+s-i}$. An *un-augmented* version of the HEGY regression obtains by setting $p^* = 0$ in (2.4); that is, omitting the lagged dependent variables from the regression.

As outlined in section S.3 of the accompanying supplement, the so-called HEGY tests for testing $H_{0,0}$, $H_{0,S/2}$ and $H_{0,k}$, $k = 1, ..., S^*$, can be formulated as standard t- and F-tests for $\pi_0 = 0$ (denoted t_0), $\pi_{S/2} = 0$ (denoted $t_{S/2}$) and $\pi_k = \pi^*_k = 0$ (denoted F_k), $k = 1, ..., S^*$, respectively, in (2.4). Joint tests for $H_0 := \cap_{k=0}^{\lfloor S/2 \rfloor} H_{0,k}$ (denoted $F_{0...\lfloor S/2 \rfloor}$) and $H_{0,\text{seas}} := \cap_{k=1}^{\lfloor S/2 \rfloor} H_{0,k}$ (denoted $F_{1...\lfloor S/2 \rfloor}$) can also be performed. In section S.5 of the supplementary appendix we also detail how the non-seasonal Phillips and Perron (1988) [PP] unit root testing principle can be implemented to test for zero and seasonal frequency unit roots in seasonally observed data based on estimating the un-augmented form of (2.4).

3 $\mathcal{M}$-Type Seasonal Unit Root Tests

In this section we propose semi-parametric seasonal unit root tests based on generalising the non-seasonal $\mathcal{M}$ unit root tests to the seasonal case. In section 3.1, as background material, we first briefly review the trinity of non-seasonal $\mathcal{M}$ unit root tests.

3.1 Non-Seasonal $\mathcal{M}$ Unit Root Tests

For the non-seasonal ($S = 1$) case, Perron and Ng (1996), Stock (1999) and Ng and Perron (2001) define the trinity of so-called $\mathcal{M}$ unit root test statistics as follows:

$$\mathcal{MZ}_0 := \frac{T^{-1}\left[(y^{\xi}_T)^2 - (y^{\xi}_0)^2\right] - \hat{\lambda}^2_0}{2T^{-2}\sum_{t=1}^{T}(y^{\xi}_{t-1})^2}, \quad \mathcal{MSB}_0 := \left(T^{-2}\sum_{n=1}^{T}(y^{\xi}_{t-1})^2/\hat{\lambda}^2_0\right)^{1/2} \tag{3.1}$$

and $\mathcal{MZ}_{t_0} := \mathcal{MZ}_0 \times \mathcal{MSB}_0$, where $\hat{\lambda}^2_0$ is a consistent estimator of the long run variance, λ^2_0. Stock (1999) shows that the first of these statistics, $\mathcal{MZ}_0$, can be re-written[1] as $\mathcal{MZ}_0 = Z_0 + \frac{T}{2}(\hat{\pi}_0)^2$, where $Z_0 := T\hat{\pi}_0 - \frac{(\hat{\lambda}^2_0 - \hat{\gamma}_0)}{2}(T^{-2}\sum_{t=1}^{T}(y^{\xi}_{t-1})^2)^{-1}$ is the non-seasonal coefficient-based PP unit root test, where $\hat{\pi}_0$ and $\hat{\gamma}_0$ are the OLS estimate of π_0 and the OLS residual variance estimate, respectively, from (2.4) with $p^* = 0$ when $S = 1$ (i.e. an un-augmented Dickey-Fuller regression). It can therefore be seen to be a modified version of the PP non-seasonal unit root test statistic, Z_0. These two statistics are asymptotically equivalent under $H_{0,c}$. The second statistic, $\mathcal{MSB}_0$, can be used as a basis for a unit root test by noting that the sums of squares of an $I(1)$ series is of $O_p(T^2)$ while that of an $I(0)$ series is of $O_p(T)$. A test

[1]The term $-T^{-1}(y^{\xi}_0)^2$ can be omitted from the numerator of $\mathcal{MZ}_0$ for the case of local GLS de-trended data; see Müller and Elliott (2003).

which rejects for small values of the $\mathcal{MSB}_0$ statistic therefore tests the unit root null hypothesis against the stationary alternative. Stock (1999) shows that $\mathcal{MSB}_0$ can be viewed as a modified version of Bhargava's (1986) R_1 statistic. The final test is based on PP's (non-seasonal) t-based unit root statistic $Z_{t_0} := \frac{\hat{\gamma}_0^{1/2}}{\hat{\lambda}_0} t_0 - \frac{(\hat{\lambda}_0^2 - \hat{\gamma}_0)}{2}(\hat{\lambda}_0^2 T^{-2} \sum_{t=1}^{T} (y_{t-1}^{\xi})^2)^{-1/2}$, where t_0 is the t-ratio on π_0 in the un-augmented form of (2.4) when $S = 1$. Noting that $Z_{t_0} = \mathcal{MSB}_0 \times Z_{t_0}$, Perron and Ng (1996) propose $\mathcal{MZ}_{t_0}$ as a modified version of the PP Z_{t_0} test. As with the corresponding coefficient-based modified statistics, $\mathcal{MZ}_{t_0}$ and Z_{t_0} are asymptotically equivalent under $H_{0,c}$.

3.2 Zero and Nyquist Frequency $\mathcal{M}$ Unit Root Tests

We now consider how we may generalise the principles underlying the trinity of non-seasonal $\mathcal{M}$ unit root tests outlined above to develop tests for unit roots at the zero and Nyquist frequencies in the seasonal case. Consider first the modified coefficient-type tests. Here, in a similar vein to the relationship that holds between $\mathcal{MZ}_0$ and Z_0 in the non-seasonal case, it is straightforward to show that $\mathcal{MZ}_{k} = Z_{k} + \frac{T}{2}(\hat{\pi}_k)^2 + o_p(1)$, $k = 0, S/2$, where for the zero ($k = 0$) and Nyquist ($k = S/2$) frequencies,

$$\mathcal{MZ}_k := \frac{T^{-1}\left[\left(y_{k,T}^{\xi}\right)^2 - \left(y_{k,0}^{\xi}\right)^2\right] - \hat{\lambda}_k^2}{2T^{-2}\sum_{Sn+s=1}^{T}\left(y_{k,Sn+s-1}^{\xi}\right)^2}, \; k = 0, S/2, \tag{3.2}$$

with $\hat{\pi}_k$ the OLS estimates of π_k, $k = 0, S/2$, from estimating (2.4) with $p^* = 0$, Z_0 and $Z_{S/2}$ the zero and Nyquist frequency coefficient-based PP statistics, respectively, defined in section S.5 of the supplementary appendix. Finally, $\hat{\lambda}_0^2$ and $\hat{\lambda}_{S/2}^2$ are consistent estimators of λ_0^2 and $\lambda_{S/2}^2$, respectively. The unit root null hypothesis at the zero and Nyquist frequencies is rejected for large negative values of the $\mathcal{MZ}_0$ and $\mathcal{MZ}_{S/2}$ statistics, respectively.

To make the $\mathcal{MZ}_k$, $k = 0, S/2$, tests operational we therefore need consistent estimators of the long run variance parameters λ_k^2, $k = 0, S/2$. Following Breitung and Franses (1998) and Gregoir (2006), these can be obtained using sums-of-covariances (or kernel-based) estimators based on the estimated un-augmented form of (2.4), and are defined as follows:

$$\hat{\lambda}_{k,WA}^2 := \sum_{j=-T+1}^{T-1} \kappa(j/m)\hat{\gamma}_j \cos(\omega_k j), \qquad k = 0, S/2 \tag{3.3}$$

where $\omega_0 = 0$ and $\omega_{S/2} = \pi$, and $\hat{\gamma}_j$ is the sample autocovariance of order j computed from the OLS residuals from estimating (2.4) setting $p^* = 0$. Analogous quantities at the harmonic seasonal frequencies can be defined as $\hat{\lambda}_{k,WA}^2$, $k = 1, ..., S^*$, by setting $\omega_k = 2\pi k/S$ for $k = 1, ..., S^*$ in the formula in (3.3). These estimators are consistent under $H_{1,\mathbf{c}}$ provided the kernel function $\kappa(\cdot)$ satisfies *e.g.* the general conditions reported in Jansson (2002, Assumption A3) and the bandwidth parameter $m \in (0, \infty)$ satisfies the rate condition $1/m + m^2/T \to 0$ as $T \to \infty$ (which corresponds to Assumption A4 of Jansson, 2002).

An alternative approach, which in the non-seasonal case has been shown to deliver unit root tests with considerably better finite sample size properties, is to use the ASD estimators originally proposed in Berk (1974) and extended to the context of the ADF regression by

Perron and Ng (1998); see, in particular, Ng and Perron (2001) and Haldrup and Jansson (2006). Following the approach in Berk (1974), the ASD analogues of the sums-of-covariances estimators in (3.3) are given by:

$$\hat{\lambda}^2_{k,AR} := s_e^2(1-\widehat{\phi}(e^{\mathrm{i}\omega_k}))^{-2}, \quad k=0,S/2. \tag{3.4}$$

Analogous quantities at the harmonic seasonal frequencies can be defined as

$$\hat{\lambda}^2_{k,AR} := \frac{s_e^2}{\left\{1-\mathcal{R}e\left(\widehat{\phi}\left(e^{(\mathrm{i}\omega_k)}\right)\right)\right\}^2+\left\{\mathcal{I}m\left(\widehat{\phi}\left(e^{(\mathrm{i}\omega_k)}\right)\right)\right\}^2}, \; k=1,\ldots,S^*. \tag{3.5}$$

In (3.4) and (3.5), s_e^2 and $\widehat{\phi}(L) := \sum_{i=1}^{p^*}\hat{\phi}_i^* L^i$ denote the OLS residual variance estimator and the fitted augmentation polynomial, respectively, from the augmented HEGY regression, (2.4), with $\hat{\phi}_j^*$ denoting the OLS estimator of ϕ_j^*, $j=1,...,p^*$, from (2.4). Consistency of the ASD estimators under $H_{1,\mathbf{c}}$ requires that: (i) the lag polynomial $\psi(z)$ is invertible, and (ii) that the lag length used in estimating (2.4) satisfies $(1/p^*)+(p^*)^3/T\to 0$ as $T\to\infty$; see Berk (1974).

Noting that the HEGY transformed level variables $y^{\xi}_{0,Sn+s}$ and $y^{\xi}_{S/2,Sn+s}$, defined just below (2.4), filter out unit roots at all but the zero and Nyquist frequency, respectively, the sums of squares of these variables can be used to form the analogues at the zero and Nyquist frequencies, respectively, of the non-seasonal $\mathcal{MSB}_0$ statistic defined in (3.1); that is,

$$\mathcal{MSB}_k := \left[\frac{1}{T^2\hat{\lambda}^2_k}\sum_{Sn+s=1}^{T}\left(y^{\xi}_{k,Sn+s-1}\right)^2\right]^{1/2}, \; k=0,S/2. \tag{3.6}$$

The unit root null at the zero and Nyquist frequencies is rejected for small values of $\mathcal{MSB}_0$ and $\mathcal{MSB}_{S/2}$, respectively. Combining (3.2) and (3.6), $\mathcal{M}$ versions of the seasonal t-based PP-type Z_{t_k}, $k=0,S/2$ tests (as defined in section S.5 of the supplementary appendix) can then be straightforwardly defined to reject for small values of the statistics

$$\mathcal{MZ}_{t_k} := \mathcal{MZ}_k \times \mathcal{MSB}_k, \;\; k=0,S/2. \tag{3.7}$$

3.3 Harmonic and Joint Frequency $\mathcal{M}$ Unit Root Tests

In order to generalise the $\mathcal{M}$ tests to the harmonic seasonal frequencies, we will consider an approach based around the use of the demodulator operator introduced by Granger and Hatanaka (1964) and used in the context of complex unit root analysis by, *inter alia*, Gregoir (1999,2006).[2]

To illustrate the principle of demodulation, consider the complex-valued process, z_{Sn+s}, near-integrated at frequency ω_k, $(1-(1+\frac{c_k}{T})e^{-\mathrm{i}\omega_k}L)z_{Sn+s}=u_{Sn+s}$, where the innovation u_{Sn+s} satisfies Assumption 1. By recursive substitution it follows that z_{Sn+s} can be written as,

$$z_{Sn+s} = e^{-\mathrm{i}\omega_k(Sn+s)}\left[(1+\frac{c_k}{T})^{(Sn+s)}z_0+\sum_{j=1}^{Sn+s}(1+\frac{c_k}{T})^{Sn+s-j}e^{\mathrm{i}\omega_k j}u_j\right]. \tag{3.8}$$

[2] An alternative approach is to define $\mathcal{M}$ tests at the harmonic frequencies analogously to the zero and Nyquist frequency $\mathcal{MZ}_k$, $\mathcal{MSB}_k$ and $\mathcal{MZ}_{t_k}$ $k=0,S/2$, tests outlined above, using the relevant filtered variables $y^{\xi}_{k,Sn+s}$ and $y^{*\xi}_{k,Sn+s}$, $k=1,...,S^*$ defined just below (2.4). Monte Carlo simulation results reported in the accompanying working paper, del Barrio Castro, Rodrigues and Taylor (2015), suggest, however, that this approach yields tests with inferior finite sample size properties to the standard augmented HEGY tests.

From the representation in (3.8) we observe that z_{Sn+s} is driven by the complex innovation $e^{\mathrm{i}\omega_k j}u_j$ and can be expressed as a complex-valued near-integrated process at the zero frequency multiplied by the demodulator operator $e^{-\mathrm{i}\omega_k(Sn+s)}$. The latter shifts the peak in the spectrum which occurs at the zero frequency with the former to a peak in the spectrum at frequency ω_k.

In order to use the demodulation-based approach to develop harmonic frequency $\mathcal{M}$-type tests we first need to define the demodulated complex conjugate variables,

$$y^{\xi,\mathtt{D}a}_{k,Sn+s} := e^{\mathrm{i}\omega_k(Sn+s)}\left(1-e^{\mathrm{i}\omega_k}L\right)\Delta^0_k(L)\,y^{\xi}_{Sn+s} \tag{3.9}$$

$$y^{\xi,\mathtt{D}b}_{k,Sn+s} := e^{-\mathrm{i}\omega_k(Sn+s)}\left(1-e^{-\mathrm{i}\omega_k}L\right)\Delta^0_k(L)\,y^{\xi}_{Sn+s} \tag{3.10}$$

in each case for $k=1,...,S^*$, where

$$\Delta^0_k(L) := (1-L)(1+L)\sum_{j\neq k,j=1}^{S^*}(1-2\cos[\omega_j]L+L^2) = \sin[\omega_k]^{-1}(\sum_{j=0}^{S-1}\sin[(j+1)\omega_k]L^j) \tag{3.11}$$

omitting the factor $(1+L)$ above when S is odd. As demonstrated in the supplementary appendix (see equation (S.17)), applying the filter $\Delta^0_k(L)$ to y^{ξ}_{Sn+s} yields a real-valued near-integrated process at frequency ω_k with associated AR(2) polynomial $(1-2\cos(\omega_k)(1+\frac{c_k}{T})L$ $+(1+\frac{c_k}{T})^2L^2)$. Consequently, the filters $(1-e^{\mathrm{i}\omega_k}L)\Delta^0_k(L)$ and $(1-e^{-\mathrm{i}\omega_k}L)\Delta^0_k(L)$ when applied to y^{ξ}_{Sn+s} deliver the complex-valued near-integrated processes with associated (complex) AR(1) polynomials $(1-(1+\frac{c_k}{T})e^{-\mathrm{i}\omega_k}L)$ and $(1-(1+\frac{c_k}{T})e^{\mathrm{i}\omega_k}L)$, respectively; see (S.18) and (S.19) in the Appendix. Finally, the demodulation by multiplication by $e^{\mathrm{i}\omega_k(Sn+s)}$ and $e^{-\mathrm{i}\omega_k(Sn+s)}$ in (3.9) and (3.10), respectively, yields the complex-valued near-integrated processes at the zero frequency, $y^{\xi,\mathtt{D}a}_{k,Sn+s}$ and $y^{\xi,\mathtt{D}b}_{k,Sn+s}$, associated with the filters $(1-(1+\frac{c_k}{T})e^{-\mathrm{i}\omega_k}L)$ and $(1-(1+\frac{c_k}{T})e^{\mathrm{i}\omega_k}L)$, respectively; see (S.27) and (S.28) in the supplementary appendix.

The following weak convergence results for $y^{\xi,\mathtt{D}a}_{k,Sn+s}$ and $y^{\xi,\mathtt{D}b}_{k,Sn+s}$ of (3.9) and (3.10), respectively, follow straightforwardly from (S.27) and (S.28) in the supplementary appendix,

$$T^{-1/2}y^{\xi,\mathtt{D}a}_{k,S\lfloor rN\rfloor+s} \Rightarrow \frac{\sigma_\varepsilon\psi\left(e^{\mathrm{i}\omega_k}\right)}{\sqrt{2}}\left[J^{\zeta}_{k,c_k}(r)+\mathrm{i}J^{\zeta*}_{k,c_k}(r)\right] =: \frac{\sigma_\varepsilon\psi\left(e^{\mathrm{i}\omega_k}\right)}{\sqrt{2}}\mathbb{J}_{k,c_k}(r) \tag{3.12}$$

$$T^{-1/2}y^{\xi,\mathtt{D}b}_{k,S\lfloor rN\rfloor+s} \Rightarrow \frac{\sigma_\varepsilon\psi\left(e^{-\mathrm{i}\omega_k}\right)}{\sqrt{2}}\left[J^{\zeta}_{k,c_k}(r)-\mathrm{i}J^{\zeta*}_{k,c_k}(r)\right] =: \frac{\sigma_\varepsilon\psi\left(e^{-\mathrm{i}\omega_k}\right)}{\sqrt{2}}\overline{\mathbb{J}_{k,c_k}(r)} \tag{3.13}$$

in each case for $k=1,...,S^*$ and where "$\Rightarrow$" denotes weak convergence, as $T\to\infty$, in the Skorohod topology. In (3.12) and (3.13), $\psi(\cdot)$ is as defined in Assumption 1, while $J^{\zeta}_{k,c_k}(r)$ and $J^{\zeta*}_{k,c_k}(r)$, $k=1,...,S^*$, are the independent Ornstein-Uhlenbeck based processes which will subsequently be defined in Theorem 4.1. Notice that $\mathbb{J}_{k,c_k}$ and $\overline{\mathbb{J}_{k,c_k}}$ in (3.12) and (3.13), respectively, form a complex conjugate pair of complex OU processes.

As the limiting representations given for $y^{\xi,\mathtt{D}a}_{k,Sn+s}$ and $y^{\xi,\mathtt{D}b}_{k,Sn+s}$ in (3.12) and (3.13) make clear, developing feasible harmonic frequency $\mathcal{M}$-type test statistics based on these demodulated variables will require taking appropriate real-valued transformations of $y^{\xi,\mathtt{D}a}_{k,Sn+s}$ and $y^{\xi,\mathtt{D}b}_{k,Sn+s}$, together with estimates of the seasonal long run variance nuisance parameters $\sigma_\varepsilon\psi(e^{\mathrm{i}\omega_k})$ and $\sigma_\varepsilon\psi(e^{-\mathrm{i}\omega_k})$ which feature in (3.12) and (3.13), respectively, which are consistent under $H_{1,\mathbf{c}}$. It is straightforward to show that the latter can be obtained, under the conditions stated for

consistent estimation in section 3.2, using the ASD estimators, $\breve{\lambda}^2_{k,AR} := s^2_e\{1 - [\widehat{\phi}(e^{\mathrm{i}\omega_k})]\}^{-2}$ and $\breve{\lambda}^{*2}_{k,AR} := s^2_e\{1 - [\widehat{\phi}(e^{-\mathrm{i}\omega_k})]\}^{-2}$, $k = 1, ..., S^*$, where s^2_e and $\widehat{\phi}(\cdot)$ are as defined below (3.5). For the former, we take the following transformations

$$y^{\mathcal{R}e,\xi}_{k,Sn+s} := \frac{1}{2}\mathcal{R}e\left(\frac{y^{\xi,\mathtt{D}a}_{k,Sn+s}}{\breve{\lambda}_{k,AR}\sqrt{T}} + \frac{y^{\xi,\mathtt{D}b}_{k,Sn+s}}{\breve{\lambda}^*_{k,AR}\sqrt{T}}\right) \tag{3.14}$$

$$y^{\mathcal{I}m,\xi}_{k,Sn+s} := \frac{1}{2}\mathcal{I}m\left(\frac{y^{\xi,\mathtt{D}a}_{k,Sn+s}}{\breve{\lambda}_{k,AR}\sqrt{T}} - \frac{y^{\xi,\mathtt{D}b}_{k,Sn+s}}{\breve{\lambda}^*_{k,AR}\sqrt{T}}\right) \tag{3.15}$$

for $k = 1, ..., S^*$. Notice that the transformations in (3.14) and (3.15) are designed such that they weakly converge to $J^{\zeta}_{k,c_k}(r)$ and $J^{\zeta*}_{k,c_k}(r)$, respectively. Other transformations with this same asymptotic property could be used instead, but we found little difference even in very small samples compared to using (3.14) and (3.15).

The sequence of transformations in (3.9)-(3.10) and (3.14)-(3.15) map the original (detrended) series y^{ξ}_{Sn+s} which admits a complex pair of (near-) unit roots at frequency ω_k into two (scaled) series, $y^{\mathcal{R}e,\xi}_{k,Sn+s}$ and $y^{\mathcal{I}m,\xi}_{k,Sn+s}$, each of which has a single (near-) unit root at the zero frequency. Consequently, under $H_{0,k}$ where y^{ξ}_{Sn+s} admits a pair of unit roots at frequency ω_k, then so the two demodulated series $y^{\mathcal{R}e,\xi}_{k,Sn+s}$ and $y^{\mathcal{I}m,\xi}_{k,Sn+s}$ will each contain a zero frequency unit root. Likewise, under H_{1,c_k}, $y^{\mathcal{R}e,\xi}_{k,Sn+s}$ and $y^{\mathcal{I}m,\xi}_{k,Sn+s}$ each admit either a stable ($c_k < 0$) or explosive ($c_k > 0$) root at frequency zero. Consequently, by analogy to the non-seasonal $\mathcal{M}$ tests in section 3.1, $H_{0,k}$ can therefore be tested against H_{1,c_k} using either $y^{\mathcal{R}e,\xi}_{k,Sn+s}$ or $y^{\mathcal{I}m,\xi}_{k,Sn+s}$ in the following harmonic frequency $\mathcal{M}$-type statistics, in each case for $k = 1, ..., S^*$,

$$\mathcal{K}\text{-}\mathcal{MSB}_k := \left[\frac{2}{T}\left(\sum_{Sn+s=1}^{T} y^{\mathcal{K},\xi}_{k,Sn+s-1}\right)^2\right]^{1/2} \tag{3.16}$$

$$\mathcal{K}\text{-}\mathcal{MZ}_k := \frac{\left(y^{\mathcal{K},\xi}_{k,T}\right)^2 - \left(y^{\mathcal{K},\xi}_{k,0}\right)^2 - 1}{\left[\mathcal{K}\text{-}\mathcal{MSB}_k\right]^2} \tag{3.17}$$

$$\mathcal{K}\text{-}\mathcal{MZ}_{t_k} := \mathcal{K}\text{-}\mathcal{MZ}_k \times \mathcal{K}\text{-}\mathcal{MSB}_k \tag{3.18}$$

where setting $\mathcal{K} = \mathcal{R}e$ in (3.16)-(3.18) denotes tests based on $y^{\mathcal{R}e,\xi}_{k,Sn+s}$, while setting $\mathcal{K} = \mathcal{I}m$ denotes the corresponding tests based on $y^{\mathcal{I}m,\xi}_{k,Sn+s}$. In parallel with the $\mathcal{M}$ tests from section 3.2, $H_{0,k}$ is rejected in favour of H_{1,c_k} for large negative values of $\mathcal{R}e\text{-}\mathcal{MZ}_k$, $\mathcal{I}m\text{-}\mathcal{MZ}_k$, $\mathcal{R}e\text{-}\mathcal{MZ}_{t_k}$ and $\mathcal{I}m\text{-}\mathcal{MZ}_{t_k}$, and for small values of $\mathcal{R}e\text{-}\mathcal{MSB}_k$ and $\mathcal{I}m\text{-}\mathcal{MSB}_k$, $k = 1, ..., S^*$.

The harmonic frequency $\mathcal{M}$-type unit root test statistics proposed in (3.16)-(3.18) will be shown in Theorem 4.1 to share the same limiting distributions as the corresponding $\mathcal{M}$-type tests defined for the zero and Nyquist frequencies in section 3.2. As a result, asymptotic critical values for the tests based on these statistics are as given for the corresponding non-seasonal tests. Moreover, this also implies that their asymptotic local power functions under H_{1,c_k} will be close to the power envelope for testing for a single unit root at either the zero or Nyquist frequency. This is known to lie considerably beneath the power envelope for testing $H_{0,k}$ against H_{1,c_k}; see, for example, Rodrigues and Taylor (2007). Consequently, one could consider joint tests which combine the $\mathcal{M}$-type statistics based on (3.14) and (3.15) in order to increase

power. To that end we propose the test which rejects for large values of the following statistic, analogous to the F_k test statistic of HEGY from section 2.3:

$$F^{\mathtt{D}}_{\mathcal{M},k} := \frac{1}{2}\left[\left(\mathcal{R}e\text{-}\mathcal{MZ}_{t_{\pi_k}}\right)^2 + \left(\mathcal{I}m\text{-}\mathcal{MZ}_{t_{\pi_k}}\right)^2\right], \;\; k = 1, ..., S^*. \tag{3.19}$$

Similarly, $\mathcal{MZ}$-type analogues of the joint frequency $F_{1,...,\lfloor S/2\rfloor}$ and $F_{0,...,\lfloor S/2\rfloor}$ HEGY tests from section 2.3 can be formed by rejecting $H_{0,\text{seas}}$ and H_0 for large values of the statistics

$$F^{\mathtt{D}}_{\mathcal{M},1...\lfloor S/2\rfloor} := \frac{1}{S-1}\left[2\sum_{k=1}^{S^*} F^{\mathtt{D}}_{\mathcal{M},k} + \left(\mathcal{MZ}_{t_{\pi_{S/2}}}\right)^2\right] \tag{3.20}$$

and

$$F^{\mathtt{D}}_{\mathcal{M},0...\lfloor S/2\rfloor} := \frac{1}{S}\left[2\sum_{k=1}^{S^*} F^{\mathtt{D}}_{\mathcal{M},k} + \left(\mathcal{MZ}_{t_{\pi_0}}\right)^2 + \left(\mathcal{MZ}_{t_{\pi_{S/2}}}\right)^2\right], \tag{3.21}$$

respectively. Analogous joint tests can also be formed by rejecting $H_{0,k}$, $H_{0,\text{seas}}$ and H_0, respectively, for small values of the $\mathcal{MSB}$-type statistics,

$$\mathcal{MSB}^{\mathtt{D}}_k := \frac{1}{2}\left[\left(\mathcal{R}e\text{-}\mathcal{MSB}_k\right)^2 + \left(\mathcal{I}m\text{-}\mathcal{MSB}_k\right)^2\right]^{1/2}, \; k = 1, ..., S^* \tag{3.22}$$

$$\mathcal{MSB}^{\mathtt{D}}_{1...\lfloor S/2\rfloor} := \frac{1}{S-1}\left\{\sum_{k=1}^{S^*}\left[\mathcal{MSB}^{\mathtt{D}}_k\right]^2 + \mathcal{MSB}^2_{S/2}\right\}^{1/2}, \tag{3.23}$$

$$\mathcal{MSB}^{\mathtt{D}}_{0...\lfloor S/2\rfloor} := \frac{1}{S}\left\{\sum_{k=1}^{S^*}\left[\mathcal{MSB}^{\mathtt{D}}_k\right]^2 + \mathcal{MSB}^2_0 + \mathcal{MSB}^2_{S/2}\right\}^{1/2}. \tag{3.24}$$

Remark 3.1: The statistics in (3.19)-(3.24) are based on the approach underlying the corresponding F-type HEGY statistics obtained from (2.4). An alternative is to follow the approach used to develop point optimal seasonal unit root tests in Rodrigues and Taylor (2007), whereby the optimal joint tests are based on the sum of the individual optimal test statistics involved. We define these test statistics as follows, $S^{\mathtt{D}}_{\mathcal{M},k} := \mathcal{R}e\text{-}\mathcal{MZ}_{t_k} + \mathcal{I}m\text{-}\mathcal{MZ}_{t_k}$, $k = 1, ..., S^*$, $S^{\mathtt{D}}_{\mathcal{M},1...\lfloor S/2\rfloor} := \sum_{k=1}^{S^*} S^{\mathtt{D}}_{\mathcal{M},k} + \mathcal{MZ}_{t_{S/2}}$ and $S^{\mathtt{D}}_{\mathcal{M},0...\lfloor S/2\rfloor} := \sum_{k=1}^{S^*} S^{\mathtt{D}}_{\mathcal{M},k} + \mathcal{MZ}_{t_0} + \mathcal{MZ}_{t_{S/2}}$, rejecting $H_{0,k}$ for large negative values of $S^{\mathtt{D}}_{\mathcal{M},k}$, $k = 1, ..., S^*$, and $H_{0,\text{seas}}$ and H_0 for large negative values of $S^{\mathtt{D}}_{\mathcal{M},1...\lfloor S/2\rfloor}$ and $S^{\mathtt{D}}_{\mathcal{M},0...\lfloor S/2\rfloor}$, respectively.

4 Asymptotic Results for the $\mathcal{M}$-Type Seasonal Unit Root Tests

We now provide representations for the limiting distributions of the seasonal $\mathcal{M}$-type unit root statistics from section 3. These are shown to have pivotal limiting distributions whose form coincides with those which obtain for serially uncorrelated shocks. Local asymptotic power functions of these tests, together with the relevant power envelopes, are also reported.

4.1 Limiting Distributions

In Theorem 4.1 we provide limiting representations for the single unit root $\mathcal{M}$-type statistics in (3.2), (3.6) and (3.7) and (3.16)-(3.18). These representations are indexed by the parameter ζ

whose value is determined by which of Cases 1-3 of μ_{Sn+s}, as outlined in section 2.1, holds and the frequency under test. For the zero frequency ω_0 tests: Case 1: $\zeta = 1$; Cases 2 and 3: $\zeta = 2$. For the seasonal frequency ω_k, $k = 1, ..., \lfloor S/2 \rfloor$, tests: Cases 1 and 2: $\zeta = 1$; Case 3: $\zeta = 2$.

Theorem 4.1. *Let y_{Sn+s} be generated by (2.1) under $H_{1,\mathbf{c}}$ and let Assumption 1 hold. Then, as $T \to \infty$:*
(i) for the zero ($k = 0$) and Nyquist ($k = S/2$) frequencies, the single $\mathcal{M}$-type seasonal unit root test statistics in (3.2), (3.6) and (3.7) satisfy,

$$\mathcal{MZ}_k \Rightarrow \left\{2\int_0^1 \left[J^{\zeta}_{k,c_k}(r)\right]^2 dr\right\}^{-1} \left\{\left[J^{\zeta}_{k,c_k}(1)\right]^2 - 1\right\}, \quad k = 0, S/2 \tag{4.1}$$

$$\mathcal{MSB}_k \Rightarrow \left\{\int_0^1 \left[J^{\zeta}_{k,c_k}(r)\right]^2 dr\right\}^{1/2} =: \mathfrak{MGB}^{\zeta}_k, \quad k = 0, S/2 \tag{4.2}$$

$$\mathcal{MZ}_{t_k} \Rightarrow \frac{1}{2}\left\{\int_0^1 \left[J^{\zeta}_{k,c_k}(r)\right]^2 dr\right\}^{-1/2} \left\{\left[J^{\zeta}_{k,c_k}(1)\right]^2 - 1\right\} =: \mathcal{T}^{\zeta}_k, \quad k = 0, S/2; \tag{4.3}$$

(ii) the harmonic frequency single unit root test statistics in (3.16)-(3.18), recalling that $\mathcal{K} = \mathcal{R}e$ relates to statistics based on $y^{\mathcal{R}e,\xi}_{k,Sn+s}$ and $\mathcal{K} = \mathcal{I}m$ relates to the corresponding statistics based on $y^{\mathcal{I}m,\xi}_{k,Sn+s}$, satisfy, in each case for $k = 1, ..., S^*$,

$$\mathcal{K}\text{-}\mathcal{MZ}_k \Rightarrow \left\{2\int_0^1 \left[\mathcal{H}^{\zeta}_{k,c_k}(r)\right]^2 dr\right\}^{-1} \left\{\left[\mathcal{H}^{\zeta}_{k,c_k}(1)\right]^2 - 1\right\} := \mathcal{K}\text{-}\mathcal{MZ}^{\zeta}_k \tag{4.4}$$

$$\mathcal{K}\text{-}\mathcal{MSB}_k \Rightarrow \left[\int_0^1 \left[\mathcal{H}^{\zeta}_{k,c_k}(r)\right]^2 dr\right]^{1/2} =: \mathcal{K}\text{-}\mathfrak{MGB}^{\zeta}_k \tag{4.5}$$

$$\mathcal{K}\text{-}\mathcal{MZ}_{t_k} \Rightarrow \mathcal{K}\text{-}\mathcal{MZ}^{\zeta}_k \times \mathcal{K}\text{-}\mathfrak{MGB}^{\zeta}_k =: \mathcal{K}\text{-}\mathcal{T}^{\zeta}_k \tag{4.6}$$

where "$\Rightarrow$" denotes weak convergence in the Skorohod topology.

In the above $\mathcal{H}^{\zeta}_{k,c_k}(r) := J^{\zeta}_{k,c_k}(r)$ if $\mathcal{K} = \mathcal{R}e$ and $\mathcal{H}^{\zeta}_{k,c_k}(r) := J^{*\zeta}_{k,c_k}(r)$ if $\mathcal{K} = \mathcal{I}m$, with $J^{\zeta}_{0,c_0}(r)$, $J^{\zeta}_{S/2,c_{S/2}}(r)$, $J^{\zeta}_{k,c_k}(r)$ and $J^{\zeta*}_{k,c_k}(r)$, $k = 1, \ldots, S^*$, $\zeta = 1, 2$, collectively forming a set of S mutually independent scalar Ornstein-Uhlenbeck [OU] processes. These limiting processes are defined as follows. First let $W_0(r)$, $W_{S/2}(r)$, $W_k(r)$ and $W^*_k(r)$, $k = 1, \ldots, S^*$, be mutually independent standard Brownian motions. Then $J^{\zeta}_{0,c_0}(r)$, $J^{\zeta}_{S/2,c_{S/2}}(r)$, $J^{\zeta}_{k,c_k}(r)$ and $J^{\zeta*}_{k,c_k}(r)$, $k = 1, \ldots, S^*$, are mutually independent functionals of these Brownian motions whose precise form depends on the de-trending index ξ and on whether y^{ξ}_{Sn+s} is formed using OLS de-trending or local GLS de-trending. In the case of local GLS de-trending: for $\zeta = 1$, these are the standard OU processes $J^1_{k,c_k}(r) := J_{k,c_k}(r) := \int_0^r \exp(c_k(r-s))dW_k(s)$, $k = 0, \ldots, \lfloor S/2 \rfloor$, and $J^{1*}_{k,c_k}(r) := J^*_{k,c_k}(r) := \int_0^r \exp(c_k(r-s))dW^*_k(s)$, $k = 1, ..., S^*$; for $\zeta = 2$, they take the form $J^2_{k,c_k}(r) := J^1_{k,c_k}(r) - r\{\frac{(1-\bar{c}_k)J^1_{k,c_k}(1)+\bar{c}^2_k\int_0^1 sJ^1_{k,c_k}(s)ds}{1-\bar{c}_k+\bar{c}^2_k/3}\}$, $k = 0, \ldots, \lfloor S/2 \rfloor$, and $J^{2*}_{k,c_k}(r) := J^{1*}_{k,c_k}(r) - r\{\frac{(1-\bar{c}_k)J^{1*}_{k,c_k}(1)+\bar{c}^2_k\int_0^1 sJ^{1*}_{k,c_k}(s)ds}{1-\bar{c}_k+\bar{c}^2_k/3}\}$, $k = 1, ..., S^*$. For OLS de-trending they are de-meaned standard OU processes for $\zeta = 1$, so that, for example, $J^1_{k,c_k}(r) := J_{k,c_k}(r) - \int_0^1 J_{k,c_k}(s)ds$, while for $\zeta = 2$ they are de-trended OU processes, so that, for example, J^2_{k,c_k} is the de-meaned and de-trended standard OU process, $J^2_{k,c_k}(r) := J^1_{k,c_k}(r) - 12\left(r - \frac{1}{2}\right)\int_0^1 \left(s - \frac{1}{2}\right) J^1_{k,c_k}(s)ds$.

Remark 4.1: The limiting distributions given for $\mathcal{MZ}_k$, $k = 0, S/2$, in (4.1), are identical (for a given value of ζ) to and independent of those given for $\mathcal{R}e\text{-}\mathcal{MZ}_k$ and $\mathcal{I}m\text{-}\mathcal{MZ}_k$, $k = 1, ..., S^*$, in (4.4). Similarly, the limiting distributions for the $\mathcal{MZ}_{t_k}$, $k = 0, S/2$, statistics of (4.3) are identical (for a given value of ζ) to and independent of those for $\mathcal{R}e\text{-}\mathcal{MZ}_{t_k}$ and $\mathcal{I}m\text{-}\mathcal{MZ}_{t_k}$ in (4.6). Moreover, it is also seen from (4.2) and (4.5) that the limiting distributions of the $\mathcal{MSB}_k$, $k = 0, S/2$, $\mathcal{R}e\text{-}\mathcal{MSB}_k$ and $\mathcal{I}m\text{-}\mathcal{MSB}_k$, $k = 1, ..., S^*$, statistics are identical (again for a given value of ζ) and are mutually independent.

Remark 4.2: The limiting distributions of the seasonal $\mathcal{M}$-type statistics given in Theorem 4.1 coincide with those of the corresponding non-seasonal $\mathcal{M}$ statistics discussed in section 3.1, and, hence, are free of any nuisance parameters arising from weak dependence in u_{Sn+s}. Selected critical values for the tests based on these statistics can therefore be obtained from Table I of Elliott *et al.* (1996, p.825) and from Table 1 of Ng and Perron (2001,p.1524). Moreover, the asymptotic local power functions of these statistics also coincide with those given for the corresponding statistics in the non-seasonal case and graphed in Figures 1-3 of Elliott *et al.* (1996, pp.822-24). Finally, the representations for $\mathcal{MZ}_{t_0}$ and $\mathcal{MZ}_{t_{S/2}}$ coincide with those given in Rodrigues and Taylor (2007) for the corresponding HEGY statistics t_0 and $t_{S/2}$, respectively.

We now detail the limiting distributions of the joint $\mathcal{M}$ tests from section 3.

Corollary 4.1. *Let the conditions of Theorem 4.1 hold. Then, as* $T \to \infty$*: (i)* $F^{\mathtt{D}}_{\mathcal{M},k} \Rightarrow \frac{1}{2}[(\mathcal{R}e\text{-}\mathcal{T}^{\zeta}_k)^2 + (\mathcal{I}m\text{-}\mathcal{T}^{\zeta}_k)^2] =: \mathcal{F}^{\mathtt{D},\zeta}_{\mathcal{M},k}$, $k = 1, ..., S^*$, $F^{\mathtt{D}}_{\mathcal{M},1...\lfloor S/2 \rfloor} \Rightarrow \frac{1}{S-1}[2\sum_{k=1}^{S^*} \mathcal{F}^{\mathtt{D},\zeta}_{\mathcal{M},k} + (\mathcal{T}^{\zeta}_{S/2})^2]$; $F^{\mathtt{D}}_{\mathcal{M},0...\lfloor S/2 \rfloor} \Rightarrow \frac{1}{S}[2\sum_{k=1}^{S^*} \mathcal{F}^{\mathtt{D},\zeta}_{\mathcal{M},k} + (\mathcal{T}^{\zeta}_0)^2 + (\mathcal{T}^{\zeta}_{S/2})^2]$; *(ii)* $\mathcal{MSB}^{\mathtt{D}}_k \Rightarrow \frac{1}{2}[(\mathcal{R}e\text{-}\mathfrak{MGSB}^{\zeta}_k)^2 + (\mathcal{I}m\text{-}\mathfrak{MGSB}^{\zeta}_k)^2]^{1/2} =: \mathfrak{MGSB}^{\mathtt{D},\zeta}_k$, $k = 1, ..., S^*$; $\mathcal{MSB}^{\mathtt{D}}_{j...\lfloor S/2 \rfloor} \Rightarrow [\sum_{k=j}^{S^*} (\mathfrak{MGSB}^{\mathtt{D},\zeta}_k)^2 + (\mathfrak{MGSB}^{\zeta}_0)^2 + (\mathfrak{MGSB}^{\zeta}_{S/2})^2]^{1/2}$, $j = 0, 1$; *and (iii)* $S^{\mathtt{D}}_{\mathcal{M},k} \Rightarrow \mathcal{R}e\text{-}\mathcal{T}^{\zeta}_k + \mathcal{I}m\text{-}\mathcal{T}^{\zeta}_k$, $k = 1, ..., S^*$, $S^{\mathtt{D}}_{\mathcal{M},1...\lfloor S/2 \rfloor} \Rightarrow \sum_{k=1}^{S^*} (\mathcal{R}e\text{-}\mathcal{T}^{\zeta}_k + \mathcal{I}m\text{-}\mathcal{T}^{\zeta}_k) + \mathcal{T}^{\zeta}_{S/2}$, *and* $S^{\mathtt{D}}_{\mathcal{M},0...\lfloor S/2 \rfloor} \Rightarrow \sum_{k=1}^{S^*} (\mathcal{R}e\text{-}\mathcal{T}^{\zeta}_k + \mathcal{I}m\text{-}\mathcal{T}^{\zeta}_k) + \mathcal{T}^{\zeta}_0 + \mathcal{T}^{\zeta}_{S/2}$.

Remark 4.3: The limiting distributions which appear in Corollary 4.1 have not appeared in the literature before. Consequently, in Table 1 for the $\mathcal{S}^{\mathtt{D}}_{\mathcal{M}}$ and $\mathcal{MSB}^{\mathtt{D}}$ tests, and in Table 2 for the $F^{\mathtt{D}}_{\mathcal{M}}$ tests, we provide selected asymptotic null critical values, for each of Cases 1–3 for the deterministic component, computed by direct simulation of the relevant limiting null distributions in Corollary 4.1, using 100,000 Monte Carlo replications and a discretisation of $N = 1000$ steps, for versions of the statistics based on either OLS de-trended data or local GLS de-trended data, the latter using the relevant values of $\bar{c}$ detailed in section 2.3.

4.2 Asymptotic Local Power Functions

Figures 1 and 2 graph the asymptotic local power functions of the seasonal $\mathcal{M}$-type unit root tests proposed in section 3, together with the seasonal point optimal-based tests of Rodrigues and Taylor (2007) and, where relevant, the HEGY tests of section 2.3.[3] Results for the zero,

[3]The seasonal unit root tests of Jansson and Nielsen (2011) have asymptotic local power functions which are almost indistinguishable from the point optimal tests and, hence, are not reported.

Nyquist and harmonic frequency unit root tests (which are independent of the seasonal aspect, S) are given in Figure 1, while results for joint frequency tests for the quarterly case, $S = 4$, are given in Figure 2. All results relate to tests based on local GLS de-trended data, with results given for $\zeta = 1$ and $\zeta = 2$, where the index ζ is as defined immediately prior to Theorem 4.1. The local GLS de-trending parameters $\bar{c}_k$ detailed in section 2.3 were used for all tests. Each graph also reports the relevant Gaussian asymptotic local power envelope, taken from either Elliott *et al.* (1996) or Rodrigues and Taylor (2007), as a benchmark. The local power functions were calculated using direct simulation methods with 80,000 Monte Carlo replications, discretising over $N = 1000$ steps. The horizontal axes of the graphs are indexed by c which is used generically to denote either the relevant frequency-specific non-centrality parameter, c_k, $k = 0, ..., \lfloor S/2 \rfloor$ (so that for tests at the zero frequency, for example, $c = c_0$) or, in the case of joint frequency tests, a common non-centrality parameter (for example, $c = c_1 = c_2$ in the case of the tests of the null hypothesis of unit roots at all of the seasonal frequencies).

Consider first Figures 1(a) and 1(b) which pertain to the zero and Nyquist frequency tests. Results are reported for the $\mathcal{M}Z_k$, $\mathcal{M}Z_{t_k}$ and $\mathcal{MSB}_k$, $k = 0, S/2$, tests from section 3.2 together with the feasible point optimal-type tests from section 4 of Rodrigues and Taylor (2007, pp.556-558), denoted $P_{k,T}$, $k = 0, S/2$, in what follows.[4] As discussed in section 4, for a given value of ζ the large sample behaviour of a given zero frequency statistic and its Nyquist frequency analogue coincide, and coincide with the behaviour of that statistic in the non-seasonal ($S = 1$) case. This is also true of the $P_{k,T}$, $k = 0, S/2$, statistics, as demonstrated in Rodrigues and Taylor (2007). For the local GLS de-meaning ($\zeta = 1$) case in Figure 1(a) it is seen that the asymptotic local power functions of the $\mathcal{M}Z_k$, $\mathcal{M}Z_{t_k}$, $\mathcal{MSB}_k$ and $P_{k,T}$, $k = 0, S/2$ tests all lie very close to the Gaussian power envelope and are almost indistinguishable from each other, echoing results in Figures 1-3 of Elliott *et al.* (1996). For the local GLS de-trended ($\zeta = 2$) case in Figure 1(b), we see a decline in the power curves and the power envelope relative to the corresponding quantities in Figure 1(a), again consonant with Figures 1-3 of Elliott *et al.* (1996). In the local GLS de-trended case the tests again all lie very close to one another and again are effectively indistinguishable from the Gaussian power envelope.

Figures 1(c) and 1(d) present the corresponding results for the harmonic frequency $\mathcal{M}$-type tests of section 3.3, the feasible point optimal $P_{k,T}$ test of Rodrigues and Taylor (2007) and the HEGY F_k test. Gaussian local power envelopes are from Gregior (2006) and Rodrigues and Taylor (2007). For a given value of ζ, the demodulated single unit root $\mathcal{M}$-type tests in (3.2)-(3.7) and (3.16)-(3.18) were virtually indistinguishable and so we only plot $\mathcal{R}e\text{-}\mathcal{MZ}_{t_k}$. The results for $\zeta = 1$ in Figure 1(c) show that the local power function of the demodulated $\mathcal{R}e\text{-}\mathcal{MZ}_{t_k}$ test lies well below both the Gaussian local power envelope and the power functions of the other harmonic frequency unit root tests, as would be expected given that each of the latter jointly test on both complex conjugate harmonic frequency unit roots. Of the other tests, the $P_{k,T}$ test displays the best power. The $\mathcal{MSB}_k^{\mathtt{D}}$ and the $S_{\mathcal{M},k}^{\mathtt{D}}$ test of Remark 3.1 are both slightly less powerful than the aforementioned test, followed by the standard HEGY F_k test

[4]The relevant HEGY tests t_k, $k = 0, S/2$, are not included in Figures 1(a) and 1(b) because they are asymptotically equivalent to $\mathcal{M}Z_{t_k}$; cf. Remark 4.2.

and the demodulated $F^{\mathtt{D}}_{\mathcal{M},1}$ test whose power functions lie close to one another. The results for $\zeta = 2$ in Figure 1(d) show the same power ordering among the tests as was seen in Figure 1(c) but the differences between these power functions are far less pronounced, with the exception of the demodulated $\mathcal{R}e\text{-}\mathcal{MZ}_{t_k}$ test whose power function still lies well below those of the other tests. As with the corresponding results in Figures 1(a) and 1(b), the power functions and the power envelope again decline relative to those in Figure 1(c).

Finally in Figure 2 we graph the Gaussian power envelopes and asymptotic local power functions of the joint frequency tests discussed in this paper which obtain in the quarterly case, $S = 4$. Specifically, Figures 2(a) and 2(b) report results, for the local GLS de-meaned and de-trended cases respectively, for the F_{12}, $F^{\mathtt{D}}_{\mathcal{M},12}$, $\mathcal{MSB}^{\mathtt{D}}_{12}$ and $S^{\mathtt{D}}_{\mathcal{M},12}$ tests and the corresponding feasible point optimal test of Rodrigues and Taylor (2007), denoted $PT_{12,T}$, while Figures 2(c) and 2(d) report results, again for the local GLS de-meaned and de-trended cases respectively, for the F_{012}, $F^{\mathtt{D}}_{\mathcal{M},012}$, $\mathcal{MSB}^{\mathtt{D}}_{012}$, $S^{\mathtt{D}}_{\mathcal{M},012}$ and $PT_{012,T}$ tests, the latter again denoting the relevant feasible point optimal test from Rodrigues and Taylor (2007). Consider first Figures 2(a) and 2(b) which pertain to tests of the null hypothesis of unit roots at all of the seasonal frequencies, $H_{0,\text{seas}} = \cap_{k=1}^{2} H_{0,k}$. The $S^{\mathtt{D}}_{\mathcal{M},12}$ test and the feasible point optimal $P_{12,T}$ test outperform the other tests regardless of whether de-meaning or de-trending is considered. For the de-meaned case, the $\mathcal{MSB}^{\mathtt{D}}_{12}$ test outperforms both the F_{12} and $F^{\mathtt{D}}_{\mathcal{M},12}$ tests, but for the de-trended case these three tests all perform quite similarly. Qualitatively similar patterns are observed in Figures 2(c) and 2(d) for the corresponding tests of the overall null hypothesis, $H_0 = \cap_{k=0}^{2} H_{0,k}$.

5 Finite Sample Results

We next investigate the finite sample size and (local) power properties of the new seasonal $\mathcal{M}$-type unit root tests of section 3, comparing them with the augmented HEGY tests of section 2.3 and the feasible point optimal tests of Rodrigues and Taylor (2007). Our simulations are based on the following quarterly ($S = 4$) DGP:

$$\left(1 - \left[1 + \frac{c_0}{4N}\right] L\right)\left(1 + \left[1 + \frac{c_2}{4N}\right] L\right)\left(1 + \left[1 + \frac{c_1}{4N}\right]^2 L^2\right) x_{4n+s} = u_{4n+s} \tag{5.1}$$

for $s = -3, ..., 0$, $n = 1, ..., N$ initialised at $x_{-3} = \cdots = x_0 = 0$, and where u_{4n+s} a stationary error whose properties will be detailed below. Results relating to finite sample size, where $c_0 = c_1 = c_2 = 0$, are reported in section 5.1, while finite sample power results, where $c_i < 0$, for some $i \in \{0, 1, 2\}$, are reported in section 5.2. Results are reported for $N = 50$ and $N = 100$.

For the long run variance estimates needed to implement both the new semi-parametric tests proposed in this paper and the corresponding feasible point optimal tests of Rodrigues and Taylor (2007), we explored both sums-of-covariances estimators based on Bartlett and Quadratic Spectral kernels and ASD estimators. Tests based on the latter displayed considerably better finite sample behaviour throughout and so we only report these results. The AR lag order used in constructing the ASD estimates was determined using the seasonal MAIC criterion of del Barrio Castro, Osborn and Taylor (2016) using Schwert's rule, $k_{\max K} := \lfloor K[\frac{4N}{100}]^{1/4} \rfloor$, with K a constant discussed below, to determine the maximum lag length allowed. As in Perron and Qu

(2007) the MAIC criterion is computed based on OLS de-trended data. Results are reported for both Case 1 (zero and seasonal frequency intercepts) and Case 3 (zero and seasonal frequency intercepts and trends). All reported results are based on local GLS de-trending.

5.1 Empirical Size

In order to explore the impact of near cancellation regions on the finite sample size, Tables 3-5 report results for the case where u_{4n+s} in (5.1) follows the MA(q) process $u_{4n+s} = \varepsilon_{4n+s} - \theta_q \varepsilon_{4n+s-q}$, with $\varepsilon_{4n+s} \sim NIID(0,1)$, for $s = -3, ..., 0$, $n = 1, ..., N$, initialised at $\varepsilon_j = 0$, $j \leq 0$. The MA order and range of values of the MA parameter which generate a near cancellation region vary according to the frequency of interest. For the zero frequency we consider $q = 1$ and $\theta_1 \in \{0, 0.2, 0.4, 0.6, 0.8, 0.9\}$. For the Nyquist frequency we consider $q = 1$ and $\theta_1 \in \{0, -0.2, -0.4, -0.6, -0.8, -0.9\}$. For the harmonic frequency, we consider $q = 2$ and $\theta_2 \in \{0, -0.04, -0.16, -0.36, -0.64, -0.81\}$. Notice that the moduli of the resulting MA roots is the same in each design. Given the values of θ_q considered, we set $K = 12$ in the formula for $k_{\max K}$ to allow for a reasonably long lag length in the AR approximation.

Consider first the results in Table 3 for zero frequency tests. Although the standard HEGY t_0 test displays reasonably good size control both when $\theta_1 = 0$ and when θ_1 is small, its empirical size rises significantly above the nominal level as θ_1 increases. This occurs in both Cases 1 and 3, with the distortions slightly lower in general under Case 3. Although ameliorated as N increases, the empirical size of t_0 remains uncomfortably large, even for $N = 100$, for large values of θ_1. To illustrate, under Case 1 and $\theta_1 = 0.9$ the empirical size of t_0 is almost 23% for $N = 50$ reducing only to 18% for $N = 100$. Consistent with findings for the non-seasonal case in Ng and Perron (2001), the trinity of zero frequency $\mathcal{M}$-type tests all display significantly better size control than the HEGY t_0 test, and show more pronounced improvements in relative size control than the HEGY tests as the sample size increases. In the example above, the three $\mathcal{M}$ tests all display empirical size of around 8% for $N = 50$, with no over-sizing seen for $N = 100$; indeed, again consistent with the simulation results in Ng and Perron (2001), the tests are all slightly under-sized in the latter case. As with the t_0 test, distortions tend to be lower under Case 3 (with the exception of the case where $\theta_1 = 0.9$ and $N = 50$); here the three $\mathcal{M}$ tests for $\theta_1 = 0.9$ are again slightly under-sized when $N = 100$ (compared to 17% size for t_0). The feasible point optimal $P_{0,T}$ test of Rodrigues and Taylor (2007) behaves very similarly to the three $\mathcal{M}$ tests. Similar observations can be made about the joint frequency tests in Table 1. The lowest size distortions are again displayed by the $\mathcal{M}$ tests from section 3 and the corresponding feasible point optimal test, $P_{012,T}$, from Rodrigues and Taylor (2007), although the latter is consistently undersized, especially so under Case 3. In particular, the $F^{\mathsf{D}}_{\mathcal{M},012}$ test displays consistently better size control than the HEGY F_{012} test.

Turning to the results for the Nyquist frequency in Tables 4a (Case 1) and 4b (Case 3), very similar patterns of size distortions are seen here as were observed in Table 3 as might be expected, given that an equivalent near cancellation effect is obtained here for a given value of θ_1 as for the zero frequency results. In addition to the joint tests considered in Table 3, Tables 4a and 4b also report the joint tests for testing the null hypothesis of unit roots at

all of the seasonal frequencies, $H_{0,\text{seas}}$. Again the same relative behaviour is seen between the HEGY-type and $\mathcal{M}$-type tests as is observed for the other tests.

Finally, we turn to the results for the seasonal harmonic frequency in Tables 5a and 5b. Consider first the results for Case 1 in Table 5a. As with the results for the HEGY tests in Tables 3 and 4a-4b, the harmonic frequency HEGY F_1 test displays good size control for small values of θ_2 but is again rather over-sized for the larger values of θ_2 considered. For example, for $\theta_2 = 0.81$ and $N = 50$ the F_1 test has size of about 12% falling to about 8% for $N = 100$. The best size control is offered by the $F^{\mathtt{D}}_{\mathcal{M},1}$ test which displays excellent size control for all values of θ_2 considered for both $N = 50$ and $N = 100$. In the example above $F^{\mathtt{D}}_{\mathcal{M},1}$ has empirical size of about 5% for $N = 50$ and 3% for $N = 100$. The single root demodulated tests $\mathcal{R}e$-$\mathcal{MZ}_1$, $\mathcal{I}m$-$\mathcal{MZ}_1$, $\mathcal{R}e$-$\mathcal{MZ}_{t_1}$, $\mathcal{I}m$-$\mathcal{MZ}_{t_1}$, $\mathcal{R}e$-$\mathcal{MSB}_1$ and $\mathcal{I}m$-$\mathcal{MSB}_1$, perform similarly to one another but do not control size as well as $F^{\mathtt{D}}_{\mathcal{M},1}$, displaying significant under-sizing when $\theta_2 = 0.81$, and some over-sizing for $\theta_2 = 0.16$ when $N = 50$. The $\mathcal{MSB}^{\mathtt{D}}_1$ and $P_{1,T}$ test of Rodrigues and Taylor (2007) behave similarly to one another, displaying slightly poorer size control than the HEGY F_1 test. As regards the joint frequency tests, here the feasible point optimal tests of Rodrigues and Taylor (2007) appear to offer the best size control overall. The joint frequency $\mathcal{M}$-type tests perform similarly to the corresponding joint frequency HEGY tests, F_{12} and F_{012}.

The results in Table 5b for Case 3 show a similar ordering of the tests as for Case 1 but with an overall deterioration seen in the finite sample size control of most of the tests. Again the best size control is shown by the $F^{\mathtt{D}}_{\mathcal{M},1}$ test, which displays fairly similar size control overall to the single root demodulated tests. These tests again display considerably better size control in the near cancellation region than the HEGY F_1 test. To illustrate when $\theta_2 = 0.81$, the HEGY F_1 test has empirical size of about 25% for $N = 50$ and 16% for $N = 100$, while the empirical sizes of $F^{\mathtt{D}}_{\mathcal{M},1}$ in these cases are about 4% and 3%, respectively, and those of the $P_{1,T}$ test are about 20% and 7%, respectively. In the case of the joint frequency tests, the joint frequency $\mathcal{M}$-type tests display arguably the best overall size control, now notably better than the corresponding joint frequency HEGY tests. The feasible point optimal tests of Rodrigues and Taylor (2007) also avoid any over-sizing but display a stronger tendency to under-sizing than the $\mathcal{M}$ tests.

5.2 Empirical Power

Figures 3–6 graph the finite sample size adjusted power functions of the tests[5] for the case where the data are generated according to (5.1) with $u_{4n+s} \sim NIID(0,1)$, with K commensurately set to zero in the formula for $k_{\max K}$. And as in Rodrigues and Taylor (2007) the power results pertain to the case where, when moving a particular non-centrality parameter c_k, $k = 0, 1, 2$ away from unity, the remaining non-centrality parameters are all held at zero. The index, c, on the horizontal axes of the graphs has the same meaning as described above for Figures 1 and 2.

From Figure 3 we observe that the zero frequency tests display very similar power, particularly under local GLS de-trending (Case 3) where, even for $N = 50$, the power functions of the various tests are almost indistinguishable. In the case of local GLS de-meaning (Case 1)

[5]Results are not reported here for the corresponding Nyquist frequency unit root tests because they were almost identical to the corresponding zero frequency tests reported in Figure 3.

and for the smaller sample size, $N = 50$, and as we move further into the stationarity region (i.e., as c becomes more negative) we note that the point optimal test, PT_0, loses some power relative to the other tests, but overall finite sample power remains very similar across the tests.

Turning to the results for the harmonic frequency unit root tests reported in Figure 4 we see that, in line with the corresponding asymptotic local power results reported in Figure 1, there is rather more variation across the finite sample power properties of the various tests, relative to the results for the zero frequency tests in Figure 3. Again consistent with the corresponding asymptotic local power results in Figures 1(c) and 1(d), we see in Figure 4 that the demodulated single unit root test $\mathcal{R}e\text{-}\mathcal{MZ}_{t_1}$ (again we only report one of these demodulated single unit root tests because they display virtually identical power properties) displays considerably lower power than the other harmonic frequency unit root tests. As for the remaining tests, under Case 1 the best performing tests are PT_1, $\mathcal{MSB}_1^D$ and $\mathcal{S}_{M,1}^D$, all outperforming the F_1 and $F_{M,1}^D$ tests, which perform very similarly, on power. These rankings hold for both $N = 50$ and $N = 100$; indeed, the local power properties of a given test alter little between the two sample sizes, suggesting again that the asymptotic local power functions provide good predictors for the finite sample powers of the tests. Under Case 3, roughly the same power ordering as was observed for Case 1 is seen, although again as predicted by the asymptotic local power functions, the power differentials between the tests are decreased relative to those seen under Case 1.

We turn now to the joint frequency tests. Consider first the joint seasonal unit root tests graphed in Figure 5. For both sample sizes and under both Cases 1 and 3 we see that the differences across the various power functions are relatively small. In terms of relative performance, under Case 1, for both sample sizes the highest power is delivered by PT_{12}, closely followed by $\mathcal{S}_{M,12}^D$ and $\mathcal{MSB}_{12}^D$, with the lowest power displayed by F_{12} and $F_{M,12}^D$, the latter two displaying almost identical power. Under Case 3, we again see that the best performing tests on power are PT_{12} and $\mathcal{S}_{M,12}^D$, while the power performances of F_{12} and $F_{M,12}^D$ are now as good and sometimes superior to that of $\mathcal{MSB}_{12}^D$. Next in Figure 6 we display finite sample power graphs for the tests of the null hypothesis of a unit root at all of the zero and seasonal frequencies. The conclusions from these graphs are qualitatively similar to those remarked on above for the joint seasonal frequency unit root tests. The only exception is for local GLS de-trending, where it is observed that F_{012}, $F_{M,012}^D$ and $\mathcal{MSB}_{012}^D$ display almost identical finite sample power.

For completeness, Figures S.1–S.4 in the Supplementary Appendix report the corresponding size *unadjusted* power results for tests based on the relevant asymptotic critical values. They highlight a degree of over-sizing seen in some of the tests, particularly the augmented HEGY tests, making meaningful power comparisons between the tests somewhat difficult when not using size adjusted power. Interestingly, the point optimal tests of Rodrigues and Taylor (2007), which were already seen in section 5.1 to show a tendency to undersize, are correspondingly seen to lack power in cases where they are under-sized relative to the other tests when comparisons are made on the basis of size unadjusted power. This would seem to further strengthen the case for the use of the $\mathcal{M}$-type tests in that they simultaneously control size well, in general, and yet avoid the low power that can be seen with the point optimal tests in small samples.

6 Conclusions

We have generalised the so-called $\mathcal{M}$ class of semi-parametric unit root tests to allow for unit root testing at the zero and seasonal frequencies in seasonally observed data. For tests involving the seasonal harmonic frequencies this was shown to necessitate the use of demodulated data. In the non-seasonal case the $\mathcal{M}$ unit root tests, combined with an autoregressive spectral density-based estimator of the long run variance, are known to considerably improve on the finite sample size control of augmented Dickey-Fuller tests in the most problematic (near-cancellation) case where the driving shocks contain a strong negative moving average component. Using Monte Carlo simulation methods we have shown that this result carries over to the seasonal case with the $\mathcal{M}$-type seasonal unit root tests we develop here displaying significantly better finite sample size control than the corresponding parametric HEGY seasonal unit root tests in near cancellation regions. As in the non-seasonal case, these improvements in finite sample size were shown not to come at the expense of any loss in power relative to the HEGY tests. Moreover, certain of the $\mathcal{M}$-type seasonal unit root tests were shown to achieve similar or better finite-sample power properties than the feasible point optimal tests of Rodrigues and Taylor (2007).

Overall, based on both the finite sample size and local power properties of the tests considered, we recommend the use of either one of the trinity of $\mathcal{M}$-type tests or the feasible point optimal test of Rodrigues and Taylor (2007), when testing for a unit root at either the zero or Nyquist frequencies. For testing for a complex pair of unit roots at one of the seasonal harmonic frequencies, we recommend the test based on $F_{M,1}^{D}$ of (3.19), because among the tests considered it was the only one which delivered reliable size control. In each case we recommend basing these test statistics on an autoregressive spectral density (seasonal) long run variance estimator using del Barrio Castro, Osborn and Taylor's (2016) seasonal implementation of the MAIC lag selection criterion of Ng and Perron (2001).

References

del Barrio Castro, T., D. R. Osborn and A.M.R. Taylor, 2016, The performance of lag selection and detrending methods for HEGY seasonal unit root tests, Econometric Reviews 35, 122–168.

del Barrio Castro, T., P.M.M. Rodrigues and A.M.R. Taylor, 2015, Semi-parametric seasonal unit root tests, Essex Finance Centre Working Paper Series number 16807, downloadable from `http://repository.essex.ac.uk/16807/`.

Berk, K.N., 1974, Consistent autoregressive spectral estimates, The Annals of Statistics 2, 389-502.

Bhargava, A., 1986, On the theory of testing for unit roots in observed time series, Review of Economic Studies 53, 369-384.

Box, G.E.P., and G.M. Jenkins, 1976, Time Series Analysis: Forecasting and Control (revised edition). San Francisco: Holden-Day.

Breitung, J. and P.H. Franses, 1998, On Phillips-Perron type tests for seasonal unit roots, Econometric Theory 14, 200-221.

Elliott, G, T.J. Rothenberg and J.H. Stock, 1996, Efficient tests for an autoregressive unit root, Econometrica 64, 813-836.

Ghysels, E. and D.R. Osborn, 2001, The Econometric Analysis of Seasonal Time Series, CUP: Cambridge.

Granger, C.W.J. and M. Hatanaka, 1964, Spectral Analysis of Economic Time Series. Princeton, NJ: Princeton University Press.

Gregoir, S., 1999, Multivariate time series with various hidden unit roots, Part I: Integral operator algebra and representation theory, Econometric Theory 15, 435-468.

Gregoir, S., 2006, Efficient tests for the presence of a pair of complex conjugate unit roots in real time series, Journal of Econometrics, 130, 45-100.

Haldrup, N. and M. Jansson, 2006, Improving power and size in unit root testing. Palgrave Handbooks of Econometrics: Vol. 1 Econometric Theory, Chapter 7. T. C. Mills and K. Patterson (eds.). Palgrave MacMillan, Basingstoke.

Hylleberg, S., R.F. Engle, C.W.J. Granger and B.S. Yoo, 1990, Seasonal integration and cointegration, Journal of Econometrics 44, 215-238.

Jansson, M., 2002, Consistent covariance matrix estimation for linear processes, Econometric Theory 18, 1449-1459.

Jansson, M. and M.Ø. Nielsen, 2011, Nearly efficient likelihood ratio tests for seasonal unit roots, Journal of Time Series Econometrics Volume 3, Issue 1, Article 5.

Müller, U.K. and G. Elliott, 2003, Tests for unit roots and the initial condition, Econometrica 71, 1269-1286.

Ng, S., and P. Perron, 2001, Lag length selection and the construction of unit root tests with good size and power, Econometrica 69, 1519-1554.

Perron, P. and Z. Qu, 2007, A simple modification to improve the finite sample properties of Ng and Perrons unit root tests, Economics Letters 94, 12–19.

Perron P., and Ng, S., 1996, Useful modifications to some unit root tests with dependent errors and their local asymptotic properties, Review of Economic Studies 63, 435–463.

Perron P., and Ng, S., 1998, An autoregressive spectral density estimator at frequency zero for nonstationarity tests, Econometric Theory 14, 560–603.

Phillips, P.C.B. and P. Perron, 1988, Testing for a unit root in time series regression, Biometrika 75, 335-346.

Rodrigues, P.M.M., and A.M.R. Taylor, 2007, Efficient tests of the seasonal unit root hypothesis, Journal of Econometrics 141, 548-573.

Smith R.J., Taylor, A.M.R., and T. del Barrio Castro, 2009, Regression-based seasonal unit root tests, Econometric Theory 25, 527-560.

Stock, J.H., 1999, A class of tests for integration and cointegration. Engle, R.F. and White, H. (eds.), Cointegration, Causality and Forecasting. A Festschrift in Honour of Clive W.J. Granger, Oxford: Oxford University Press, 137-167.

Table 1: Asymptotic critical values for the $\mathcal{MSB}^{\mathtt{D}}$-type and $S^{\mathtt{D}}_{\mathcal{M}}$-type tests

	Case 1				**Case 2**				**Case 3**			
	0.010	0.025	0.050	0.100	0.010	0.025	0.050	0.100	0.010	0.025	0.050	0.100
OLS de-trended												
$\mathcal{MSB}^{\mathtt{D}}_{1}$	0.140	0.153	0.166	0.182	0.140	0.153	0.166	0.182	0.111	0.118	0.125	0.134
$\mathcal{MSB}^{\mathtt{D}}_{12}$	0.259	0.280	0.301	0.327	0.259	0.280	0.301	0.327	0.200	0.212	0.223	0.237
$\mathcal{MSB}^{\mathtt{D}}_{012}$	0.363	0.390	0.416	0.449	0.333	0.355	0.376	0.402	0.274	0.289	0.302	0.319
$\mathcal{S}^{\mathtt{D}}_{\mathcal{M}.1}$	-5.733	-5.312	-4.953	-4.541	-5.733	-5.312	-4.953	-4.541	-6.825	-6.419	-6.079	-5.691
$\mathcal{S}^{\mathtt{D}}_{\mathcal{M}.12}$	-7.904	-7.377	-6.939	-6.426	-7.904	-7.377	-6.939	-6.426	-9.576	-9.073	-8.653	-8.175
$\mathcal{S}^{\mathtt{D}}_{\mathcal{M}.012}$	-9.944	-9.347	-8.833	-8.250	-10.504	-9.920	-9.436	-8.847	-12.23	-11.636	-11.164	-10.615
Local GLS de-trended												
$\mathcal{MSB}^{\mathtt{D}}_{1}$	0.176	0.197	0.219	0.250	0.176	0.197	0.219	0.250	0.125	0.135	0.144	0.156
$\mathcal{MSB}^{\mathtt{D}}_{12}$	0.330	0.368	0.402	0.451	0.333	0.369	0.405	0.453	0.224	0.239	0.253	0.271
$\mathcal{MSB}^{\mathtt{D}}_{012}$	0.474	0.519	0.565	0.624	0.415	0.453	0.488	0.533	0.308	0.327	0.344	0.366
$\mathcal{S}^{\mathtt{D}}_{\mathcal{M}.1}$	-3.951	-3.506	-3.115	-2.648	-3.951	-3.506	-3.115	-2.648	-5.758	-5.350	-5.025	-4.642
$\mathcal{S}^{\mathtt{D}}_{\mathcal{M}.12}$	-5.197	-4.624	-4.168	-3.596	-5.197	-4.623	-4.167	-3.596	-8.012	-7.512	-7.106	-6.647
$\mathcal{S}^{\mathtt{D}}_{\mathcal{M}.012}$	-6.307	-5.679	-5.137	-4.496	-7.245	-6.648	-6.121	-5.519	-10.136	-9.603	-9.134	-8.614

Notes: Case 1 indicates that the deterministic component used consists of a zero and seasonal frequency intercepts; Case 2 indicates that zero and seasonal frequency intercepts and a zero frequency trend were used; and Case 3 indicates that zero and seasonal frequency intercepts and trends were used.

Table 2: Asymptotic critical values for the $F^{\mathtt{D}}_{\mathcal{M}}$-type tests

	Case 1				**Case 2**				**Case 3**			
	0.900	0.950	0.975	0.990	0.900	0.950	0.975	0.990	0.900	0.950	0.975	0.990
OLS de-trended												
$F^{\mathtt{D}}_{\mathcal{M}.1}$	5.540	6.555	7.496	8.648	5.540	6.555	7.496	8.648	8.420	9.615	10.667	12.028
$F^{\mathtt{D}}_{\mathcal{M}.12}$	5.087	5.867	6.592	7.498	2.333	2.869	3.384	4.064	7.847	8.778	9.607	10.682
$F^{\mathtt{D}}_{\mathcal{M}.012}$	6.403	7.278	8.083	9.063	7.338	8.261	9.081	10.069	10.010	11.039	11.967	13.182
Local GLS de-trended												
$F^{\mathtt{D}}_{\mathcal{M}.1}$	2.555	3.259	3.961	4.880	2.555	3.259	3.961	4.880	5.731	6.695	7.565	8.765
$F^{\mathtt{D}}_{\mathcal{M}.12}$	2.352	2.880	3.414	4.052	2.333	2.869	3.384	4.064	5.343	6.089	6.782	7.648
$F^{\mathtt{D}}_{\mathcal{M}.012}$	2.208	2.647	3.073	3.616	3.956	4.620	5.249	6.035	5.099	5.723	6.318	7.016

Note: See notes to Table 1

Table 3: Empirical size of zero frequency unit root tests. MAIC lag selection.

DGP (5.1) with $c = 0$ and $u_{4n+s} = \varepsilon_{4n+s} - \theta_1 \varepsilon_{4n+s-1}$.

Case 1: Local GLS de-trended data

N	θ_1	t_0	$\mathcal{MZ}_0$	$\mathcal{MZ}_{t_0}$	$\mathcal{MSB}_0$	$P_{0.T}$	F_{012}	$F^{\mathrm{D}}_{\mathcal{M}.012}$	$\mathcal{MSB}^{\mathrm{D}}_{012}$	$P_{012.T}$	$S^{\mathrm{D}}_{\mathcal{M}.012}$
50	0.0	0.068	0.079	0.083	0.077	0.067	0.065	0.064	0.117	0.042	0.115
	0.2	0.073	0.094	0.098	0.087	0.079	0.068	0.064	0.119	0.046	0.111
	0.4	0.086	0.105	0.111	0.100	0.091	0.075	0.069	0.123	0.046	0.108
	0.6	0.102	0.108	0.115	0.100	0.096	0.076	0.073	0.131	0.051	0.116
	0.8	0.133	0.062	0.069	0.053	0.064	0.086	0.068	0.099	0.043	0.105
	0.9	0.227	0.081	0.086	0.074	0.082	0.151	0.102	0.061	0.027	0.110
100	0.0	0.063	0.066	0.069	0.064	0.061	0.060	0.052	0.073	0.034	0.072
	0.2	0.064	0.073	0.073	0.073	0.065	0.056	0.054	0.079	0.032	0.069
	0.4	0.070	0.079	0.079	0.077	0.074	0.057	0.057	0.077	0.036	0.072
	0.6	0.079	0.078	0.080	0.077	0.072	0.060	0.060	0.076	0.033	0.075
	0.8	0.103	0.046	0.050	0.040	0.050	0.070	0.050	0.071	0.032	0.069
	0.9	0.182	0.028	0.031	0.025	0.032	0.109	0.056	0.048	0.024	0.066

Case 3: Local GLS de-trended data

N	θ_1	t_0	$\mathcal{MZ}_0$	$\mathcal{MZ}_{t_0}$	$\mathcal{MSB}_0$	$P_{0.T}$	F_{012}	$F^{\mathrm{D}}_{\mathcal{M}.012}$	$\mathcal{MSB}^{\mathrm{D}}_{012}$	$P_{012.T}$	$S^{\mathrm{D}}_{\mathcal{M}.012}$
50	0.0	0.045	0.042	0.045	0.049	0.040	0.067	0.026	0.039	0.019	0.033
	0.2	0.053	0.059	0.065	0.067	0.057	0.069	0.028	0.038	0.019	0.033
	0.4	0.063	0.079	0.084	0.088	0.076	0.069	0.025	0.033	0.015	0.027
	0.6	0.079	0.080	0.084	0.089	0.074	0.092	0.034	0.031	0.017	0.037
	0.8	0.117	0.063	0.067	0.071	0.059	0.121	0.042	0.015	0.010	0.035
	0.9	0.232	0.137	0.140	0.145	0.133	0.205	0.101	0.006	0.003	0.062
100	0.0	0.042	0.040	0.041	0.041	0.046	0.057	0.032	0.042	0.021	0.036
	0.2	0.045	0.051	0.052	0.051	0.056	0.056	0.031	0.043	0.021	0.036
	0.4	0.060	0.065	0.067	0.063	0.072	0.061	0.034	0.043	0.020	0.038
	0.6	0.065	0.056	0.059	0.057	0.065	0.067	0.042	0.051	0.026	0.048
	0.8	0.082	0.020	0.022	0.019	0.027	0.077	0.034	0.023	0.013	0.033
	0.9	0.165	0.023	0.025	0.022	0.029	0.127	0.041	0.007	0.005	0.033

Notes: Case 1 indicates that the deterministic component used consists of zero and seasonal frequency intercepts; Case 3 indicates that zero and seasonal frequency intercepts and trends were used.

Table 4: Empirical size of Nyquist frequency unit root tests. MAIC lag selection.

DGP (5.1) with $c = 0$ and $u_{4n+s} = \varepsilon_{4n+s} + \theta_1 \varepsilon_{4n+s-1}$.

Local GLS de-trended data; Case 1 (zero and seasonal frequency intercepts)

N	θ_1	t_2	$\mathcal{MZ}_2$	$\mathcal{MZ}_{t_2}$	$\mathcal{MSB}_2$	$P_{2.T}$	$P_{12.T}$	$P_{012.T}$	F_{12}	F_{012}	$F^{D}_{\mathcal{M}.12}$	$F^{D}_{\mathcal{M}.012}$	$\mathcal{MSB}^{D}_{12}$	$\mathcal{MSB}^{D}_{012}$	$S^{D}_{\mathcal{M}.12}$	$S^{D}_{\mathcal{M}.012}$
50	0.0	0.067	0.081	0.085	0.075	0.067	0.041	0.051	0.068	0.073	0.063	0.070	0.092	0.121	0.060	0.118
	0.2	0.075	0.097	0.103	0.092	0.080	0.043	0.047	0.065	0.070	0.057	0.065	0.093	0.116	0.056	0.106
	0.4	0.082	0.105	0.108	0.101	0.089	0.042	0.048	0.063	0.072	0.060	0.070	0.096	0.123	0.058	0.110
	0.6	0.100	0.103	0.111	0.097	0.092	0.050	0.051	0.070	0.077	0.067	0.076	0.108	0.129	0.067	0.117
	0.8	0.131	0.063	0.068	0.055	0.062	0.044	0.046	0.092	0.094	0.066	0.076	0.079	0.096	0.067	0.115
	0.9	0.216	0.078	0.080	0.072	0.079	0.036	0.028	0.153	0.151	0.086	0.097	0.060	0.055	0.071	0.108
100	0.0	0.062	0.070	0.069	0.068	0.063	0.030	0.032	0.056	0.056	0.056	0.054	0.063	0.073	0.040	0.068
	0.2	0.065	0.074	0.076	0.073	0.068	0.035	0.030	0.055	0.055	0.050	0.055	0.069	0.077	0.043	0.072
	0.4	0.072	0.081	0.082	0.079	0.073	0.036	0.035	0.060	0.061	0.059	0.056	0.075	0.079	0.045	0.071
	0.6	0.073	0.071	0.076	0.070	0.072	0.035	0.035	0.055	0.055	0.055	0.057	0.072	0.077	0.047	0.075
	0.8	0.098	0.043	0.046	0.037	0.045	0.031	0.034	0.067	0.065	0.048	0.052	0.060	0.070	0.042	0.071
	0.9	0.173	0.027	0.030	0.024	0.032	0.024	0.022	0.111	0.097	0.052	0.058	0.035	0.041	0.042	0.065

Local GLS de-trended data; Case 3 (zero and seasonal frequency intercepts and trends)

N	θ_1	t_2	$\mathcal{MZ}_2$	$\mathcal{MZ}_{\pi_2}$	$\mathcal{MSB}_2$	$P_{2.T}$	$P_{12.T}$	$P_{012.T}$	F_{12}	F_{012}	$F^{D}_{\mathcal{M}.12}$	$F^{D}_{\mathcal{M}.012}$	$\mathcal{MSB}^{D}_{12}$	$\mathcal{MSB}^{D}_{012}$	$S^{D}_{\mathcal{M}.12}$	$S^{D}_{\mathcal{M}.012}$
50	0.0	0.043	0.035	0.040	0.034	0.041	0.023	0.019	0.062	0.069	0.031	0.027	0.038	0.035	0.037	0.033
	0.2	0.054	0.063	0.067	0.058	0.067	0.027	0.018	0.062	0.070	0.037	0.026	0.048	0.036	0.039	0.030
	0.4	0.068	0.084	0.088	0.081	0.090	0.033	0.018	0.061	0.072	0.042	0.029	0.056	0.037	0.044	0.031
	0.6	0.076	0.076	0.082	0.071	0.088	0.041	0.017	0.082	0.090	0.049	0.031	0.062	0.032	0.054	0.033
	0.8	0.121	0.068	0.072	0.064	0.077	0.035	0.011	0.112	0.122	0.066	0.046	0.048	0.015	0.063	0.038
	0.9	0.228	0.133	0.136	0.130	0.142	0.030	0.004	0.202	0.207	0.124	0.098	0.055	0.007	0.101	0.058
100	0.0	0.049	0.047	0.048	0.047	0.052	0.020	0.023	0.054	0.060	0.039	0.037	0.039	0.044	0.041	0.041
	0.2	0.051	0.057	0.058	0.056	0.062	0.025	0.021	0.054	0.058	0.038	0.035	0.049	0.044	0.041	0.039
	0.4	0.059	0.067	0.069	0.066	0.073	0.028	0.021	0.052	0.055	0.044	0.035	0.054	0.041	0.048	0.039
	0.6	0.065	0.059	0.061	0.058	0.065	0.034	0.022	0.065	0.062	0.055	0.041	0.059	0.044	0.058	0.044
	0.8	0.081	0.018	0.019	0.017	0.025	0.018	0.013	0.071	0.073	0.039	0.033	0.025	0.023	0.043	0.033
	0.9	0.166	0.025	0.026	0.023	0.029	0.013	0.004	0.130	0.125	0.052	0.042	0.017	0.006	0.046	0.031

Table 5a: Empirical size of harmonic frequency unit root tests. MAIC lag selection. Order selection based on MAIC.

DGP (5.1) with $c = 0$ and $u_{4n+s} = \varepsilon_{4n+s} + \theta_2 \varepsilon_{4n+s-2}$. Local GLS de-trended data; Case 1 (zero and seasonal frequency intercepts).

N	θ_2	F_1	F_{12}	F_{012}	$F^{\mathtt{D}}_{\mathcal{M}.1}$	$F^{\mathtt{D}}_{\mathcal{M}.12}$	$F^{\mathtt{D}}_{\mathcal{M}.012}$	$\mathcal{MSB}^{\mathtt{D}}_{1}$	$\mathcal{MSB}^{\mathtt{D}}_{12}$	$\mathcal{MSB}^{\mathtt{D}}_{012}$	$P_{1.T}$	$P_{12.T}$	$P_{012.T}$
50	0.00	0.055	0.065	0.071	0.048	0.058	0.061	0.075	0.096	0.115	0.067	0.040	0.047
	0.04	0.053	0.057	0.063	0.054	0.060	0.059	0.080	0.092	0.112	0.072	0.043	0.043
	0.16	0.052	0.054	0.054	0.064	0.067	0.066	0.104	0.099	0.118	0.093	0.047	0.046
	0.36	0.051	0.061	0.071	0.060	0.080	0.093	0.105	0.124	0.154	0.100	0.061	0.067
	0.64	0.069	0.068	0.067	0.049	0.070	0.086	0.123	0.131	0.156	0.127	0.064	0.069
	0.81	0.116	0.119	0.120	0.050	0.094	0.124	0.121	0.135	0.163	0.146	0.080	0.084
100	0.00	0.044	0.050	0.051	0.048	0.049	0.051	0.060	0.062	0.072	0.056	0.031	0.032
	0.04	0.050	0.048	0.050	0.052	0.051	0.051	0.067	0.060	0.068	0.064	0.030	0.031
	0.16	0.046	0.049	0.050	0.049	0.053	0.053	0.069	0.069	0.077	0.064	0.033	0.034
	0.36	0.042	0.047	0.050	0.056	0.063	0.068	0.074	0.072	0.081	0.071	0.038	0.039
	0.64	0.055	0.052	0.053	0.046	0.056	0.062	0.092	0.087	0.094	0.092	0.045	0.046
	0.81	0.082	0.077	0.076	0.025	0.045	0.060	0.081	0.090	0.094	0.100	0.050	0.049

N	θ_2	$S^{\mathtt{D}}_{\mathcal{M}.1}$	$S^{\mathtt{D}}_{\mathcal{M}.12}$	$S^{\mathtt{D}}_{\mathcal{M}.012}$	$\mathcal{R}$e-$\mathcal{MZ}_1$	$\mathcal{R}$e-$\mathcal{MSB}_1$	$\mathcal{R}$e-$\mathcal{MZ}_{t_1}$	$\mathcal{I}$m-$\mathcal{MZ}_1$	$\mathcal{I}$m-$\mathcal{MSB}_1$	$\mathcal{I}$m-$\mathcal{MZ}_{t_1}$
50	0.00	0.062	0.055	0.109	0.052	0.052	0.052	0.055	0.054	0.058
	0.04	0.069	0.063	0.114	0.062	0.062	0.062	0.057	0.057	0.059
	0.16	0.090	0.070	0.122	0.070	0.069	0.070	0.073	0.073	0.075
	0.36	0.090	0.087	0.159	0.065	0.063	0.066	0.064	0.066	0.065
	0.64	0.095	0.091	0.168	0.046	0.043	0.048	0.050	0.052	0.044
	0.81	0.093	0.105	0.196	0.035	0.032	0.038	0.036	0.039	0.031
100	0.00	0.052	0.039	0.064	0.053	0.051	0.052	0.050	0.050	0.051
	0.04	0.060	0.044	0.070	0.055	0.055	0.055	0.053	0.054	0.055
	0.16	0.058	0.047	0.075	0.052	0.052	0.054	0.050	0.049	0.051
	0.36	0.065	0.053	0.084	0.055	0.056	0.056	0.058	0.059	0.058
	0.64	0.073	0.057	0.094	0.050	0.046	0.053	0.049	0.049	0.047
	0.81	0.058	0.052	0.091	0.017	0.014	0.020	0.018	0.021	0.014

Table 5b: Empirical size of harmonic frequency unit root tests. MAIC lag selection. Order selection based on MAIC.

DGP (5.1) with $c = 0$ and $u_{4n+s} = \varepsilon_{4n+s} + \theta_2 \varepsilon_{4n+s-2}$. Local GLS de-trended data; Case 3 (zero and seasonal frequency intercepts and trends).

N	θ_2	F_1	F_{12}	F_{012}	$F^{\mathtt{D}}_{\mathcal{M}.1}$	$F^{\mathtt{D}}_{\mathcal{M}.12}$	$F^{\mathtt{D}}_{\mathcal{M}.012}$	$\mathcal{MSB}^{\mathtt{D}}_{1}$	$\mathcal{MSB}^{\mathtt{D}}_{12}$	$\mathcal{MSB}^{\mathtt{D}}_{012}$	$P_{1.T}$	$P_{12.T}$	$P_{012.T}$
50	0.00	0.048	0.059	0.068	0.028	0.028	0.026	0.033	0.034	0.037	0.044	0.021	0.022
	0.04	0.063	0.068	0.070	0.042	0.035	0.028	0.045	0.036	0.032	0.060	0.021	0.019
	0.16	0.067	0.070	0.069	0.056	0.046	0.037	0.067	0.044	0.032	0.085	0.030	0.020
	0.36	0.070	0.090	0.109	0.059	0.063	0.064	0.081	0.066	0.068	0.101	0.043	0.043
	0.64	0.113	0.122	0.130	0.072	0.072	0.069	0.106	0.061	0.047	0.133	0.044	0.027
	0.81	0.246	0.250	0.259	0.036	0.036	0.036	0.174	0.043	0.030	0.202	0.036	0.018
100	0.00	0.046	0.052	0.057	0.036	0.036	0.036	0.039	0.042	0.044	0.044	0.023	0.022
	0.04	0.052	0.053	0.054	0.043	0.041	0.034	0.052	0.041	0.038	0.054	0.023	0.021
	0.16	0.053	0.060	0.064	0.047	0.049	0.049	0.059	0.056	0.052	0.065	0.031	0.028
	0.36	0.054	0.060	0.063	0.055	0.057	0.057	0.066	0.059	0.060	0.072	0.033	0.033
	0.64	0.079	0.079	0.081	0.041	0.047	0.049	0.062	0.059	0.056	0.076	0.034	0.032
	0.81	0.160	0.146	0.143	0.031	0.044	0.045	0.052	0.040	0.034	0.066	0.023	0.017

N	θ_2	$S^{\mathtt{D}}_{\mathcal{M}.1}$	$S^{\mathtt{D}}_{\mathcal{M}.12}$	$S^{\mathtt{D}}_{\mathcal{M}.012}$	$\mathcal{R}e$-$\mathcal{MZ}_1$	$\mathcal{R}e$-$\mathcal{MSB}_1$	$\mathcal{R}e$-$\mathcal{MZ}_{t_1}$	$\mathcal{I}m$-$\mathcal{MZ}_1$	$\mathcal{I}m$-$\mathcal{MSB}_1$	$\mathcal{I}m$-$\mathcal{MZ}_{t_1}$
50	0.00	0.028	0.032	0.032	0.031	0.030	0.032	0.031	0.031	0.031
	0.04	0.042	0.040	0.033	0.037	0.036	0.037	0.036	0.037	0.036
	0.16	0.059	0.051	0.042	0.044	0.043	0.045	0.045	0.047	0.044
	0.36	0.066	0.072	0.074	0.041	0.039	0.042	0.040	0.042	0.038
	0.64	0.085	0.078	0.070	0.034	0.032	0.035	0.039	0.040	0.037
	0.81	0.036	0.039	0.042	0.035	0.034	0.036	0.037	0.039	0.036
100	0.00	0.036	0.039	0.042	0.035	0.034	0.036	0.037	0.039	0.036
	0.04	0.045	0.044	0.038	0.040	0.039	0.040	0.040	0.039	0.040
	0.16	0.050	0.054	0.053	0.041	0.040	0.042	0.040	0.040	0.039
	0.36	0.060	0.062	0.062	0.047	0.046	0.049	0.046	0.047	0.045
	0.64	0.050	0.053	0.052	0.021	0.019	0.023	0.019	0.020	0.018
	0.81	0.039	0.042	0.038	0.013	0.013	0.014	0.012	0.013	0.012

Figure 1: Gaussian asymptotic local power envelopes and asymptotic local power functions of zero, Nyquist and harmonic frequency local GLS de-trended unit root tests

(a) de-meaned zero ($k = 0$) and Nyquist ($k = S/2$) frequency tests

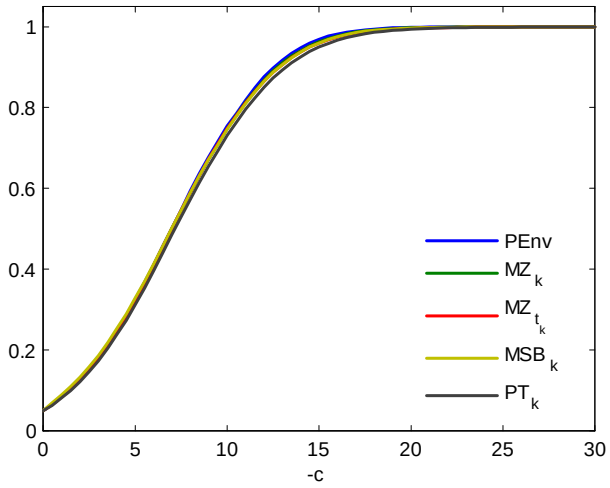

(b) de-trended zero ($k = 0$) and Nyquist ($k = S/2$) frequency tes

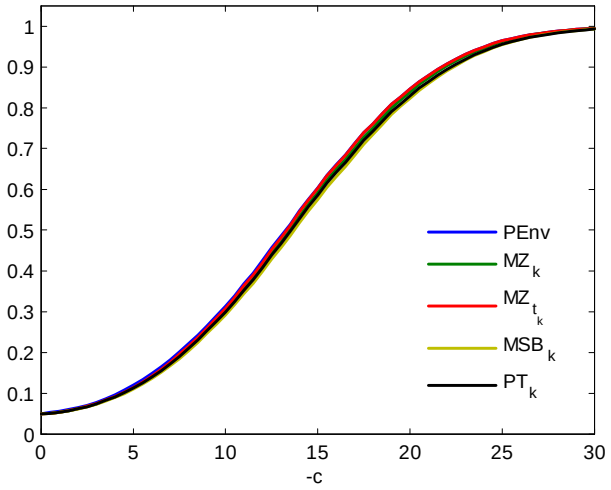

(c) de-meaned harmonic frequency tests ($k \in \{1, ..., S^*\}$)

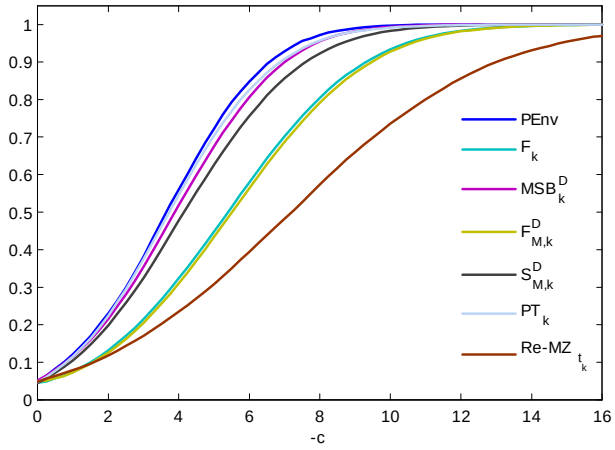

(d) de-trended harmonic frequency tests ($k \in \{1, ..., S^*\}$)

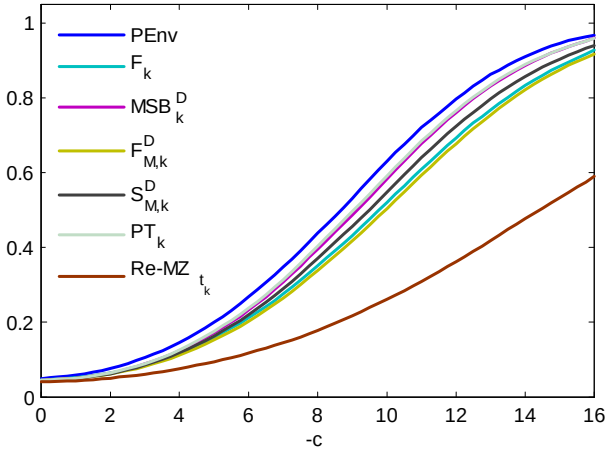

Figure 2: Gaussian asymptotic local power envelopes and asymptotic local power functions of joint frequency local GLS de-trended unit root tests for the quarterly case ($S = 4$)

(a) de-meaned joint seasonal frequency tests

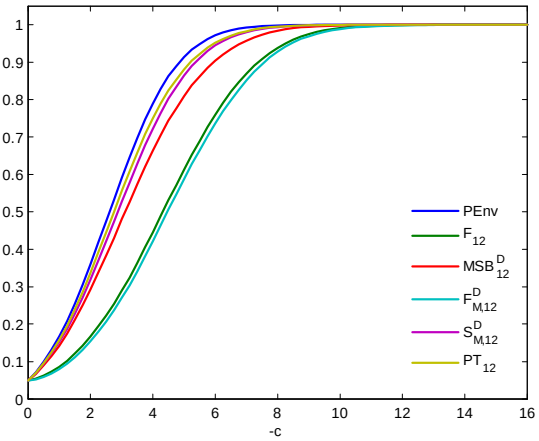

(b) de-trended joint seasonal frequency tests

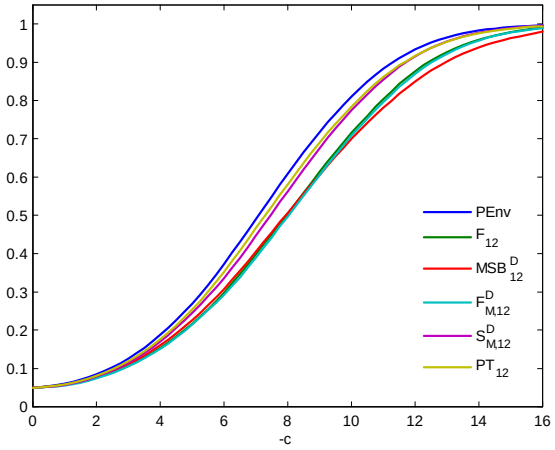

(c) de-meaned joint zero and seasonal frequency tests

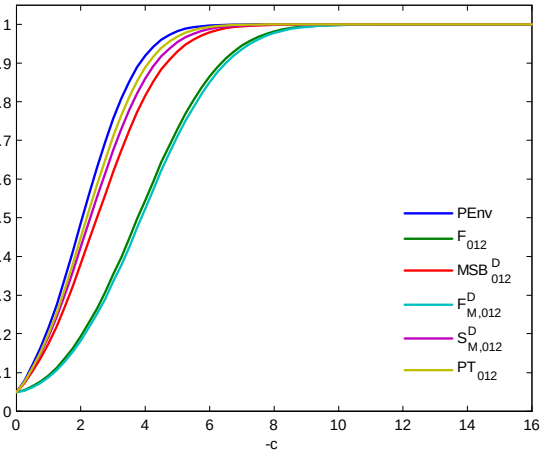

(d) de-trended joint zero and seasonal frequency tests

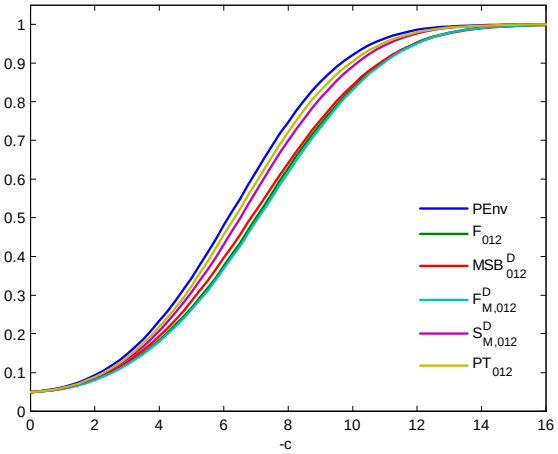

Figure 3: Finite sample size-adjusted power functions of zero frequency unit root tests (quarterly case, $S = 4$)

(a) local GLS de-meaned tests - $N = 50$

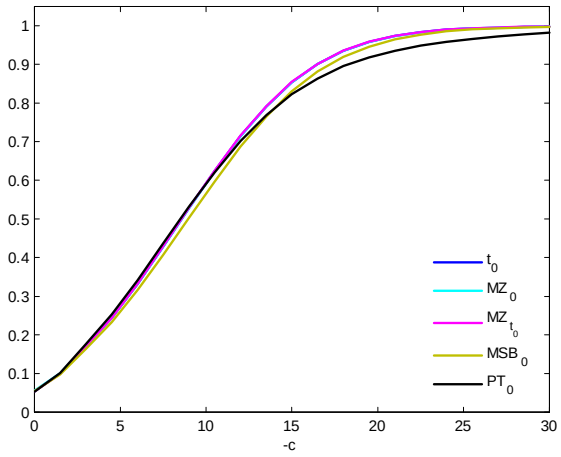

(b) local GLS de-meaned tests - $N = 100$

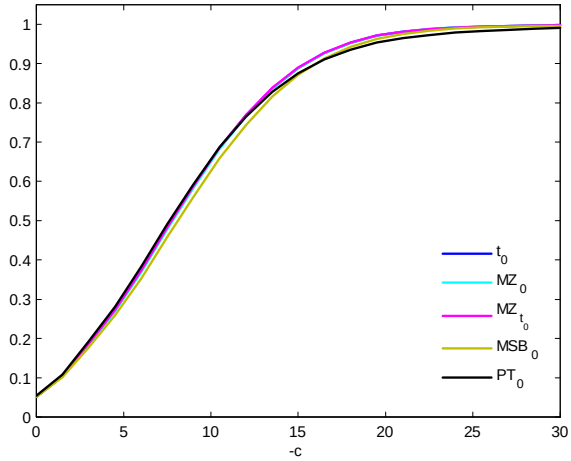

(c) local GLS de-trended tests - $N = 50$

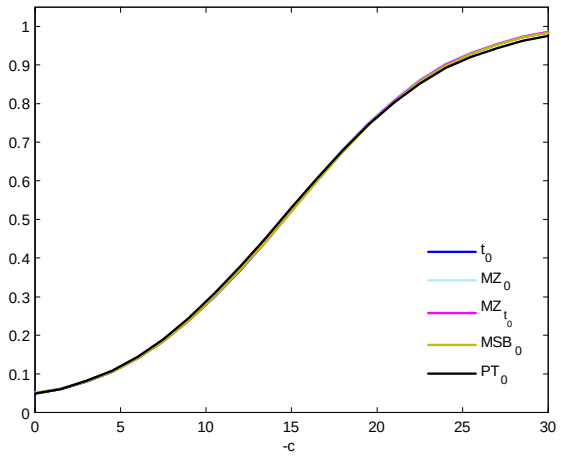

(d) local GLS de-trended tests - $N = 100$

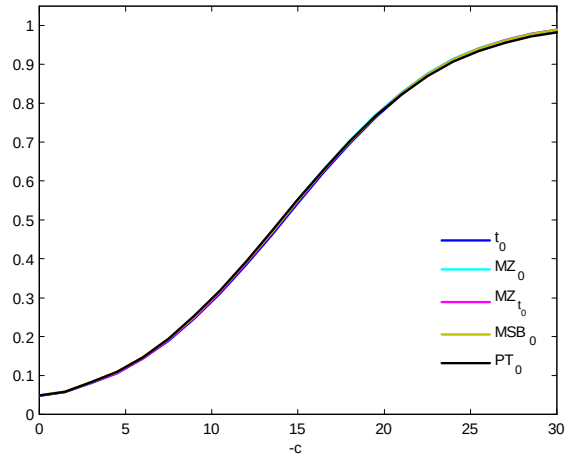

Figure 4: Finite sample size-adjusted power functions of harmonic frequency unit root tests (quarterly case, $S = 4$)

(a) local GLS de-meaned tests - $N = 50$

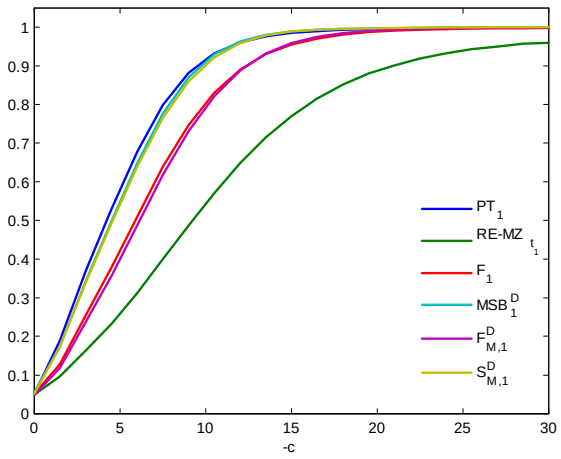

(b) local GLS de-meaned tests - $N = 100$

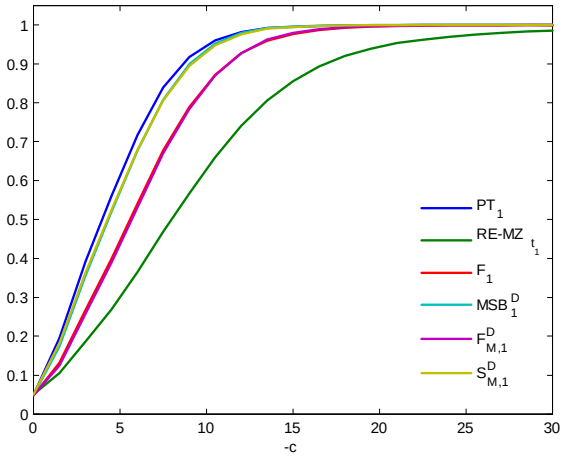

(c) local GLS de-trended tests - $N = 50$

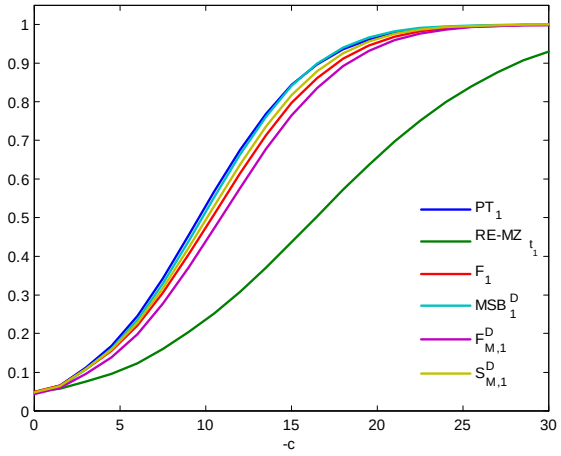

(d) local GLS de-trended tests - $N = 100$

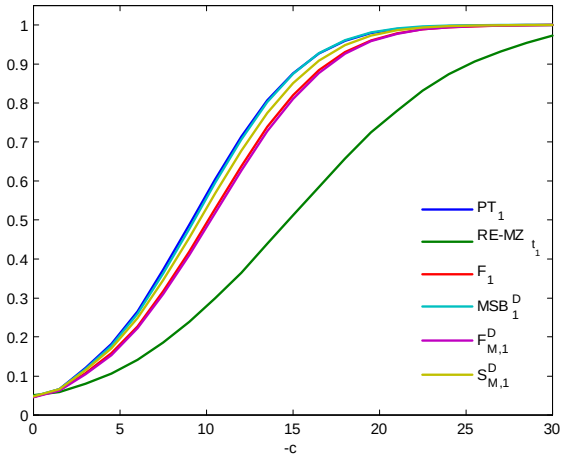

Figure 5: Finite sample size-adjusted power functions of joint seasonal frequency tests (quarterly case, $S = 4$)

(a) local GLS de-meaned tests - $N = 50$

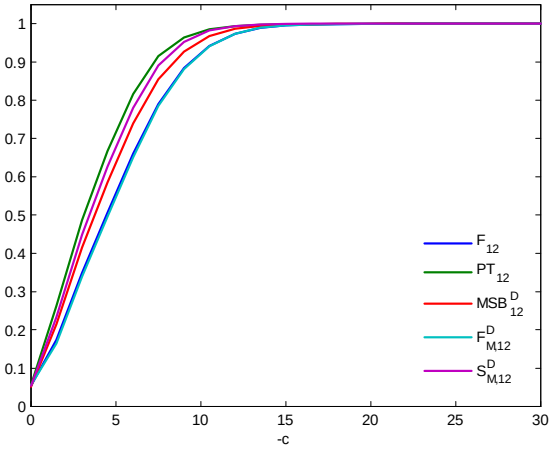

(b) local GLS de-meaned tests - $N = 100$

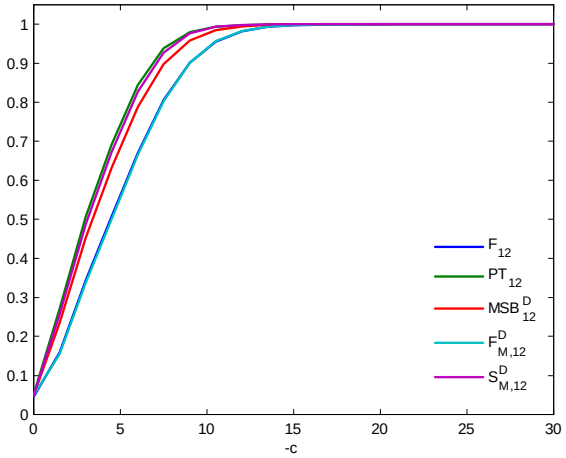

(c) local GLS de-trended tests - $N = 50$

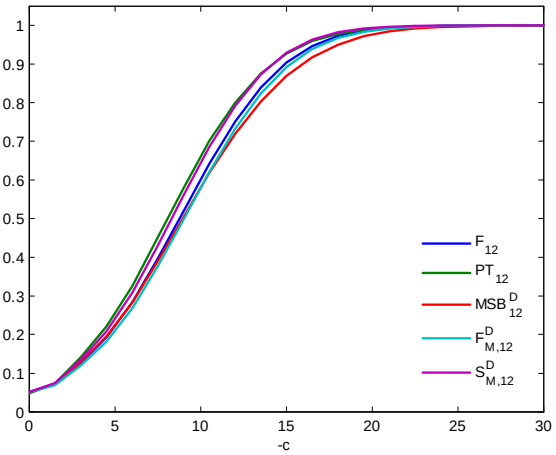

(d) local GLS de-trended tests - $N = 100$

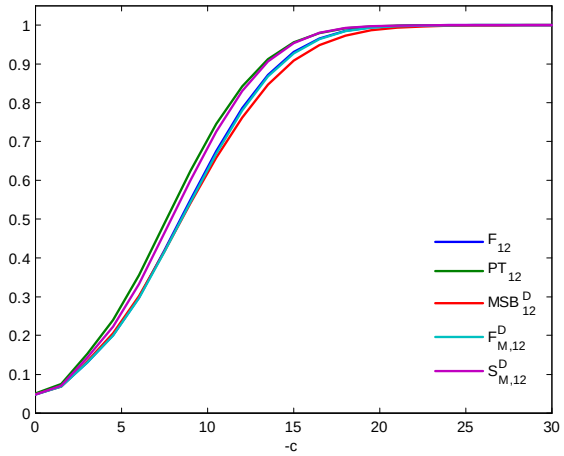

Figure 6: Finite sample size-adjusted power functions of joint zero and seasonal frequency tests (quarterly case, $S = 4$)

(a) local GLS de-meaned tests - $N = 50$

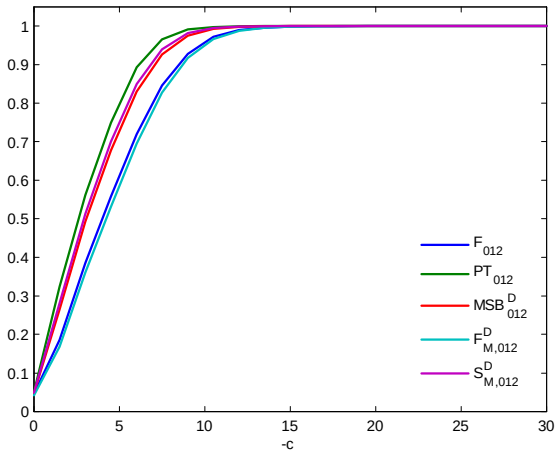

(b) local GLS de-meaned tests - $N = 100$

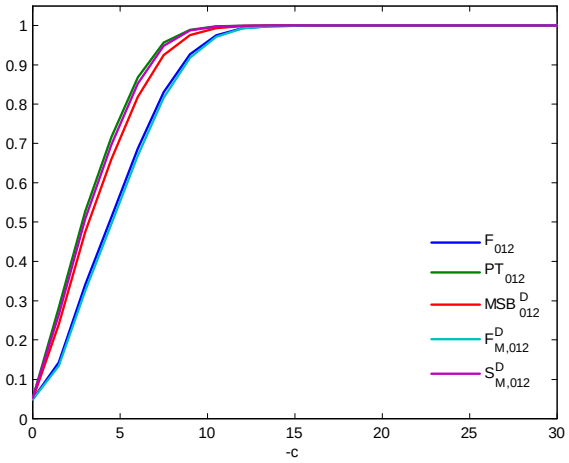

(c) local GLS de-trended tests - $N = 50$

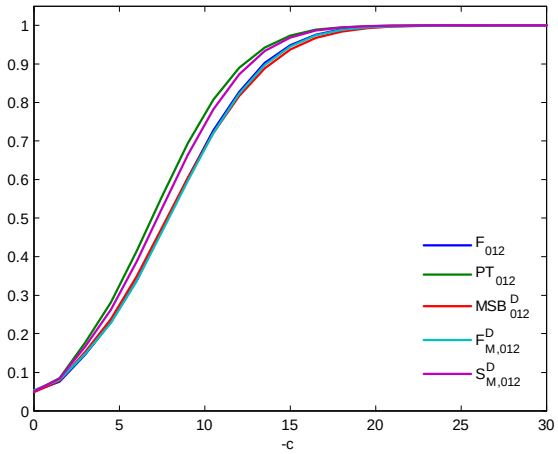

(d) local GLS de-trended tests - $N = 100$

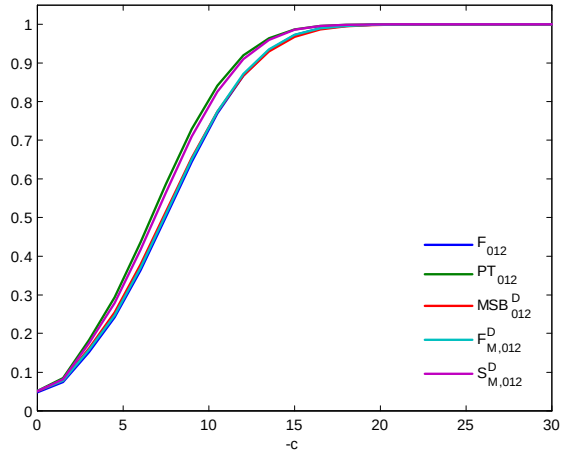

Supplementary Online Appendix

to

Semi-Parametric Seasonal Unit Root Tests

by

T. del Barrio Castro, P.M.M. Rodrigues and A.M.R. Taylor

Date: March 7, 2017

S.1 Introduction

This supplement contains supporting material for our paper "Semi-Parametric Seasonal Unit Root Tests". Equation references (S.n) for $n \geq 1$ refer to equations in this supplement and other equation references are to the main paper.

The supplement is organised as follows. Proofs of the main theoretical results in the paper can be found in section S.2. A more detailed outline of the augmented HEGY seasonal unit root tests are given in section S.3. Section S.4 details the limiting distributions of the lag un-augmented HEGY seasonal unit root tests which obtain from (2.4) with p^* set to zero. These are shown in Theorem S.1 to be non-pivotal depending on any (un-modelled) serial correlation present in u_{Sn+s} of (2.1b). Seasonal implementations of the PP unit root tests are outlined in section S.5 and their limiting distributions are given in Theorem S.2 in section S.6. The proofs of Theorems S.1 and S.2 are provided in section S.7. Additional Monte Carlo results relating to size unadjusted finite sample power results are reported in section S.8. All additional references are included at the end of the supplement.

S.2 Proofs of Main Results

S.2.1 Preliminary Results

Before providing the proofs of the main results given in the paper, a number of preliminary results are needed first. To that end, we first note that under (2.3), x_{Sn+s} in (2.1b) can be written as,

$$\Delta_0^{c_0}\Delta_{S/2}^{c_{S/2}}\prod_{k=1}^{S^*}\Delta_k^{c_k}x_{Sn+s}=u_{Sn+s} \tag{S.1}$$

where $\Delta_0^{c_0}:=1-\alpha_0L=1-\left(1+\frac{c_0}{SN}\right)L$, $\Delta_{S/2}^{c_{S/2}}:=1+\alpha_{S/2}L=1+\left(1+\frac{c_{S/2}}{SN}\right)L$, and $\Delta_k^{c_k}:=1-2\cos\left[\omega_k\right]\alpha_kL+\alpha_k^2L^2=1-2\cos\left[\omega_k\right]\left(1+\frac{c_k}{SN}\right)L+\left(1+\frac{c_k}{SN}\right)^2L^2$, for $k=1,...,S^*$. Consequently, (S.1) can be equivalently written as,

$$x_{Sn+s}=\left[S_{0,c_0}\left(Sn+s\right)\right]\left[S_{S/2,c_{S/2}}\left(Sn+s\right)\right]\left[\prod_{k=1}^{S^*}S_{k,c_k}\left(Sn+s\right)\right]u_{Sn+s} \tag{S.2}$$

where, for $\omega_0=0$ and $\omega_{S/2}=\pi$,

$$S_{i,c_i}\left(Sn+s\right):=\sum_{j=1}^{Sn+s}\cos\left[\left(\left(Sn+s\right)-j\right)\omega_i\right]\alpha_i^{Sn+s-j}L^{Sn+s-j},\ i=0,S/2$$

and, for $\omega_k=(2\pi k)/S, k=1,...,S^*$,

$$\begin{aligned}S_{k,c_k}\left(Sn+s\right) &:= \sin\left[\omega_k\right]^{-1}\sum_{j=0}^{Sn+s-1}\sin\left[\left(\left(Sn+s\right)+1-j\right)\omega_k\right]\alpha_k^{Sn+s-j}L^{Sn+s-j}\\ &= \sin\left[\omega_k\right]^{-1}\left(\sin\left[\left(\left(Sn+s\right)+1\right)\omega_k\right]S_{k,c_k}^{\alpha}\left(Sn+s\right)\right.\\ &\qquad\left.-\cos\left[\left(\left(Sn+s\right)+1\right)\omega_k\right]S_{k,c_k}^{\beta}\left(Sn+s\right)\right)\end{aligned}$$

with

$$S^{\alpha}_{k,c_k}(Sn+s) := \sum_{j=1}^{Sn+s} \cos[j\omega_k]\,\alpha_k^{Sn+s-j} L^{Sn+s-j}$$

$$S^{\beta}_{k,c_k}(Sn+s) := \sum_{j=1}^{Sn+s} \sin[j\omega_k]\,\alpha_k^{Sn+s-j} L^{Sn+s-j}.$$

In view of the foregoing, the identities given in Gregoir (1999, p. 463) can be extended to the terms in (2.3) as follows,

$$\frac{\Delta_0^{c_0}}{2} + \frac{\Delta_{S/2}^{c_{S/2}}}{2} = 1 + \frac{1}{2}\left(\frac{c_{S/2}-c_0}{SN}\right)L = 1 + O(1/N) \tag{S.3}$$

$$\begin{aligned}\frac{\Delta_k^{c_k} + (1-2\cos[\omega_k]+L)\,\Delta_0^{c_0}}{2\kappa_0(\omega_k)} &= 1 - \frac{c_0}{2\kappa_0(\omega_k)SN}L - \frac{2\cos[\omega_k]}{2\kappa_0(\omega_k)}\frac{(c_k-c_0)}{SN}L \\ &\quad + \frac{(2c_k-c_0)}{2\kappa_0(\omega_k)SN}L^2 + \frac{c_k^2}{2\kappa_0(\omega_k)(SN)^2}L^2 \\ &= 1 - O\left(\frac{1}{N}\right) - O\left(\frac{1}{N}\right) + O\left(\frac{1}{N}\right) + O\left(\frac{1}{N^2}\right)\end{aligned} \tag{S.4}$$

$$\begin{aligned}\frac{\Delta_k^{c_k} + (1+2\cos[\omega_k]-L)\,\Delta_{S/2}^{c_{S/2}}}{2\kappa_{S/2}(\omega_k)} &= 1 + \frac{c_{S/2}}{2\kappa_{S/2}(\omega_k)SN}L + \frac{2\cos[\omega_k]}{2\kappa_{S/2}(\omega_k)}\frac{(c_{S/2}-c_k)}{SN}L \\ &\quad + \frac{(2c_k-c_{S/2})}{2\kappa_{S/2}(\omega_k)SN}L^2 + \frac{c_k^2}{2\kappa_{S/2}(\omega_k)(SN)^2}L^2 \\ &= 1 + O\left(\frac{1}{N}\right) + O\left(\frac{1}{N}\right) + O\left(\frac{1}{N}\right) + O\left(\frac{1}{N^2}\right)\end{aligned} \tag{S.5}$$

and

$$\begin{aligned}&\frac{2\cos[\omega_k]-L}{2\kappa(\omega_{kj})}\Delta_j^{c_j} + \frac{2\cos[\omega_j]-L}{2\kappa(\omega_{jk})}\Delta_k^{c_k} \\ &= 1 - \frac{4\cos[\omega_k]\cos[\omega_j]}{2\kappa(\omega_{kj})}\frac{(c_j-c_k)}{SN}L + \frac{2\left[\cos[\omega_j]\frac{c_j}{SN} - \cos[\omega_k]\frac{c_k}{SN}\right]}{2\kappa(\omega_{kj})}L^2 \\ &\quad + \frac{4\left[\cos[\omega_k]\frac{c_j}{SN} - \cos[\omega_j]\frac{c_k}{SN}\right]}{2\kappa(\omega_{kj})}L^2 - \frac{2}{2\kappa(\omega_{kj})}\frac{(c_j-c_k)}{SN}L^3 \\ &\quad + \frac{2\left[\cos[\omega_k]\left(\frac{c_j}{SN}\right)^2 - \cos[\omega_j]\left(\frac{c_k}{SN}\right)^2\right]}{2\kappa(\omega_{kj})}L^2 - \frac{1}{2\kappa(\omega_{kj})}\frac{\left(c_j^2-c_k^2\right)}{(SN)^2}L^3 \\ &= 1 - O\left(\frac{1}{N}\right) + O\left(\frac{1}{N}\right) + O\left(\frac{1}{N}\right) - O\left(\frac{1}{N}\right) + O\left(\frac{1}{N^2}\right) - O\left(\frac{1}{N^2}\right)\end{aligned} \tag{S.6}$$

where $\kappa_0(\omega_k) := 1-\cos[\omega_k]$, $\kappa_{S/2}(\omega_k) := 1+\cos[\omega_k]$ and $\kappa(\omega_{kj}) := \cos[\omega_k]-\cos[\omega_j]$, $j,k = 1,...,S^*$.

Consequently, noting that $\Delta_k^{c_k} S_{k,c_k}(Sn+s) = 1$ and using (S.3)-(S.6), it follows from (S.2) after some tedious algebra and using the standard trigonometric identities, $\sin[((Sn+s)+1)\,\omega_k]$

$\equiv \cos[\omega_k]\sin[(Sn+s)\omega_k]+\sin[\omega_k]\cos[(Sn+s)\omega_k]$ and $\cos[((Sn+s)+1)\omega_k] \equiv \cos[\omega_k]\cos[(Sn+s)\omega_k]$ $-\sin[\omega_k]\sin[(Sn+s)\omega_k]$, that x_{Sn+s} can be decomposed into the sum of frequency specific partial sums plus an asymptotically negligible term (see also Gregoir, 1999); that is,

$$\begin{aligned} x_{Sn+s} &= \frac{1}{S}S_{0,c_0}(Sn+s)\,u_{Sn+s} + \frac{1}{S}S_{S/2,c_{S/2}}(Sn+s)\,u_{Sn+s} \\ &\quad + \frac{2}{S}\sum_{k=1}^{S^*}\Big[\cos[(Sn+s)\omega_k]\,S^{\alpha}_{k,c_k}(Sn+s)\,u_{Sn+s} \\ &\qquad + \sin[(Sn+s)\omega_k]\,S^{\beta}_{k,c_k}(Sn+s)\,u_{Sn+s}\Big] + o_p(1). \end{aligned} \tag{S.7}$$

Defining $X_n := [x_{Sn-(S-1)}, x_{Sn-(S-2)}, ..., x_{Sn}]'$, $n = 0, ..., N$, and $U_n := [u_{Sn-(S-1)}, u_{Sn-(S-2)}, ..., u_{Sn}]'$, $n = 1, ..., N$, and noting that $\sum_{j=1}^{n}\exp\left(\frac{c_k}{SN}\right)^{S(n-j)}U_j = \sum_{j=1}^{n}\exp\left(\frac{c_k}{N}\right)^{n-j}U_j$, it will prove convenient, for the analysis that follows, to re-write (S.7) in the so-called vector-of-seasons representation:

$$X_n = \sum_{k=0}^{\lfloor S/2\rfloor}\left(\frac{1+\delta_k}{S}\right)C_k\sum_{i=1}^{n}\exp\left(\frac{c_k}{N}\right)^{n-i}U_i + o_p(1) \tag{S.8}$$

where $\delta_k := 0$ for $k = 0$ and $k = S/2$ and $\delta_k := 1$ otherwise, and where $C_i := \mathsf{Circ}[\cos[0], \cos[\omega_i], \cos[2\omega_i], \ldots, \cos[(S-1)\omega_i]]$, $i = 0, \ldots, \lfloor S/2\rfloor$, such that C_0 and $C_{S/2}$ are $S \times S$ circulant matrices of rank 1, while for $\omega_i = 2\pi i/S$ with $i = 1, \ldots, S^*$, C_i are $S \times S$ circulant matrices of rank 2. For further details on these circulant matrices see, for example, Osborn and Rodrigues (2002) and Smith *et al.* (2009).

Remark S.1: In order to relate (S.8) to (S.7) we have made use of the fact that the circulant matrices involved can be written as $C_0 = \mathbf{v}_0\mathbf{v}_0{}'$, where $\mathbf{v}_0{}' := [1, 1, 1, ..., 1]$, $C_{S/2} = \mathbf{v}_{S/2}\mathbf{v}_{S/2}{}'$, where $\mathbf{v}_{S/2}{}' := [-1, 1, -1, ..., 1]$, and for $j = 1, ..., S^*$, $C_j = \mathbf{v}_j\mathbf{v}_j'$ and finally the matrix $\overline{C}_j := \mathsf{Circ}[\sin[0], \sin[(S-1)\omega_j], \sin[(S-2)\omega_j], \ldots, \sin[\omega_j]]$, with $\overline{C}_j = \mathbf{v}_j\mathbf{v}_j^{*\prime}$, which will be used later in lemma S.1 where

$$\mathbf{v}_j' := \begin{bmatrix} \cos[\omega_j(1-S)] & \cos[\omega_j(2-S)] & \cdots & \cos[0] \\ \sin[\omega_j(1-S)] & \sin[\omega_j(2-S)] & \cdots & \sin[0] \end{bmatrix} =: \begin{bmatrix} \mathbf{h}_j' \\ \mathbf{h}_j^{*\prime} \end{bmatrix}$$

and

$$\mathbf{v}_j^{*\prime} := \begin{bmatrix} -\sin[\omega_j(1-S)] & -\sin[\omega_j(2-S)] & \cdots & -\sin[0] \\ \cos[\omega_j(1-S)] & \cos[\omega_j(2-S)] & \cdots & \cos[0] \end{bmatrix} =: \begin{bmatrix} -\mathbf{h}_j^{*\prime} \\ \mathbf{h}_j' \end{bmatrix},$$

$j = 1, \ldots, S^*$. □

Remark S.2: As shown in Burridge and Taylor (2001), the error process, U_n, defined above (S.8) satisfies the vector $MA(\infty)$ representation

$$U_n = \sum_{j=0}^{\infty}\mathbf{\Psi}_j E_{n-j} \tag{S.9}$$

where $E_n := [\varepsilon_{Sn-(S-1)}, \varepsilon_{Sn-(S-2)}, ..., \varepsilon_{Sn}]'$ is a vector of IID errors, and the $S \times S$ matrices $\mathbf{\Psi}_0$, $\mathbf{\Psi}_j$, $j = 1, 2, \ldots$, are given by

$$\mathbf{\Psi}_0 := \begin{bmatrix} 1 & 0 & 0 & 0 & \cdots & 0 \\ \psi_1 & 1 & 0 & 0 & \cdots & 0 \\ \psi_2 & \psi_1 & 1 & 0 & \cdots & 0 \\ \psi_3 & \psi_2 & \psi_1 & 1 & \cdots & 0 \\ \vdots & \vdots & \vdots & \vdots & \ddots & \vdots \\ \psi_{S-1} & \psi_{S-2} & \psi_{S-3} & \psi_{S-4} & \cdots & 1 \end{bmatrix}$$

and

$$\mathbf{\Psi}_j := \begin{bmatrix} \psi_{jS} & \psi_{jS-1} & \psi_{jS-2} & \psi_{jS-3} & \cdots & \psi_{jS-(S-1)} \\ \psi_{jS+1} & \psi_{jS} & \psi_{jS-1} & \psi_{jS-2} & \cdots & \psi_{jS-(S-2)} \\ \psi_{jS+2} & \psi_{jS+1} & \psi_{jS} & \psi_{jS-1} & \cdots & \psi_{jS-(S-3)} \\ \psi_{jS+3} & \psi_{jS+2} & \psi_{jS+1} & \psi_{jS} & \cdots & \psi_{jS-(S-4)} \\ \vdots & \vdots & \vdots & \vdots & \ddots & \vdots \\ \psi_{jS+S-1} & \psi_{jS+S-2} & \psi_{jS+S-3} & \psi_{jS+S-4} & \cdots & \psi_{jS} \end{bmatrix}, \quad j \geq 1.$$

□

Next in Lemma S.1 we provide a multivariate invariance principle for $Y_n^{\xi} := [y^{\xi}_{Sn-(S-1)}, y^{\xi}_{Sn-(S-2)}, ..., y^{\xi}_{Sn}]'$, where $y^{\xi}_{Sn+s} := x_{Sn+s} - \hat{\delta}' z_{Sn+s,\xi}$, and where it is recalled that the parameter $\xi \in \{1, 2, 3\}$ denotes the deterministic Case of interest.

Lemma S.1. *Let the conditions of Theorem 4.1 hold. Then, as $N \to \infty$,*

$$\begin{aligned} N^{-1/2} Y^{\xi}_{\lfloor rN \rfloor} &\Rightarrow \frac{\sigma_\varepsilon}{S} \sum_{i=0}^{\lfloor S/2 \rfloor} (1 + \delta_i) \left(C_i \mathbf{\Psi}(1) \mathbf{J}^{\xi}_{c_i}(r) \right), \ r \in [0, 1] \\ &= \frac{\sigma_\varepsilon}{S} \left[\psi(1) C_0 \mathbf{J}^{\xi}_{c_0}(r) + \psi(-1) C_{S/2} \mathbf{J}^{\xi}_{c_{S/2}}(r) + 2 \sum_{i=1}^{S^*} \left(b_i C_i \mathbf{J}^{\xi}_{c_i}(r) + a_i \overline{C}_i \mathbf{J}^{\xi}_{c_i}(r) \right) \right] \end{aligned} \tag{S.10}$$

where $\{\delta_i\}_{i=0}^{\lfloor S/2 \rfloor}$, are as defined below (S.8)*; $\mathbf{J}^{\xi}_{c_k}(r) := [J^{\xi}_{c_k,1-S}(r), J^{\xi}_{c_k,2-S}(r), ..., J^{\xi}_{c_k,0}(r)]'$ is an $S \times 1$ vector OU process such that $d\mathbf{J}^{\xi}_{c_k}(r) = c\mathbf{J}^{\xi}_{c_k}(r)\, dr + d\mathbf{W}^{\xi}(r)$ and $\mathbf{W}^{\xi}(r)$ is an $S \times 1$ vector Brownian motion process; $a_i := \mathcal{I}m(\psi[\exp(\mathrm{i}\omega_i)])$ and $b_i := \mathcal{R}e(\psi[\exp(\mathrm{i}\omega_i)])$, $i = 1, ..., S^*$, with $\mathcal{R}e(\cdot)$ and $\mathcal{I}m(\cdot)$ denoting the real and imaginary parts of their arguments, respectively; and C_0, $C_{S/2}$, C_i and $\overline{C}_i$, $i = 1, \ldots, S^*$, are the $S \times S$ circulant matrices defined in Remark S.1. Finally, with OLS de-trending:*

$$\begin{aligned} J^1_{c_k,s}(r) &:= J_{c_k,s}(r) - \int_0^1 J_{c_k,s}(r)\, dr \\ J^2_{c_k,s}(r) &:= J^1_{c_k,s}(r) - 12 \left(r - \frac{1}{2} \right) \int_0^1 \left(r - \frac{1}{2} \right) \left[\frac{1}{S} \sum_{s=1-S}^{0} J^1_{c_k,s}(r) \right] dr \\ J^3_{c_k,s}(r) &:= J^1_{c_k,s}(r) - 12 \left(r - \frac{1}{2} \right) \int_0^1 \left(r - \frac{1}{2} \right) J^1_{c_k,s}(r)\, dr \end{aligned}$$

and with local GLS de-trending:

$$\begin{aligned} J^1_{c_k,s}(r) &:= J_{c_k,s}(r) \\ J^2_{c_k,s}(r) &:= J_{c_k,s}(r) - r\left[\frac{1}{S}\sum_{s=1-S}^{0}\left(\lambda J_{c_k,s}(1) + 3(1-\lambda)\int_0^1 h J_{c_k,s}(h)\,dh\right)\right] \\ J^3_{c_k,s}(r) &:= J_{c_k,s}(r) - r\left[\lambda J_{c_k,s}(1) + 3(1-\lambda)\int_0^1 h J_{c_k,s}(h)\,dh\right] \end{aligned}$$

with $\lambda := (1-\overline{c})/\left(1+\overline{c}+\overline{c}^2/3\right)$*, in all cases for the indices* $s = 1-S, ..., 0$ *and* $k = 0, ..., \lfloor S/2 \rfloor$.

Proof of Lemma S.1: Following along the same lines as for the proof of Lemma 1 in del Barrio Castro, Osborn and Taylor (2012) and Phillips (1988) it follows that, as $N \to \infty$,

$$\frac{\sigma_\varepsilon^{-1}}{\sqrt{N}}\sum_{i=1}^{\lfloor rN \rfloor}\exp\left(\frac{c_k}{N}\right)^{\lfloor rN \rfloor - i} E_i \;\Rightarrow\; \mathbf{J}_{c_k}(r), \quad r \in [0,1] \tag{S.11}$$

$$\begin{aligned} \frac{\sigma_\varepsilon^{-1}}{\sqrt{N}}\sum_{i=1}^{\lfloor rN \rfloor}\exp\left(\frac{c_k}{N}\right)^{\lfloor rN \rfloor - i} U_i &= \frac{\sigma_\varepsilon^{-1}\boldsymbol{\Psi}(1)}{\sqrt{N}}\sum_{i=1}^{\lfloor rN \rfloor}\exp\left(\frac{c_k}{N}\right)^{\lfloor rN \rfloor - i} E_i + o_p(1) \\ &\Rightarrow \boldsymbol{\Psi}(1)\mathbf{J}_{c_k}(r), \quad r \in [0,1] \end{aligned} \tag{S.12}$$

where E_i and U_i are as previously defined, $d\mathbf{J}_{c_k}(r) = c_k \mathbf{J}_{c_k}(r)\,dr + d\mathbf{W}(r)$, $\mathbf{W}(r)$ is an $S \times 1$ vector standard Brownian motion and $\mathbf{J}_{c_k}(r)$ is an $S \times 1$ vector standard OU process. Next observe from (S.8) and (S.9), that

$$\begin{aligned} N^{-1/2}X_{\lfloor rN \rfloor} &= \sum_{k=0}^{\lfloor S/2 \rfloor}\left(\frac{1+\delta_k}{S}\right)C_k N^{-1/2}\sum_{i=1}^{\lfloor rN \rfloor}\exp\left(\frac{c_k}{N}\right)^{\lfloor rN \rfloor - i} U_i + o_p(1) \\ &= \sum_{k=0}^{\lfloor S/2 \rfloor}\left(\frac{1+\delta_k}{S}\right)C_k \boldsymbol{\Psi}(1) N^{-1/2}\sum_{i=1}^{\lfloor rN \rfloor}\exp\left(\frac{c_k}{N}\right)^{\lfloor rN \rfloor - i} E_i + o_p(1) \end{aligned} \tag{S.13}$$

where $\{\delta_k\}_{k=0}^{\lfloor S/2 \rfloor}$, are as defined below (S.8), and the approximation in (S.13) follows from (S.12) and using similar arguments to those used in Boswijk and Franses (1996, p.238). From (S.11), (S.13) and the continuous mapping theorem [CMT] the result in (S.10) follows immediately. Noting that $\boldsymbol{\Psi}(1)$ is also a circulant matrix, then by the properties of products of circulant matrices it can be shown that $C_0\boldsymbol{\Psi}(1) = \psi(1)C_0$, $C_{S/2}\boldsymbol{\Psi}(1) = \psi(-1)C_{S/2}$, $C_j\boldsymbol{\Psi}(1) = b_j C_j + a_j\overline{C}_j$ and $\overline{C}_j\boldsymbol{\Psi}(1) = -a_j C_j + b_j\overline{C}_j$ for $j = 1, \ldots S^*$; see, *inter alia*, Davis (1979, Theorem 3.2.4), Gray (2006, Theorem 3.1) and Smith *et al.* (2009) for further details. The stated result then follows immediately. □

Remark S.3: Note that the circulant matrices C_0 and $C_{S/2}$ are associated with the auxiliary variables $y^{\xi}_{0,Sn+s}$ and $y^{\xi}_{S/2,Sn+s}$, respectively. Moreover, the circulant matrices C^k, $k = 1, ..., S^*$ (see Remark 2 in Smith, Taylor and del Barrio Castro, 2009) defined as:

$$\begin{aligned} C^k &:= \mathsf{Circ}\left[\frac{\sin[\omega_k]}{\sin[\omega_k]}, \frac{\sin[S\omega_k]}{\sin[\omega_k]}, \frac{\sin[(S-1)\omega_k]}{\sin[\omega_k]}, \ldots, \frac{\sin[2\omega_k]}{\sin[\omega_k]}\right] \\ &= C_k + \frac{\cos[\omega_k]}{\sin[\omega_k]}\overline{C}_k, \quad k = 1, ..., S^* \end{aligned} \tag{S.14}$$

where C_k and $\overline{C}_k$, $k = 1, ..., S^*$, are as defined in Remark S.1 and are associated with the filter $\Delta_k^0(L) = \sin[\omega_k]^{-1}\left(\sum_{j=0}^{S-1}\sin[(j+1)\omega_k]L^j\right)$ in (3.11). Finally the circulant matrices $D_{\omega_k}^+$ and $D_{\omega_k}^-$, $k = 1, ..., S^*$, defined as, $D_{\omega_k}^+ := \mathsf{Circ}\left[1, 0, 0, \cdots, 0, e^{\mathrm{i}\omega_k}\right]$ and $D_{\omega_k}^- := \mathsf{Circ}\left[1, 0, 0, \cdots, 0, e^{-\mathrm{i}\omega_k}\right]$ are associated with the filters $\left(1 - e^{\mathrm{i}\omega_k}L\right)$ and $\left(1 - e^{-\mathrm{i}\omega_k}L\right)$, respectively. □

In order to obtain results for the asymptotic distributions of the test statistics discussed in this paper, the limiting results collected together in the following Lemma will prove useful.

Lemma S.2. *Let the conditions of Lemma S.1 hold. Then, as* $N \to \infty$,

$$N^{-1/2}C_0Y_{\lfloor rN\rfloor}^{\xi} \Rightarrow \sigma_\varepsilon\,\psi(1)\,C_0\mathbf{J}_{c_0}^{\xi}(r) \tag{S.15}$$

$$N^{-1/2}C_{S/2}Y_{\lfloor rN\rfloor}^{\xi} \Rightarrow \sigma_\varepsilon\,\psi(-1)\,\mathbf{J}_{c_{S/2}}^{\xi}(r) \tag{S.16}$$

$$N^{-1/2}C^kY_{\lfloor rN\rfloor}^{\xi} \Rightarrow \sigma_\varepsilon\left(C_k + \frac{\cos[\omega_k]}{\sin[\omega_k]}\overline{C}_k\right)\Psi(1)\,\mathbf{J}_{c_k}^{\xi}(r), k = 1, \ldots, S^* \tag{S.17}$$

$$\frac{1}{\sqrt{N}}D_{\omega_k}^+C^kY_{\lfloor rN\rfloor}^{\xi} \Rightarrow \sigma_\varepsilon C_k^-\Psi(1)\,\mathbf{J}_{c_k}^{\xi}(r) = \sigma_\varepsilon\psi\left(e^{\mathrm{i}\omega_k}\right)\mathcal{E}_{1,k}^-\mathcal{E}_{2,k}^{-\prime}\mathbf{J}_{c_k}^{\xi}(r), k = 1, \ldots, S^* \tag{S.18}$$

$$\frac{1}{\sqrt{N}}D_{\omega_k}^-C^kY_{\lfloor rN\rfloor}^{\xi} \Rightarrow \sigma_\varepsilon C_k^+\Psi(1)\,\mathbf{J}_{c_k}^{\xi}(r) = \sigma_\varepsilon\psi\left(e^{-\mathrm{i}\omega_k}\right)\mathcal{E}_{1,k}^+\mathcal{E}_{2,k}^{+\prime}\mathbf{J}_{c_k}^{\xi}(r), k = 1, \ldots, S^* \tag{S.19}$$

where the vector OU processes, $\mathbf{J}_{c_i}^{\xi}(r)$, $i = 0, \ldots, \lfloor S/2\rfloor$, *and the circulant matrices,* C_i, $i = 0, \ldots, \lfloor S/2\rfloor$ *and* $\overline{C}_i$, $i = 1, \ldots, S^*$, *are defined in Lemma S.1,* C^k *is defined in (S.14),* $D_{\omega_k}^+ := \mathsf{Circ}\left[1, 0, 0, \cdots, 0, e^{\mathrm{i}\omega_k}\right]$, $D_{\omega_k}^- := \mathsf{Circ}\left[1, 0, 0, \cdots, 0, e^{-\mathrm{i}\omega_k}\right]$, $C_k^- := \mathsf{Circ}\left[1, e^{-\mathrm{i}(S-1)\omega_k}, e^{-\mathrm{i}(S-2)\omega_k}, \cdots, e^{-\mathrm{i}\omega_k}\right]$, $C_k^+ := \mathsf{Circ}\left[1, e^{\mathrm{i}(S-1)\omega_k}, e^{\mathrm{i}(S-2)\omega_k}, \cdots, e^{\mathrm{i}\omega_k}\right]$, $k = 1, \ldots, S^*$, $\mathcal{E}_{1,k}^- := [1, e^{-\mathrm{i}\omega_k}, e^{-\mathrm{i}2\omega_k}, ..., e^{-\mathrm{i}(S-1)\omega_k}]'$, $\mathcal{E}_{2,k}^- := [1, e^{-\mathrm{i}(S-1)\omega_k}, e^{-\mathrm{i}(S-2)\omega_k}, ..., e^{-\mathrm{i}\omega_k}]'$, $\mathcal{E}_{1,k}^+ := [1, e^{\mathrm{i}\omega_k}, e^{\mathrm{i}2\omega_k}, ..., e^{\mathrm{i}(S-1)\omega_k}]'$ *and* $\mathcal{E}_{2,k}^+ := [1, e^{\mathrm{i}(S-1)\omega_k}, e^{\mathrm{i}(S-2)\omega_k}, ..., e^{\mathrm{i}\omega_k}]'$.

Proof of Lemma S.2: The results in (S.15) to (S.17) follow immediately from Lemma S.1 using the following identities: $C_0C_0 \equiv SC_0$,$C_{S/2}C_{S/2} \equiv SC_{S/2}$, $C_kC_k \equiv \frac{S}{2}C_k$ and $\overline{C}_kC_k \equiv \frac{S}{2}\overline{C}_k$, recalling that the matrix products between C_0, $C_{S/2}$, C_j and $\overline{C}_j$, $j = 1, \ldots, S^*$ are all zero matrices, and that multiplication between circulant matrices is commutative, and finally that $C^k := \left(C_k + \frac{\cos[\omega_k]}{\sin[\omega_k]}\overline{C}_k\right)$. Consider next the results in (S.18) and (S.19). We first note, using Property 1.3 and expression (2) in Gregoir (2006), that

$$C^k = \frac{e^{-\mathrm{i}\omega_k}}{e^{-\mathrm{i}\omega_k} - e^{\mathrm{i}\omega_k}}C_k^- + \frac{e^{\mathrm{i}\omega_k}}{e^{\mathrm{i}\omega_k} - e^{-\mathrm{i}\omega_k}}C_k^+ \tag{S.20}$$

with $C_k^- := \mathsf{Circ}\left[1, e^{-\mathrm{i}(S-1)\omega_k}, e^{-\mathrm{i}(S-2)\omega_k}, \cdots, e^{-\mathrm{i}\omega_k}\right]$ and $C_k^+ := \mathsf{Circ}\left[1, e^{\mathrm{i}(S-1)\omega_k}, e^{\mathrm{i}(S-2)\omega_k}, \cdots, e^{\mathrm{i}\omega_k}\right]$. Moreover, $D_{\omega_k}^-C_k^- = D_{\omega_k}^+C_k^+ = 0$, $\frac{e^{-\mathrm{i}\omega_k}}{e^{-\mathrm{i}\omega_k} - e^{\mathrm{i}\omega_k}}D_{\omega_k}^+C_k^- = C_k^-$, and $\frac{e^{\mathrm{i}\omega_k}}{e^{\mathrm{i}\omega_k} - e^{-\mathrm{i}\omega_k}}D_{\omega_k}^-C_k^+ = C_k^+$, each of which follows from the properties of the product of circulant matrices. Also, because $\Psi(1)$ is a circulant matrix, by the properties of products of circulant matrices it further holds that $C_k^-\Psi(1) = \psi\left(e^{\mathrm{i}\omega_k}\right)C_k^-$ and $C_k^+\Psi(1) = \psi\left(e^{-\mathrm{i}\omega_k}\right)C_k^+$. Finally as both C_k^- and C_k^+ are $S \times S$ circulant matrices of rank 1 we can write $C_k^- = \mathcal{E}_{1,k}^-\mathcal{E}_{2,k}^-$ and $C_k^+ = \mathcal{E}_{1,k}^+\mathcal{E}_{2,k}^{+\prime}$. The stated results then follow immediately. □

S.2.2 Proof of Theorem 4.1

Using the results that C_0 and $C_{S/2}$ are symmetric and orthogonal both to one another and to C_i and $\overline{C}_i$, $i = 1, ..., S^*$, and the fact that $C_jC_jC_j \equiv S^2C_j$ for $j = 0, S/2$, then appealing to the multivariate invariance principle in (S.10) and using an application of the CMT we have that

$$\begin{aligned} T^{-2}\sum_{n=1}^{N}\sum_{s=1-S}^{0}\left(y^{\xi}_{j,Sn+s-1}\right)^2 &= T^{-2}\sum_{n=1}^{N} S\left(Y^{\xi\prime}_{n-1}C_jY^{\xi}_{n-1}\right)+o_p(1) \\ &\Rightarrow \frac{\sigma^2_\varepsilon}{S^2}\frac{\psi\left(\cos[\omega_j]\right)^2}{S}\int_0^1 \mathbf{J}^{\xi}_{c_j}(r)'\,C_j'C_jC_j\mathbf{J}^{\xi}_{c_j}(r)\,dr \\ &= \sigma^2_\varepsilon\psi\left(\cos[\omega_j]\right)^2\int_0^1 \mathbf{J}^{\xi*}_{c_j}(r)'\,C_j\mathbf{J}^{\xi*}_{c_j}(r)\,dr, j=0,S/2 \quad \text{(S.21)} \end{aligned}$$

where $\omega_0 = 0$, $\omega_{S/2} = \pi$ and $\mathbf{J}^{\xi*}_{c_j}(r) := \frac{1}{\sqrt{S}}\mathbf{J}^{\xi}_{c_j}(r)$ for $j = 0, S/2$.

Using Remark S.1, together with the results in (S.15) and (S.16), for the zero and Nyquist frequencies, applications of the multivariate FCLT and CMT establish that, as $N \to \infty$,

$$\begin{aligned} N^{-1/2}y^{\xi}_{0,S\lfloor rN\rfloor+s} &\Rightarrow \sigma_\varepsilon\sqrt{S}\psi(1)\,\mathbf{v}_1'\frac{1}{\sqrt{S}}\mathbf{J}^{\xi}_{c_0}(r) =: \sigma_\varepsilon\sqrt{S}\psi(1)\,\mathbf{v}_1'\mathbf{J}^{\xi*}_{c_0}(r) \\ &=: \sigma_\varepsilon\sqrt{S}\psi(1)\,J^{\zeta}_{0,c_0}(r) \quad \text{(S.22)} \\ N^{-1/2}y^{\xi}_{S/2,S\lfloor rN\rfloor+s} &\Rightarrow \sigma_\varepsilon\sqrt{S}\psi(-1)(-1)^s\,\mathbf{v}_{S/2}'\frac{1}{\sqrt{S}}\mathbf{J}^{\xi}_{c_{S/2}}(r) =: \sigma_\varepsilon\sqrt{S}\psi(-1)(-1)^s\,\mathbf{v}_{S/2}'\mathbf{J}^{\xi*}_{c_{S/2}}(r) \\ &=: \sigma_\varepsilon\sqrt{S}\psi(-1)(-1)^s\,J^{\zeta}_{S/2,c_{S/2}}(r) \quad \text{(S.23)} \end{aligned}$$

where $\mathbf{v}_1'$ and $\mathbf{v}_{S/2}'$ are defined in Remark S.1, and $J^{\zeta}_{0,c_0}(r)$ and $J^{\zeta}_{S/2,c_{S/2}}(r)$ are as defined in Theorem 4.1. Consequently, for the $\mathcal{MZ}_k$, $k = 0, S/2$ tests we obtain from (S.22) and (S.23) that,

$$\begin{aligned} (SN)^{-1/2}y^{\xi}_{0,SN} &\Rightarrow \sigma_\varepsilon\psi(1)\,J^{\zeta}_{0,c_0}(1) \quad \text{(S.24)} \\ (SN)^{-1/2}y^{\xi}_{S/2,SN} &\Rightarrow \sigma_\varepsilon\psi(-1)(-1)^S\,J^{\zeta}_{S/2,c_{S/2}}(1). \quad \text{(S.25)} \end{aligned}$$

Using the results in (S.24), (S.25) and (S.21) and the fact that $\hat{\lambda}^2_0 \xrightarrow{p} \sigma^2_\varepsilon\psi(1)^2$ and $\hat{\lambda}^2_{S/2} \xrightarrow{p} \sigma^2_\varepsilon\psi(-1)^2$, it therefore follows that,

$$\mathcal{MZ}_k \Rightarrow \frac{\sigma^2_\varepsilon\psi\left(\cos[\omega_k]\right)^2 J^{\zeta}_{k,c_k}(1)^2 - \sigma^2_\varepsilon\psi\left(\cos[\omega_k]\right)^2}{2\sigma^2_\varepsilon\psi\left(\cos[\omega_k]\right)^2\int_0^1\left[J^{\zeta}_{k,c_k}(r)\right]^2dr} = \frac{\left[J^{\zeta}_{k,c_k}(1)\right]^2-1}{2\int_0^1\left[J^{\zeta}_{k,c_k}(r)\right]^2dr},\ k=0,S/2 \quad \text{(S.26)}$$

where $\omega_0 = 0$ and $\omega_{S/2} = \pi$. The results for the $\mathcal{MSB}_k$, $k = 0, S/2$, statistics are obtained straightforwardly from (S.21). Combining the results for $\mathcal{MSB}_k$ with (S.26), the limit of $\mathcal{MZ}_{t_k}$ then follows straightforwardly.

Turning to the harmonic frequency statistics, note first that the vector of seasons representations of (3.9) and (3.10) with $Y^{\xi,\mathtt{D}h}_{k,n} := \left[y^{\xi,\mathtt{D}h}_{k,Sn-(S-1)},\ y^{\xi,\mathtt{D}h}_{k,Sn-(S-2)},\cdots,y^{\xi,\mathtt{D}h}_{k,Sn}\right]'$, $h \in \{a, b\}$,

based on (S.18) and (S.19) are such that, for $k = 1, ..., S^*$,

$$\begin{aligned}
\frac{1}{\sqrt{SN}} Y^{\xi,\mathtt{D}a}_{k,\lfloor rN \rfloor} &\Rightarrow \frac{\sigma_\varepsilon}{\sqrt{S}} \psi\left(e^{\mathrm{i}\omega_k}\right)\left(e^{\mathrm{i}\omega_k}\mathbf{1}\right)\mathcal{E}^{-\prime}_{2,k}\mathbf{J}^{\xi}_{c_k}(r) = \frac{\sigma_\varepsilon}{\sqrt{S}} \psi\left(e^{\mathrm{i}\omega_k}\right)\mathbf{1}e^{\mathrm{i}\omega_k}\mathcal{E}^{+\prime}_{1,k}\mathbf{J}^{\xi}_{c_k}(r) \\
&= \frac{\sigma_\varepsilon}{\sqrt{2}} \psi\left(e^{\mathrm{i}\omega_k}\right)\mathbf{1}\left[\mathbf{h}'_k \frac{1}{\sqrt{S/2}}\mathbf{J}^{\xi}_{c_k}(r) + \mathrm{i}\mathbf{h}^{*\prime}_k \frac{1}{\sqrt{S/2}}\mathbf{J}^{\xi}_{c_k}(r)\right] \\
&= \frac{\sigma_\varepsilon}{\sqrt{2}} \psi\left(e^{\mathrm{i}\omega_k}\right)\mathbf{1}\left[\mathbf{h}'_k \mathbf{J}^{\xi\dagger}_{c_k}(r) + \mathrm{i}\mathbf{h}^{*\prime}_k \mathbf{J}^{\xi\dagger}_{c_k}(r)\right] \\
&= \frac{\sigma_\varepsilon}{\sqrt{2}} \psi\left(e^{\mathrm{i}\omega_k}\right)\mathbf{1}\left[J^{\zeta}_{k,c_k}(r) + \mathrm{i}J^{\zeta*}_{k,c_k}(r)\right] \qquad \text{(S.27)}
\end{aligned}$$

and

$$\begin{aligned}
\frac{1}{\sqrt{SN}} Y^{\xi,\mathtt{D}b}_{k,\lfloor rN \rfloor} &\Rightarrow \frac{\sigma_\varepsilon}{\sqrt{S}} \psi\left(e^{-\mathrm{i}\omega_k}\right)\left(e^{-\mathrm{i}\omega_k}\mathbf{1}\right)\mathcal{E}^{+\prime}_{2,k}\mathbf{J}^{\xi}_{c_k}(r) = \frac{\sigma}{\sqrt{S}} \psi\left(e^{-\mathrm{i}\omega_k}\right)\mathbf{1}e^{-\mathrm{i}\omega_k}\mathcal{E}^{-\prime}_{1,k}\mathbf{J}^{\xi}_{c_k}(r) \\
&= \frac{\sigma_\varepsilon}{\sqrt{2}} \psi\left(e^{-\mathrm{i}\omega_k}\right)\mathbf{1}\left[\mathbf{h}'_k \frac{1}{\sqrt{S/2}}\mathbf{J}^{\xi}_{c_k}(r) - \mathrm{i}\mathbf{h}^{*\prime}_k \frac{1}{\sqrt{S/2}}\mathbf{J}^{\xi}_{c_k}(r)\right] \\
&= \frac{\sigma_\varepsilon}{\sqrt{2}} \psi\left(e^{-\mathrm{i}\omega_k}\right)\mathbf{1}\left[\mathbf{h}'_k \mathbf{J}^{\xi\dagger}_{c_k}(r) - \mathrm{i}\mathbf{h}^{*\prime}_k \mathbf{J}^{\xi\dagger}_{c_k}(r)\right] \\
&= \frac{\sigma_\varepsilon}{\sqrt{2}} \psi\left(e^{-\mathrm{i}\omega_k}\right)\mathbf{1}\left[J^{\zeta}_{k,c_k}(r) - \mathrm{i}J^{\zeta*}_{k,c_k}(r)\right], \qquad \text{(S.28)}
\end{aligned}$$

respectively, where $\mathbf{1}$ is an $S \times 1$ vector of ones, $\mathbf{h}_k$ and $\mathbf{h}^*_k$, are defined in Remark S.1, $\mathbf{J}^{\xi}_{c_k}(r)$ and $\mathbf{J}^{\xi\dagger}_{c_k}(r)$ are defined in Lemma S.1, and where $J^{\zeta}_{k,c_k}(r)$ and $J^{\zeta*}_{k,c_k}(r)$ are as defined in Theorem 4.1.

Using the consistency of the estimators $\breve{\lambda}_{k,AR} := s_e\{1 - [\widehat{\phi}(e^{\mathrm{i}\omega_k})]\}^{-1}$ and $\breve{\lambda}^*_{k,AR} := s_e\{1 - [\widehat{\phi}(e^{-\mathrm{i}\omega_k})]\}^{-1}$ of $\sigma_\varepsilon\psi\left(e^{\mathrm{i}\omega_k}\right)$ and $\sigma_\varepsilon\psi\left(e^{-\mathrm{i}\omega_k}\right)$, respectively, $k = 1, ..., S^*$, it is then possible to show that, in each case for $k = 1, ..., S^*$,

$$(\breve{\lambda}^2_{k,AR}T)^{-1/2} y^{\xi,\mathtt{D}a}_{k,S\lfloor rN \rfloor + s} \Rightarrow \frac{1}{\sqrt{2}}\left[J^{\zeta}_{k,c_k}(r) + \mathrm{i}J^{\zeta*}_{k,c_k}(r)\right] =: \frac{1}{\sqrt{2}}\mathbb{J}_{k,c_k}(r)$$

$$(\breve{\lambda}^{*2}_{k,AR}T)^{-1/2} y^{\xi,\mathtt{D}b}_{k,S\lfloor rN \rfloor + s} \Rightarrow \frac{1}{\sqrt{2}}\left[J^{\zeta}_{k,c_k}(r) - \mathrm{i}J^{\zeta*}_{k,c_k}(r)\right] =: \frac{1}{\sqrt{2}}\overline{\mathbb{J}_{k,c_k}(r)}.$$

Noting that the auxiliary variables $y^{\mathcal{R}e,\xi}_{k,Sn+s}$ and $y^{\mathcal{I}m,\xi}_{k,Sn+s}$ defined in (3.14) and (3.15) are free from nuisance parameters, it is then straightforward to obtain the representations given for the asymptotic distributions of the $\mathcal{K}$-$\mathcal{MZ}_k$, $\mathcal{K}$-$\mathcal{MSB}_k$ and $\mathcal{K}$-$\mathcal{MZ}_{t_k}$ statistics in (4.4), (4.5) and (4.6), together with the results for the joint frequency statistics from section 3.3 given in Corollary 4.1 □

Remark S.4: Note that the deterministic kernels considered for the de-meaning and de-trending of the variables, have different impacts on the frequency specific OU processes. These set of processes at each frequency for each case are summarised for convenience as follows,

$$\begin{aligned}
&\textit{Case 1 } (\xi = 1) \quad : \quad J^1_{0,c_0}(r),\ J^1_{S/2,c_{S/2}}(r),\ J^1_{i,c_i}(r),\ J^{1*}_{i,c_i}(r),\ i = 1, ..., S^* \\
&\textit{Case 2 } (\xi = 2) \quad : \quad J^2_{0,c_0}(r),\ J^1_{S/2,c_{S/2}}(r),\ J^1_{i,c_i}(r),\ J^{1*}_{i,c_i}(r),\ i = 1, ..., S^* \\
&\textit{Case 3 } (\xi = 3) \quad : \quad J^2_{0,c_0}(r),\ J^2_{S/2,c_{S/2}}(r),\ J^2_{i,c_i}(r),\ J^{2*}_{i,c_i}(r),\ i = 1, ..., S^*
\end{aligned}$$

where it is to be recalled that $\zeta = 1$ and $\zeta = 2$ correspond to de-meaned and de-trended OU processes, respectively. These are defined as: $J^{\zeta}_{0,c_0}(r) := \mathbf{v}_1' \mathbf{J}^{\xi *}_{c_0}(r)$, $J^{\zeta}_{S/2,c_{S/2}}(r) := \mathbf{v}_{S/2}' \mathbf{J}^{\xi *}_{c_{S/2}}(r)$, $J^{\zeta}_{k,c_k}(r) := \mathbf{h}_k' \mathbf{J}^{\xi \dagger}_{c_k}(r)$ and $J^{\zeta\,*}_{k,c_k}(r) := \mathbf{h}_k^{*\prime} \mathbf{J}^{\xi \dagger}_{c_k}(r)$ for $k = 1, \ldots, S^*$. □

S.3 Augmented HEGY Seasonal Unit Root Tests

Unit roots at the zero, Nyquist and harmonic seasonal frequencies imply that $\pi_0 = 0$, $\pi_{S/2} = 0$ and $\pi_k = \pi_k^* = 0$, $k = 1, ..., S^*$, respectively, in (2.4); see Smith *et al.* (2009). Consequently, tests for the presence or otherwise of a unit root at the zero and Nyquist frequencies are conventional lower tailed regression t-tests, denoted t_0 and $t_{S/2}$, for the exclusion of $y^{\xi}_{0,Sn+s-1}$ and $y^{\xi}_{S/2,Sn+s-1}$, respectively, from (2.4). Notice that for $S = 1$, t_0 is the standard non-seasonal ADF unit root test statistic. Similarly, the hypothesis of a pair of complex unit roots at the kth harmonic seasonal frequency may be tested by the lower-tailed t_k and two-tailed t_k^* regression t-tests from (2.4) for the exclusion of $y^{\xi}_{k,Sn+s-1}$ and $y^{*\xi}_{k,Sn+s-1}$, respectively, or by the (upper-tailed) regression F-test, denoted F_k, for the exclusion of both $y^{\xi}_{k,Sn+s-1}$ and $y^{*\xi}_{k,Sn+s-1}$ from (2.4). Ghysels *et al.* (1994) also consider the joint frequency (upper-tail) regression F-tests from (2.4), $F_{1...\lfloor S/2 \rfloor}$ for the exclusion of $y^{\xi}_{S/2,Sn+s-1}$, $\{y^{\xi}_{j,Sn+s-1}\}_{j=1}^{S^*}$ and $\{y^{*\xi}_{k,Sn+s-1}\}_{k=1}^{S^*}$, and $F_{0...\lfloor S/2 \rfloor}$ for the exclusion of $y^{\xi}_{0,Sn+s-1}$, $y^{\xi}_{S/2,Sn+s-1}$, $\{y^{\xi}_{j,Sn+s-1}\}_{j=1}^{S^*}$ and $\{y^{*\xi}_{k,Sn+s-1}\}_{k=1}^{S^*}$. The former tests the null hypothesis of unit roots at all of the seasonal frequencies, defined as $H_{0,\text{seas}} := \cap_{k=1}^{\lfloor S/2 \rfloor} H_{0,k}$, while the latter tests the null hypothesis of unit roots at the zero and all of the seasonal frequencies, defined as $H_0 := \cap_{k=0}^{\lfloor S/2 \rfloor} H_{0,k}$. Observe that $\alpha(L) = \Delta_S$ under H_0.

The limiting null distributions of the OLS de-trended HEGY statistics are given for the case where $\psi(z) = 1$ in (2.1b) and accordingly $p^* = 0$ in (2.4) by Smith and Taylor (1998). In the case where $\psi(z)$ is invertible with (unique) inverse $\phi(z)$, with $\phi(z)$ a pth order, $0 \leq p < \infty$, lag polynomial, Burridge and Taylor (2001) and Smith *et al.* (2009) show that the limiting null distributions of the OLS de-trended t_0, $t_{S/2}$ and F_k, $k = 1, ..., S^*$, statistics from (2.4) are as for $p = 0$, provided $p^* \geq p$ in (2.4). They show that this is not true, however, for the t_k and t_k^*, $k = 1, ..., S^*$, statistics whose limit distributions depend on functions of the parameters characterising the serial dependence in u_{Sn+s} in (2.1b). Representations for the corresponding limiting distributions under near seasonally integrated alternatives are given in Rodrigues and Taylor (2004) and again shown to be free of nuisance parameters with the exception of the t_k and t_k^*, $k = 1, ..., S^*$, statistics. Corresponding results for the local GLS de-trended HEGY-type statistic are given in Rodrigues and Taylor (2007) and here it is also the case that the harmonic frequency t-statistics depend on nuisance parameters arising from the serial correlation in u_{Sn+s}. Where $\phi(z)$ is (potentially) infinite-ordered, del Barrio Castro *et al.* (2012) show that provided the lag length p^* in (2.4) is such that $1/p^* + (p^*)^3/T \to 0$, as $T \to \infty$, then limiting distributions of the OLS and local GLS de-trended HEGY statistics will be of the same form as derived for those statistics under finite p.

S.4 Limiting Distributions of the Lag Un-augmented HEGY Statistics

In Theorem S.1 we now provide representations for the limiting distributions of the normalised OLS estimates together with the corresponding regression t- and F-statistics computed from the un-augmented HEGY regression given by (2.4) with the lag augmentation length, p^*, set to zero. These representations are again indexed by the parameter ζ which has exactly the same meaning as was given prior to Theorem 4.1.

Theorem S.1. *Let y_{Sn+s} be generated by (2.1) under $H_{1,\mathbf{c}}$ and let Assumption 1 hold. Then the HEGY-type statistics computed from (2.4) with $p^* = 0$ are such that, as $T \to \infty$,*

$$T\hat{\pi}_k \Rightarrow \frac{\int_0^1 J^{\zeta}_{k,c_k}(r)dJ^{\zeta}_{k,c_k}(r) + \mathcal{D}_k \int_0^1 J^{\zeta *}_{k,c_k}(r)dJ^{\zeta *}_{k,c_k}(r) + \frac{\lambda_k^2-\gamma_0}{2\lambda_k^2}}{\frac{(2-\mathcal{D}_k)}{2}\left\{\int_0^1 \left[J^{\zeta}_{k,c_k}(r)\right]^2 dr + \mathcal{D}_k \int_0^1 \left[J^{\zeta *}_{k,c_k}(r)\right]^2 dr\right\}}, \quad k = 0, ..., \lfloor S/2 \rfloor \tag{S.29}$$

$$T\hat{\pi}^*_k \Rightarrow \frac{\int_0^1 J^{\zeta *}_{k,c_k}(r)dJ^{\zeta}_{k,c_k}(r) - \int_0^1 J^{\zeta}_{k,c_k}(r)dJ^{\zeta *}_{k,c_k}(r) + \frac{\lambda_k^{*2}-\gamma_0}{2\lambda_k^2}}{\frac{1}{2}\left\{\int_0^1 \left[J^{\zeta}_{k,c_k}(r)\right]^2 dr + \int_0^1 \left[J^{\zeta *}_{k,c_k}(r)\right]^2 dr\right\}}, \quad k = 1, ..., S^* \tag{S.30}$$

and

$$t_k \Rightarrow \frac{\lambda_k}{\gamma_0^{1/2}} \frac{\int_0^1 J^{\zeta}_{k,c_k}(r)dJ^{\zeta}_{k,c_k}(r) + \mathcal{D}_k \int_0^1 J^{\zeta *}_{k,c_k}(r)dJ^{\zeta *}_{k,c_k}(r) + \frac{\lambda_k^2-\gamma_0}{2\lambda_k^2}}{\left\{\int_0^1 \left[J^{\zeta}_{k,c_k}(r)\right]^2 dr + \mathcal{D}_k \int_0^1 \left[J^{\zeta *}_{k,c_k}(r)\right]^2 dr\right\}^{1/2}} =: \Upsilon^{\zeta}_k, \; k = 0, ..., \lfloor S/2 \rfloor \tag{S.31}$$

$$t^*_k \Rightarrow \frac{\lambda_k}{\gamma_0^{1/2}} \frac{\int_0^1 J^{\zeta *}_{k,c_k}(r)dJ^{\zeta}_{k,c_k}(r) - \int_0^1 J^{\zeta}_{k,c_k}(r)dJ^{\zeta *}_{k,c_k}(r) + \frac{\left(\lambda_k^{*2}-\gamma_0\right)}{2\lambda_k^2}}{\left\{\int_0^1 \left[J^{\zeta}_{k,c_k}(r)\right]^2 dr + \int_0^1 \left[J^{\zeta *}_{k,c_k}(r)\right]^2 dr\right\}^{1/2}} =: \Upsilon^{*\zeta}_k, \quad k = 1, ..., S^* \tag{S.32}$$

where $\mathcal{D}_k := 0$, for $k = 0$, $S/2$ and $\mathcal{D}_k := 1$, for $k = 1, ..., S^*$, $\lambda_k^{*2} := \gamma_0 + 2\sum_{i=1}^{\infty} \sin(\omega_k i)\gamma_k$, $k = 1, ..., S^*$, and where the limiting processes, $J^{\zeta}_{0,c_0}(r)$, $J^{\zeta}_{S/2,c_{S/2}}(r)$, $J^{\zeta}_{k,c_k}(r)$ and $J^{\zeta *}_{k,c_k}(r)$, $k = 1, \ldots, S^*$, are as defined in Theorem 4.1.

Remark S.5. Representations for the limiting distributions of the corresponding joint F statistics, F_k, $k = 1, ..., S^*$, $F_{1...\lfloor S/2 \rfloor}$ and $F_{0...\lfloor S/2 \rfloor}$ are given by the average of the squares of the limiting distributions for the t-statistics involved in their formulation given in Theorem S.1. So that, for example, $F_k \Rightarrow \frac{1}{2}\left[(\Upsilon^{\zeta}_k)^2 + (\Upsilon^{*\zeta}_k)^2\right]$, $k = 1, ..., S^*$. □

Remark S.6. The results in Theorem S.1 (and consequently also in Remark S.5) show that the limiting distributions (under both null and local alternatives) of the uncorrected un-augmented HEGY tests depend on nuisance parameters which arise when u_{Sn+s} is weakly dependent. When u_{Sn+s} is IID, which occurs where $\psi(z) = 1$, then the true lag order in (2.4) is $p^* = 0$, and the representations in (S.29)-(S.32) are pivotal because here $\lambda_k^2 = \gamma_0$, $k = 0, \ldots, \lfloor S/2 \rfloor$,

and $\lambda_k^{*2} = \gamma_0$, $k = 1, \ldots, S^*$. Indeed, these pivotal forms, for the statistics at the zero and Nyquist frequencies and for all of the F-type tests coincide with those which obtain from the appropriately augmented HEGY tests discussed in section S.3. Relative to these pivotal distributions, we see that in the presence of weak dependence in u_{Sn+s} the un-augmented HEGY statistics have limiting distributions whose numerator includes an additional term arising from the difference between the short run variance of u_{Sn+s} and the long run variance(s) of u_{Sn+s} at the frequency component relating to that statistic and, in the case of the t-statistics (and, hence, the F-statistics), are also scaled by the ratio of the long and short run variances of u_{Sn+s} at that frequency. □

The representations given for the limiting distributions of the un-augmented HEGY statistics in Theorem S.1 are useful because they enable us to see immediately how, given consistent estimators for γ_0, λ_k^2, $k = 0, \ldots, \lfloor S/2 \rfloor$, and λ_k^{*2}, $k = 1, \ldots, S^*$, these statistics can be transformed to obtain modified statistics whose limiting distributions coincide with those which obtain in the case where $\psi(z) = 1$. To that end in section S.5 we now propose seasonal analogues of the non-seasonal PP tests.

S.5 Phillips-Perron-Type Seasonal Unit Root Tests

The finite sample size control of seasonal Phillips-Perron type tests under weak dependence was found to be very poor relative to both augmented HEGY tests and the seasonal $\mathcal{M}$ tests; see the accompanying working paper, del Barrio Castro, Rodrigues and Taylor (2015).

Computation of seasonal versions of the non-seasonal PP unit root tests will require consistent estimators of the nuisance parameters which feature in the limit distributions, given in Theorem S.1, of the un-augmented HEGY statistics which obtain from estimating (2.4) with p^* set to zero. Consistent sums-of-covariances and ASD estimators for λ_k^2, $k = 0, \ldots, \lfloor S/2 \rfloor$, were discussed in section 3.2. Corresponding estimators for λ_k^{*2}, $k = 1, \ldots, S^*$, which are also consistent under the conditions given in section 3.2, can be defined as follows, where notation is the same as used in section 3.2. First, the sum-of-covariances estimators

$$\hat{\lambda}_{k,WA}^{*2} := \sum_{j=-T+1}^{T-1} \kappa(j/m)\hat{\gamma}_j \cos(\pi/2 + \omega_k j), \qquad k = 1, \ldots, S^*. \tag{S.33}$$

Second the corresponding ASD estimators

$$\hat{\lambda}_{k,AR}^{*2} := \frac{s_e^2}{\left\{1 - \sum_{j=1}^{p^*} \hat{\phi}_j^* \cos\left(\left[j\omega_k + \frac{\pi}{2}\right]\right)\right\}^2 + \left\{\sum_{j=1}^{p^*} \hat{\phi}_j^* \sin\left(\left[j\omega_k + \frac{\pi}{2}\right]\right)\right\}^2}, \; k = 1, \ldots, S^*. \tag{S.34}$$

Based on the estimators $\hat{\lambda}_{0,h}^2$, $\hat{\lambda}_{S/2,h}^2$, $\hat{\lambda}_{k,h}^2$ and $\hat{\lambda}_{k,h}^{*2}$, $h = WA$, AR, $k = 1, \ldots, S^*$, defined in (3.3), (S.33), (3.4), (3.5) and (S.34), seasonal analogues of the non-seasonal PP unit root statistics can be derived from the functional forms of the limit distributions of the un-augmented

HEGY statistics given in Theorem S.1, as follows:

$$Z_k := \quad T\hat{\pi}_k - \frac{\left(\hat{\lambda}^2_{k,h} - \hat{\gamma}_0\right)}{2}\left[\frac{1}{T^2}\sum_{Sn+s=1}^{T}\left(y^{\xi}_{k,Sn+s-1}\right)^2\right]^{-1}, \quad k = 0, ..., \lfloor S/2 \rfloor \quad \text{(S.35)}$$

$$Z^*_k := \quad T\hat{\pi}^*_k - \frac{\left(\hat{\lambda}^{*2}_{k,h} - \hat{\gamma}_0\right)}{2}\left[\frac{1}{T^2}\sum_{Sn+s=1}^{T}\left(y^{*\xi}_{k,Sn+s-1}\right)^2\right]^{-1}, \quad k = 1, \ldots, S^* \quad \text{(S.36)}$$

and

$$Z_{t_k} := \quad \frac{\hat{\gamma}_0^{1/2}}{\hat{\lambda}_{k,h}}t_k - \frac{\left(\hat{\lambda}^2_{k,h} - \hat{\gamma}_0\right)}{2}\left[\frac{\hat{\lambda}^2_{k,h}}{T^2}\sum_{Sn+s=1}^{T}\left(y^{\xi}_{k,Sn+s-1}\right)^2\right]^{-1/2}, \quad k = 0, ..., \lfloor S/2 \rfloor \text{(S.37)}$$

$$Z^*_{t_k} := \quad \frac{\hat{\gamma}_0^{1/2}}{\hat{\lambda}_{k,h}}t^*_k - \frac{\left(\hat{\lambda}^{*2}_{k,h} - \hat{\gamma}_0\right)}{2}\left[\frac{\hat{\lambda}^2_{k,h}}{T^2}\sum_{Sn+s=1}^{T}\left(y^{*\xi}_{k,Sn+s-1}\right)^2\right]^{-1/2}, \quad k = 1, \ldots, S^* \quad \text{(S.38)}$$

where $\hat{\gamma}_0$ is the OLS residual variance estimate from estimating (2.4) with p^* set to zero.

Remark S.7. Notice that for $S = 1$, $Z_{\ }$ in (S.35) and Z_{t_0} in (S.37) reduce to the non-seasonal unit root tests proposed in PP and defined in section 3.1. □

Remark S.8. PP-type analogues of the F-type statistics F_k, $k = 1, ..., S^*$, $F_{1,...,\lfloor S/2 \rfloor}$ and $F_{0,...,\lfloor S/2 \rfloor}$ discussed in section S.3 can also be constructed using the corrected normalised coefficient estimate statistics in (S.35) and (S.36). With an obvious notation we will denote these statistics as $F_{PP,k}$, $k = 1, \ldots, S^*$, $F_{PP,1...\lfloor S/2 \rfloor}$, and $F_{PP,0...\lfloor S/2 \rfloor}$. These statistics can be defined generically as follows:

$$F_{PP} := \frac{1}{\upsilon}(R\mathbf{Z})'\left[R\Lambda\mathbf{Y}'\mathbf{Y}R'\right](R\mathbf{Z}) \quad \text{(S.39)}$$

where υ denotes the number of restrictions being tested; $Z := [Z_0, Z_1, Z^*_1, Z_2, Z^*_2, \ldots, Z_{S^*}, Z^*_{S^*}, Z_{S/2}]'$ is $S \times 1$; $Y := [\mathbf{y}_0|\mathbf{y}_1|\mathbf{y}^*_1|\mathbf{y}_2|\mathbf{y}^*_2| \ \ldots \ |\mathbf{y}_{S^*}|\mathbf{y}^*_{S^*}|\mathbf{y}_{S/2}]$ is a $T \times S$ matrix where $\mathbf{y}_i$, $i = 0, S/2$, are $T \times 1$ vectors with generic element $y^{\xi}_{i,Sn+s-1}$, and $\mathbf{y}_i$ and $\mathbf{y}^*_i$, $i = 1, ..., S^*$ are $T \times 1$ vectors with generic elements $y^{\xi}_{i,Sn+s-1}$ and $y^{*\xi}_{i,Sn+s-1}$, respectively; Λ is an $S \times S$ diagonal matrix such that, $\Lambda := T^{-2}diag\left\{1/\hat{\lambda}^2_{0,h}, 1/\hat{\lambda}^2_{1,h}, 1/\hat{\lambda}^2_{1,h}, 1/\hat{\lambda}^2_{2,h}, 1/\hat{\lambda}^2_{2,h} \ \ldots, 1/\hat{\lambda}^2_{S^*,h}, 1/\hat{\lambda}^2_{S^*,h}, 1/\hat{\lambda}^2_{S/2,h}\right\}$, and finally R is the relevant $\upsilon \times S$ selection matrix; for example, setting

$$R = \begin{bmatrix} 0 & 1 & 0 & 0 & \ldots & 0 \\ 0 & 0 & 1 & 0 & \ldots & 0 \end{bmatrix},$$

yields the $F_{PP,1}$ statistic, whilst setting $R = I_S$, where I_q denotes the $q \times q$ identity matrix for any positive integer q, results in $F_{PP,0...\lfloor S/2 \rfloor}$. □

S.6 Asymptotic Results for the Seasonal PP Tests

In Theorem S.2 we now present the large sample distributions of the seasonal PP-type unit root test statistics proposed in section S.5. In particular, we show that these have pivotal limiting distributions whose form coincides with those which obtain in the case where the shocks are serially uncorrelated.

Theorem S.2. *Let the conditions of Theorem 4.1 hold. Then, as $T \to \infty$, the PP-type coefficient statistics introduced in section S.2 and Remark S.4 satisfy,*

$$Z_k \Rightarrow \frac{(1+\mathcal{D}_k)\left[\int_0^1 J^{\zeta}_{k,c_k}(r)dJ^{\zeta}_{k,c_k}(r) + \mathcal{D}_k \int_0^1 J^{\zeta*}_{k,c_k}(r)dJ^{\zeta*}_{k,c_k}(r)\right]}{\int_0^1 \left[J^{\zeta}_{k,c_k}(r)\right]^2 dr + \mathcal{D}_k \int_0^1 \left[J^{\zeta*}_{k,c_k}(r)\right]^2 dr}, \; k = 0, \ldots, \lfloor S/2 \rfloor \quad \text{(S.40)}$$

$$Z^*_k \Rightarrow \frac{2\left[\int_0^1 J^{\zeta*}_{k,c_k}(r)dJ^{\zeta}_{k,c_k}(r) - \int_0^1 J^{\zeta}_{k,c_k}(r)dJ^{\zeta*}_{k,c_k}(r)\right]}{\int_0^1 \left[J^{\zeta}_{k,c_k}(r)\right]^2 dr + \int_0^1 \left[J^{\zeta*}_{k,c_k}(r)\right]^2 dr}, \quad k = 1, \ldots, S^* \quad \text{(S.41)}$$

while the corresponding t- and F−type statistics satisfy

$$Z_{t_k} \Rightarrow \frac{\int_0^1 J^{\zeta}_{k,c_k}(r)dJ^{\zeta}_{k,c_k}(r) + \mathcal{D}_k \int_0^1 J^{\zeta*}_{k,c_k}(r)dJ^{\zeta*}_{k,c_k}(r)}{\left\{\int_0^1 \left[J^{\zeta}_{k,c_k}(r)\right]^2 dr + \mathcal{D}_k \int_0^1 \left[J^{\zeta*}_{k,c_k}(r)\right]^2 dr\right\}^{1/2}} =: \mathcal{T}^{\zeta}_k, \quad k = 0, ..., \lfloor S/2 \rfloor \quad \text{(S.42)}$$

$$Z^*_{t_k} \Rightarrow \frac{\int_0^1 J^{\zeta*}_{k,c_k}(r)dJ^{\zeta}_{k,c_k}(r) - \int_0^1 J^{\zeta}_{k,c_k}(r)dJ^{\zeta*}_{k,c_k}(r)}{\left\{\int_0^1 \left[J^{\zeta}_{k,c_k}(r)\right]^2 dr + \int_0^1 \left[J^{\zeta*}_{k,c_k}(r)\right]^2 dr\right\}^{1/2}} =: \mathcal{T}^{*\zeta}_k, \quad k = 1, \ldots, S^* \quad \text{(S.43)}$$

$$F_{PP,k} \Rightarrow \frac{1}{2}\left[\left(\mathcal{T}^{\zeta}_k\right)^2 + \left(\mathcal{T}^{*\zeta}_k\right)^2\right], \quad k = 1, \ldots, S^* \quad \text{(S.44)}$$

$$F_{PP,j...\lfloor S/2 \rfloor} \Rightarrow \frac{1}{S-j}\left[\sum_{i=j}^{\lfloor S/2 \rfloor}\left(\mathcal{T}^{\zeta}_i\right)^2 + \sum_{k=1}^{S^*}\left(\mathcal{T}^{*\zeta}_k\right)^2\right], \; j = 0, 1 \quad \text{(S.45)}$$

where $\mathcal{D}_k = 0$, for $k = 0, S/2$ and $\mathcal{D}_k = 1$, for $k = 1, ..., S^*$, and the limiting processes, $J^{\zeta}_{0,c_0}(r)$, $J^{\zeta}_{S/2,c_{S/2}}(r)$, $J^{\zeta}_{k,c_k}(r)$ and $J^{\zeta*}_{k,c_k}(r)$, $k = 1, \ldots, S^*$, are as defined in Theorem 4.1.

Remark S.9: The limiting null distributions of the PP-type statistics from section S.5 are obtained on setting $c_k = 0$ (so that, correspondingly, $H_{0,k}$ holds) in the representations given in Theorem S.2. These limiting null distributions coincide with those reported in Smith *et al.* (2009) and Rodrigues and Taylor (2007), for OLS and local GLS de-trending respectively, for the corresponding HEGY statistics from (2.4) in the case where u_{Sn+s} is serially uncorrelated. Notice also that, contrary to what is shown in, *inter alia*, Burridge and Taylor (2001) and del Barrio Castro, Osborn and Taylor (2012), for the corresponding t_k and t^*_k augmented HEGY statistics from (2.4), when u_{Sn+s} is serially correlated the limiting null distributions of the harmonic frequency PP-type test statistics Z_k, Z_{t_k}, Z^*_k and $Z^*_{t_k}$, $k = 1, ..., S^*$, are free from nuisance parameters. Indeed, the asymptotic null distributions of Z^*_k and $Z^*_{t_k}$ coincide with those reported for the augmented HEGY t_k and t^*_k statistics, $k = 1, ..., S^*$, in Burridge and Taylor (2001) and del Barrio Castro, Osborn and Taylor (2012) for the case where $a_k = 0$ and $b_k = 1$; that is, in the absence of serial correlation in u_{Sn+s}. The foregoing asymptotic equivalence results between the HEGY and corresponding PP-type statistics also hold under the local alternative, $H_{1,\mathbf{c}}$. □

Remark S.10: Selected critical values for tests based on the statistics in (S.40)-(S.43) and (S.44)-(S.45) (for the quarterly, $S = 4$, and monthly, $S = 12$, cases) are provided for the case of OLS de-trended tests in HEGY, Ghysels *et al.* (1994) and Smith and Taylor (1998), and for GLS de-trended tests in Rodrigues and Taylor (2007). Notice that the limiting null distribution in (S.40) for both $k = 0$ and $k = \lfloor S/2 \rfloor$ coincides with the limiting null distribution of the standard normalised bias statistic of Dickey and Fuller (1979), with relevant critical values provided in Fuller (1996). Furthermore, the limiting null distribution in (S.40), for $k = 1, ..., S^*$, coincides with the limiting null distribution of the Dickey *et al.* (1984) unit root test statistic, from where relevant critical values can be obtained. □

S.7 Proofs of Theorems S.1 and S.2

First re-write (2.4) with p^* set to zero in vector form, *viz*, $\mathbf{y} = \mathbf{Y}\beta_0 + \mathbf{u}$, where $\mathbf{y}$ is a $T \times 1$ vector with generic element $\Delta_S y^{\xi}_{Sn+s}$; $\mathbf{Y} := [\mathbf{y}_0|\mathbf{y}_1|\mathbf{y}_1^*|\mathbf{y}_2|\mathbf{y}_2^*| \ \ldots |\mathbf{y}_{S^*}|\mathbf{y}_{S^*}^*|\mathbf{y}_{S/2}]$ is a $T \times S$ matrix where $\mathbf{y}_i$, $i = 0$, ..., $\lfloor S/2 \rfloor$ are $T \times 1$ vectors with generic elements $y^{\xi}_{i,Sn+s-1}$, and $\mathbf{y}_i^*$, $i = 1, ..., S^*$ are $T \times 1$ vectors with generic elements $y^{*\xi}_{i,Sn+s-1}$, respectively, and $\beta_0 := [\pi_0, \pi_1\pi_1^*, \pi_2, \pi_2^*, \ldots, \pi_{S^*}, \pi_{S^*}^*, \pi_{S/2,}]'$. The OLS estimator from the un-augmented form of (2.4), may then be defined via,

$$T\hat{\beta}_0 := \left[T^{-2}\mathbf{Y}'\mathbf{Y}\right]^{-1}\left[T^{-1}\mathbf{Y}'\mathbf{y}\right]. \tag{S.46}$$

Because $T^{-2}\mathbf{Y}'\mathbf{Y}$ weakly converges to an $S \times S$ diagonal matrix, this as a consequence of the asymptotic orthogonality of the HEGY auxiliary variables discussed previously, we may therefore separately derive the large sample behavior of the OLS estimators of π_j, $j = 0, ..., \lfloor S/2 \rfloor$, and π_i^*, $i = 1, ..., S^*$. To that end, the so-called *normalised bias* statistics then satisfy the following,

$$T\widehat{\pi}_j = \frac{T^{-1}\mathbf{y}_j'\mathbf{y}}{T^{-2}\mathbf{y}_j'\mathbf{y}_j} + o_p(1) = \frac{T^{-1}\sum_{n=1}^{N}\sum_{s=1-S}^{0} y^{\xi}_{j,Sn+s-1}\Delta_S y^{\xi}_{Sn+s}}{T^{-2}\sum_{n=1}^{N}\sum_{s=1-S}^{0}\left(y^{\xi}_{j,Sn+s-1}\right)^2} + o_p(1), \quad j = 0, ..., \lfloor S/2 \rfloor \tag{S.47}$$

and

$$T\widehat{\pi}_i^* = \frac{T^{-1}\mathbf{y}_i^{*\prime}\mathbf{y}}{T^{-2}\mathbf{y}_i^{*\prime}\mathbf{y}_i^*} + o_p(1) = \frac{T^{-1}\sum_{n=1}^{N}\sum_{s=1-S}^{0} y^{*\xi}_{i,Sn+s-1}\Delta_S y^{\xi}_{Sn+s}}{T^{-2}\sum_{n=1}^{N}\sum_{s=1-S}^{0}\left(y^{*\xi}_{i,Sn+s-1}\right)^2} + o_p(1), \quad i = 1, ..., S^*. \tag{S.48}$$

Consider first the numerators of (S.47) and (S.48). For (S.47) observe first that,

$$T^{-1}\sum_{n=1}^{N}\sum_{s=1-S}^{0} y^{\xi}_{j,Sn+s-1}\Delta_S y^{\xi}_{Sn+s} = T^{-1}\sum_{n=1}^{N} Y_{n-1}^{\xi\prime} C_j \Delta_S Y_n^{\xi} + \mathbf{A}_j + o_p(1), \quad j = 0, S/2 \tag{S.49}$$

where $\mathbf{A}_j := S^{-1}\sum_{i=1}^{S-1}(S-i)\cos[i\omega_j]\, N^{-1}\sum_{n=1}^{N}\left(u^{\xi}_{S-i,n}u^{\xi}_{Sn}\right)$, and where $\Delta_S Y_n^{\xi} := [\Delta_S y^{\xi}_{Sn-(S-1)}, \Delta_S\ y^{\xi}_{Sn-(S-2)}, \ ..., \ \Delta_S\ y^{\xi}_{Sn}]'$. Notice then that $\mathbf{A}_j \to \Psi_j := S^{-1}\sum_{i=1}^{S-1}(S-i)\cos[i\omega_j]\,\gamma_i$ for

$\omega_j = \frac{2\pi j}{S}$, $j = 0, S/2$. Similarly, for $j = 1, \ldots, S^*$, we have that

$$T^{-1}\sum_{n=1}^{N}\sum_{s=1-S}^{0} y^{\xi}_{j,Sn+s-1}\Delta_S y^{\xi}_{Sn+s} = T^{-1}\sum_{n=1}^{N} Y^{\xi\prime}_{n-1} C_j \Delta_S Y^{\xi}_n + \mathbf{A}_j + o_p(1) \quad \text{(S.50)}$$

$$T^{-1}\sum_{n=1}^{N}\sum_{s=1-S}^{0} y^{*\xi}_{j,Sn+s-1}\Delta_S y^{\xi}_{Sn+s} = T^{-1}\sum_{n=1}^{N} Y^{\xi\prime}_{n-1} \overline{C}_j \Delta_S Y^{\xi}_n + \overline{\mathbf{A}}_j + o_p(1) \quad \text{(S.51)}$$

where $\mathbf{A}_j := S^{-1}\sum_{i=1}^{S-1}(S-i)\cos[i\omega_j]\, N^{-1}\sum_{n=1}^{N}\left(u^{\xi}_{S-i,n}u^{\xi}_{Sn}\right)$ and $\overline{\mathbf{A}}_j := -S^{-1}\sum_{i=1}^{S-1}(S-i)\sin[i\omega_j]$ $N^{-1}\sum_{n=1}^{N}\left(u^{\xi}_{S-i,n}u^{\xi}_{Sn}\right)$. We observe that $\mathbf{A}_j \to \Psi^1_j := S^{-1}\sum_{i=1}^{S-1}(S-i)\cos[i\omega_j]\,\gamma_i$ and $\overline{\mathbf{A}}_j \to \Psi^2_j := -S^{-1}\sum_{i=1}^{S-1}(S-i)\sin[i\omega_j]\,\gamma_i$ for $\omega_j = \frac{2\pi j}{S}$, $\quad j = 1, \ldots, S^*$.

Again using (S.10), applications of the CMT, the identities $C_kC_kC_k \equiv S^2C_k$ for $k = 0, S/2$, and $C'_jC_jC_j \equiv \left(\frac{S}{2}\right)^2 C_j$, $C'_jC_j\overline{C}_j \equiv \left(\frac{S}{2}\right)^2 \overline{C}_j$,$\overline{C}'_j\, C_jC_j \equiv -\left(\frac{S}{2}\right)^2 \overline{C}_j$, $\overline{C}'_j\, C_j\overline{C}_j \equiv \left(\frac{S}{2}\right)^2 C_j$, $C'_j\overline{C}_jC_j \equiv \left(\frac{S}{2}\right)^2 \overline{C}_j$, $C'_j\overline{C}_j\overline{C}_j \equiv -\left(\frac{S}{2}\right)^2 C_j$, $\overline{C}'_jC_jC_j \equiv \left(\frac{S}{2}\right)^2 C_j$ and $\overline{C}'_j\overline{C}_j\overline{C}_j \equiv \left(\frac{S}{2}\right)^2 \overline{C}_j$ for $j = 1, ..., S^*$, the orthogonality between the circulant matrices and Theorem 2.6 in Phillips (1988), the following results are obtained:

i) For the zero and Nyquist frequencies ($k = 0, S/2$),

$$\begin{aligned} T^{-1}\sum_{n=1}^{N} Y^{\xi\prime}_{n-1} C_k \Delta_S Y^{\xi}_n &\Rightarrow \frac{\sigma^2_\varepsilon}{S}\frac{\psi(\cos[\omega_k])}{S^2}\int_0^1 \mathbf{J}^{\xi}_{c_k}(r)'\, C'_kC_kC_k\mathbf{\Psi}(1)\, d\mathbf{J}^{\xi}_{c_k}(r) + \frac{1}{S}\sum_{j=2}^{\infty} E\left(U^{\xi\prime}_1 C_k U^{\xi}_j\right) \\ &= \frac{\sigma^2_\varepsilon}{S}\psi(\cos[\omega_k])^2\int_0^1 \mathbf{J}^{\xi}_{c_k}(r)'\, C_k d\mathbf{J}^{\xi}_{c_k}(r) + \frac{1}{S}\sum_{j=2}^{\infty} E\left(U^{\xi\prime}_1 C_k U^{\xi}_j\right) \\ &= \sigma^2_\varepsilon\psi(\cos[\omega_k])^2\int_0^1 \mathbf{J}^{\xi*}_{c_k}(r)'\, C_k d\mathbf{J}^{\xi*}_{c_k}(r) + \frac{1}{S}\sum_{j=2}^{\infty} E\left(U^{\xi\prime}_1 C_k U^{\xi}_j\right) \quad \text{(S.52)} \end{aligned}$$

where $\omega_0 = 0$ and $\omega_{S/2} = \pi$.

ii) For the harmonic frequencies ($j = 1, ..., S^*$),

$$\begin{aligned} T^{-1}\sum_{n=1}^{N} Y^{\xi\prime}_{n-1} C_j \Delta_S Y^{\xi}_n &\Rightarrow \frac{\sigma^2_\varepsilon}{S}\left(\frac{2}{S}\right)^2 b_j\int_0^1 \mathbf{J}^{\xi}_{c_j}(r)'\, C'_jC_j\left(b_jC_j + a_j\overline{C}_j\right) d\mathbf{J}^{\xi}_{c_j}(r) \\ &\quad + \frac{\sigma^2_\varepsilon}{S}\left(\frac{2}{S}\right)^2 a_j\int_0^1 \mathbf{J}^{\xi}_{c_j}(r)'\, \overline{C}'_jC_j\left(b_jC_j + a_j\overline{C}_j\right) d\mathbf{J}^{\xi}_{c_j}(r) + \frac{1}{S}\sum_{k=2}^{\infty} E\left(U^{\xi\prime}_1 C_j U^{\xi}_k\right) \\ &= \frac{\sigma^2_\varepsilon}{S}b_j^2\int_0^1 \mathbf{J}^{\xi}_{c_j}(r)'\, C_j d\mathbf{J}^{\xi}_{c_j}(r) + \frac{\sigma^2_\varepsilon}{S}a_jb_j\int_0^1 \mathbf{J}^{\xi}_{c_j}(r)'\, \overline{C}_j d\mathbf{J}^{\xi}_{c_j}(r) \\ &\quad + \frac{\sigma^2_\varepsilon}{S}a_j^2\int_0^1 \mathbf{J}^{\xi}_{c_j}(r)'\, C_j d\mathbf{J}^{\xi}_{c_j}(r) - \frac{\sigma^2_\varepsilon}{S}a_jb_j\int_0^1 \mathbf{J}^{\xi}_{c_j}(r)'\, \overline{C}_j d\mathbf{J}^{\xi}_{c_j}(r) \\ &\quad + \frac{1}{S}\sum_{k=2}^{\infty} E\left(U^{\xi\prime}_1 C_j U^{\xi}_k\right) \\ &= \frac{\sigma^2_\varepsilon\left(a_j^2 + b_j^2\right)}{2}\int_0^1 \mathbf{J}^{\xi\dagger}_{c_j}(r)'\, C_j d\mathbf{J}^{\xi\dagger}_{c_j}(r) + \frac{1}{S}\sum_{k=2}^{\infty} E\left(U^{\xi\prime}_1 C_j U^{\xi}_k\right), \quad \text{(S.53)} \end{aligned}$$

$$
\begin{aligned}
T^{-1}\sum_{n=1}^{N} Y_{n-1}^{\xi\prime}\overline{C}_j\Delta_S Y_n^{\xi} \;\Rightarrow\; & \frac{\sigma_\varepsilon^2}{S}\left(\frac{2}{S}\right)^2 b_j\int_0^1 \mathbf{J}_{c_j}^{\xi}(r)'\,C_j'\overline{C}_j\left(b_jC_j+a_j\overline{C}_j\right)d\mathbf{J}_{c_j}^{\xi}(r) \\
& +\frac{\sigma_\varepsilon^2}{S}\left(\frac{2}{S}\right)^2 a_j\int_0^1 \mathbf{J}_{c_j}^{\xi}(r)'\,\overline{C}_j'\overline{C}_j\left(b_jC_j+a_j\overline{C}_j\right)d\mathbf{J}_{c_j}^{\xi}(r)+\frac{1}{S}\sum_{k=2}^{\infty}E\left(U_1^{\xi\prime}\overline{C}_jU_k^{\xi}\right) \\
= \; & \frac{\sigma_\varepsilon^2}{S}b_j^2\int_0^1 \mathbf{J}_{c_j}^{\xi}(r)'\,\overline{C}_j d\mathbf{J}_{c_j}^{\xi}(r)-\frac{\sigma_\varepsilon^2}{S}b_ja_j\int_0^1 \mathbf{J}_{c_j}^{\xi}(r)'\,C_j d\mathbf{J}_{c_j}^{\xi}(r) \\
& +\frac{\sigma_\varepsilon^2}{S}a_jb_j\int_0^1 \mathbf{J}_{c_j}^{\xi}(r)'\,C_j d\mathbf{J}_{c_j}^{\xi}(r)+\frac{\sigma_\varepsilon^2}{S}a_j^2\int_0^1 \mathbf{J}_{c_j}^{\xi}(r)'\,\overline{C}_j d\mathbf{J}_{c_j}^{\xi}(r) \\
& +\frac{1}{S}\sum_{k=2}^{\infty}E\left(U_1^{\xi\prime}C_jU_k^{\xi}\right) \\
= \; & \frac{\sigma_\varepsilon^2\left(a_j^2+b_j^2\right)}{2}\int_0^1 \mathbf{J}_{c_j}^{\xi\dagger}(r)'\,\overline{C}_j d\mathbf{J}_{c_j}^{\xi\dagger}(r)+\frac{1}{S}\sum_{k=2}^{\infty}E\left(U_1^{\xi\prime}\overline{C}_jU_k^{\xi}\right) \qquad \text{(S.54)}
\end{aligned}
$$

where $\mathbf{J}_{c_j}^{\xi\dagger}(r):=\frac{1}{\sqrt{S/2}}\mathbf{J}_{c_j}^{\xi}(r)$.

Moreover, for $k=0$ and $k=S/2$,

$$
\frac{1}{S}\sum_{j=2}^{\infty}E\left(U_1^{\xi\prime}C_kU_j^{\xi}\right)+\Psi_k=\sum_{i=1}^{\infty}\cos\left[i\omega_k\right]\gamma_i=\frac{1}{2}(\lambda_k^2-\gamma_k) \qquad \text{(S.55)}
$$

and for $j=1,2,\ldots,S^*$,

$$
\begin{aligned}
\frac{1}{S}\sum_{k=2}^{\infty}E\left(U_1^{\xi\prime}C_jU_k^{\xi}\right)+\Psi_j^1 &= \sum_{i=1}^{\infty}\cos\left[(S-i)\,\omega_j\right]\gamma_i=\frac{1}{4}(\lambda_j^2-\gamma_0) \qquad \text{(S.56)} \\
\frac{1}{S}\sum_{k=2}^{\infty}E\left(U_1^{\xi\prime}\overline{C}_jU_k^{\xi}\right)+\Psi_j^2 &= -\sum_{i=1}^{\infty}\sin\left[(S-i)\,\omega_j\right]\gamma_i=\frac{1}{4}(\lambda_j^{*2}-\gamma_0) \qquad \text{(S.57)}
\end{aligned}
$$

with $\omega_j=\frac{2\pi j}{S}$.

In the case of the denominator of (S.47) the required results for $j=0$ and $j=S/2$ are collected in (S.21). Consider next the denominators of (S.47) and (S.48) over the values $1,...,S^*$ of the index parameters j and i, respectively. Here we have the results that C_i, $i=1,...,S^*$, is symmetric and that $\overline{C}_i'=-\overline{C}_i$, and noting also that C_i and $\overline{C}_i$ are orthogonal to C_0 and $C_{S/2}$ and that $C_iC_iC_i\equiv\left(\frac{S}{2}\right)^2C_i$, $C_iC_i\overline{C}_i\equiv\left(\frac{S}{2}\right)^2\overline{C}_i$, $\overline{C}_i'C_iC_i\equiv-\left(\frac{S}{2}\right)^2\overline{C}_i$ and $\overline{C}_i'C_i\overline{C}_i\equiv\left(\frac{S}{2}\right)^2C_i$. Using these results we have that,

$$
T^{-2}\sum_{n=1}^{N}\sum_{s=1-S}^{0}\left(y_{i,Sn+s-1}^{\xi}\right)^2=T^{-2}\sum_{n=1}^{N}\left(\frac{S}{2}\right)\left(Y_{n-1}^{\xi\prime}C_i\,Y_{n-1}^{\xi}\right)+o_p(1)
$$

$$
T^{-2}\sum_{n=1}^{N}\sum_{s=1-S}^{0}\left(y_{i,Sn+s-1}^{*\xi}\right)^2=T^{-2}\sum_{n=1}^{N}\left(\frac{S}{2}\right)\left(Y_{n-1}^{\xi\prime}C_i\,Y_{n-1}^{\xi}\right)+o_p(1)
$$

$$T^{-2}\sum_{n=1}^{N}\left(\frac{S}{2}\right)\left(Y_{n-1}^{\xi\prime}C_i\,Y_{n-1}^{\xi}\right)\Rightarrow \quad \frac{\sigma_\varepsilon^2}{S^2}\left(\frac{S}{2}\right)b_i^2\left(\frac{2}{S}\right)^2\int_0^1 \mathbf{J}_{c_i}^{\xi}(r)'\,C_iC_iC_i\mathbf{J}_{c_i}^{\xi}(r)\,dr +$$
$$\frac{\sigma_\varepsilon^2}{S^2}\left(\frac{S}{2}\right)b_ia_i\left(\frac{2}{S}\right)^2\int_0^1 \mathbf{J}_{c_i}^{\xi}(r)'\,C_iC_i\overline{C}_i\mathbf{J}_{c_i}^{\xi}(r)\,dr +$$
$$\frac{\sigma_\varepsilon^2}{S^2}\left(\frac{S}{2}\right)b_ia_i\left(\frac{2}{S}\right)^2\int_0^1 \mathbf{J}_{c_i}^{\xi}(r)'\,\overline{C}_i'C_iC_i\mathbf{J}_{c_i}^{\xi}(r)\,dr +$$
$$\frac{\sigma_\varepsilon^2}{S^2}\left(\frac{S}{2}\right)a_i^2\left(\frac{2}{S}\right)^2\int_0^1 \mathbf{J}_{c_i}^{\xi}(r)'\,\overline{C}_i'C_i\overline{C}_i\mathbf{J}_{c_i}^{\xi}(r)\,dr$$
$$= \frac{\sigma_\varepsilon^2\left(a_i^2+b_i^2\right)}{4}\int_0^1 \mathbf{J}_{c_i}^{\xi\dagger}(r)'\,C_i\mathbf{J}_{c_i}^{\xi\dagger}(r)\,dr \tag{S.58}$$

where $i=1,\ldots,S^*$ and $\mathbf{J}_{c_i}^{\xi\dagger}(r):=\frac{1}{\sqrt{S/2}}\mathbf{J}_{c_i}^{\xi}(r)$.

Combining the results in (S.49)-(S.57) with (S.21) and (S.58) we establish that for $k=0$ ($\omega_0=0$) and $k=S/2$ ($\omega_{S/2}=\pi$),

$$T\widehat{\pi}_k\Rightarrow\frac{\int_0^1\mathbf{J}_{c_k}^{\xi*}(r)'\,C_k d\mathbf{J}_{c_k}^{\xi*}(r)+\left(\sum_{i=1}^{\infty}\cos\left[i\omega_k\right]\gamma_i\right)/\sigma_\varepsilon^2\left[\psi\left(\cos[\omega_k]\right)\right]^2}{\int_0^1\mathbf{J}_{c_k}^{\xi*}(r)'\,C_k\mathbf{J}_{c_k}^{\xi*}(r)\,dr} \tag{S.59}$$

and for $j=1,...,S^*$ that,

$$T\widehat{\pi}_j \Rightarrow \frac{\frac{\sigma_\varepsilon^2\left(a_j^2+b_j^2\right)}{2}\int_0^1\mathbf{J}_{c_j}^{\xi\dagger}(r)'\,C_j d\mathbf{J}_{c_j}^{\xi\dagger}(r)+\left(\sum_{i=1}^{\infty}\cos\left[(S-i)\,\omega_j\right]\gamma_i\right)}{\frac{\sigma_\varepsilon^2\left(a_j^2+b_j^2\right)}{4}\int_0^1\mathbf{J}_{c_j}^{\xi\dagger}(r)'\,C_j\mathbf{J}_{c_j}^{\xi\dagger}(r)\,dr} \tag{S.60}$$

$$T\widehat{\pi}_j^* \Rightarrow \frac{\frac{\sigma_\varepsilon^2\left(a_j^2+b_j^2\right)}{2}\int_0^1\mathbf{J}_{c_j}^{\xi\dagger}(r)'\,\overline{C}_j d\mathbf{J}_{c_j}^{\xi\dagger}(r)+\left(\sum_{i=1}^{\infty}\sin\left[(S-i)\,\omega_j\right]\gamma_i\right)}{\frac{\sigma_\varepsilon^2\left(a_j^2+b_j^2\right)}{4}\int_0^1\mathbf{J}_{c_j}^{\xi\dagger}(r)'\,C_j\mathbf{J}_{c_j}^{\xi\dagger}(r)\,dr}. \tag{S.61}$$

Next observe that the corresponding t-statistics from the un-augmented form of (2.4) can be written as

$$t_k = \widehat{\gamma}_0^{-1/2}T\widehat{\pi}_k\left[T^{-2}\sum_{n=1}^{N}\sum_{s=1-S}^{0}\left(y_{k,Sn+s}^{\xi}\right)^2\right]^{1/2}+o_p(1),\quad k=0,...,\lfloor S/2\rfloor \tag{S.62}$$

$$t_i^* = \widehat{\gamma}_0^{-1/2}T\widehat{\pi}_i^*\left[T^{-2}\sum_{n=1}^{N}\sum_{s=1-S}^{0}\left(y_{i,Sn+s}^{*\xi}\right)^2\right]^{1/2}+o_p(1),\quad i=1,\ldots,S^* \tag{S.63}$$

where $\widehat{\gamma}_0$ is the usual OLS variance estimator from the un-augmented form of (2.4); that is, $\widehat{\gamma}_0:=T^{-1}\sum_{n=1}^{N}\sum_{s=1-S}^{0}(\hat{u}_{Sn+s}^{\xi})^2$. Observe from the results in (S.59)-(S.61) that $\widehat{\pi}_j=o_p(1)$ and $\widehat{\pi}_j^*=o_p(1)$, and hence $\widehat{\gamma}_0:=T^{-1}\sum_{n=1}^{N}\sum_{s=1-S}^{0}(\Delta_S y_{Sn+s}^{\xi})^2+o_p(1)$ so that $\widehat{\gamma}_0\xrightarrow{p}\sigma_\varepsilon^2\left(1+\sum_{j=1}^{\infty}\psi_j^2\right)$.

Substituting the result that $\widehat{\gamma}_0\xrightarrow{p}\sigma_\varepsilon^2\left(1+\sum_{j=1}^{\infty}\psi_j^2\right)$, the results in Remark S.1, and the results in (S.59)-(S.61), (S.21) and (S.58) into (S.62)-(S.63) and using applications of the CMT, after some simple manipulations, we finally obtain the stated results in Theorem S.1, where we have defined the independent standard OU processes $J_{i,c_i}^{\zeta}(r):=\mathbf{v}_i'\mathbf{J}_{c_i}^{\xi*}(r)$, $i=0,S/2$, $J_{j,c_j}^{\zeta}(r):=\mathbf{h}_j'\mathbf{J}_{c_j}^{\xi\dagger}(r)$ and $J_{j,c_j}^{\zeta*}(r):=\mathbf{h}_j^{*\prime}\mathbf{J}_{c_j}^{\xi\dagger}(r)$ where $\mathbf{h}_j'$ and $\mathbf{h}_j^{*\prime}$ are the first and second rows of $\mathbf{v}_j'$, respectively, for $j=1,\ldots,S^*$ (see Remarks S.1 and S.3). The proof of Theorem S.2 then follows directly from these results and the consistency properties of the long and short run variance estimators used in the construction of the PP-type statistics. □

S.8 Additional Monte Carlo Results

Figures S.1-S.4 report complementary finite sample local power figures to those given in Figures 3-6 in the main text for the case where the tests are not size-adjusted but rather were run using the relevant asymptotic critical values (obtained from the sources given in Remarks 4.2 and 4.3). The Monte Carlo DGP and set-up of these experiments were otherwise exactly as detailed in Section 5.2.

Additional References

Boswijk, H.P., and P.H. Franses, 1996, Unit roots in periodic autoregressions, Journal of Time Series Analysis 17, 221-245.

Burridge, P. and A.M.R.Taylor, 2001, On the properties of regression-based tests for seasonal unit roots in the presence of higher-order serial correlation, Journal of Business and Economic Statistics 19, 374-379.

del Barrio Castro, T., D. R. Osborn and A.M.R. Taylor, 2012, On augmented HEGY tests For seasonal unit roots, Econometric Theory 28, 1121-1143.

Davis, P.J., 1979, Circulant Matrices. Wiley-Interscience: New York.

Dickey, D.A., D.P. Hasza and W.A. Fuller, 1984, Testing for unit roots in seasonal time series, Journal of the American Statistical Association 79, 355-367.

Dickey, D.A. and W.A. Fuller, 1979, Distribution of the estimators for autoregressive time series with a unit root, Journal of the American Statistical Association 74, 427-431.

Fuller, W.A., 1996, Introduction to Statistical Time Series, Second Edition, Wiley: New York.

Ghysels, E., H.S. Lee and J. Noh, 1994, Testing for unit roots in seasonal time series: some theoretical extensions and a Monte Carlo investigation, Journal of Econometrics 62, 415-442.

Gray, R. M., 2006, Toeplitz and Circulant Matrices, A Review. Foundation and Trends(R) in Communications and Information Theory: Now Publishers Inc.

Osborn, D.R. and P.M.M. Rodrigues, 2002, The asymptotic distributions of seasonal unit root tests: a unifying approach, Econometric Reviews 21, 221-241.

Phillips, P.C.B., 1988, Regression theory for near-integrated time series, Econometrica 56, 1021-43.

Rodrigues, P.M.M. and A.M.R. Taylor, 2004, Asymptotic distributions for regression-based seasonal unit root test statistics in a near-integrated model, Econometric Theory 20, 645-670.

Said, S.E. and D.A. Dickey, 1984, Test for unit roots in autoreressive-moving average models of unknown order, Biometrika 71, 599-609.

Smith, R.J. and A.M.R. Taylor, 1998, Additional critical values and asymptotic representations for seasonal unit root tests, Journal of Econometrics 85, 269-288.

Figure S.1: Finite sample size-unadjusted power functions of zero frequency unit root tests (quarterly case, $S = 4$)

(a) local GLS de-meaned tests - $N = 50$

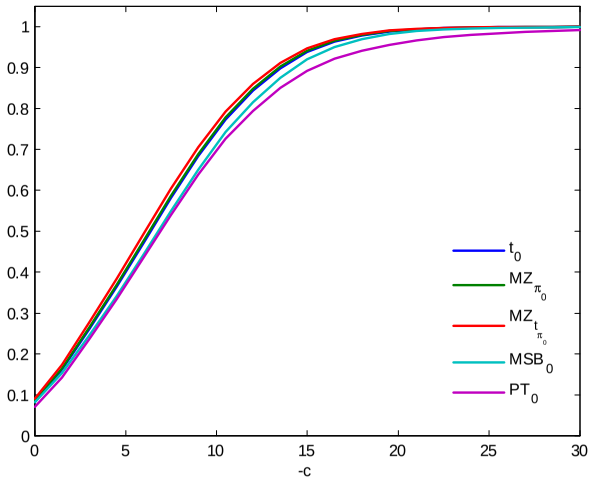

(b) local GLS de-meaned tests - $N = 100$

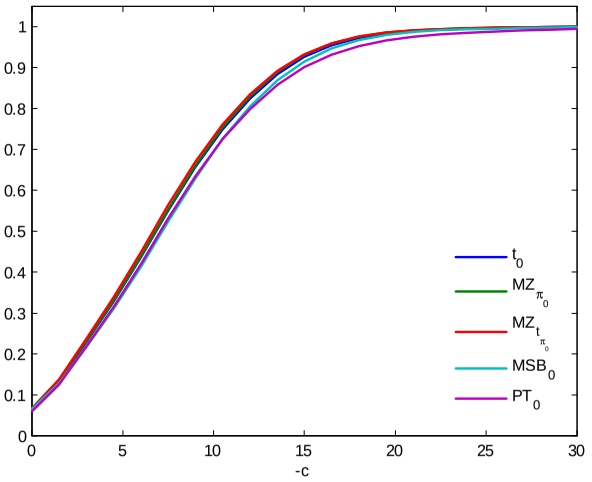

(c) local GLS de-trended tests - $N = 50$

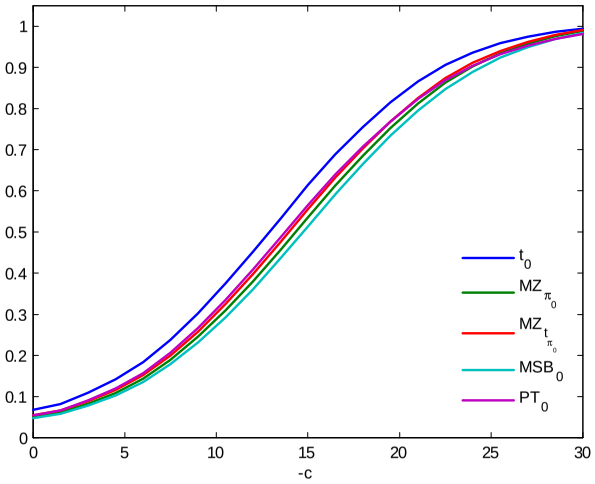

(d) local GLS de-trended tests - $N = 100$

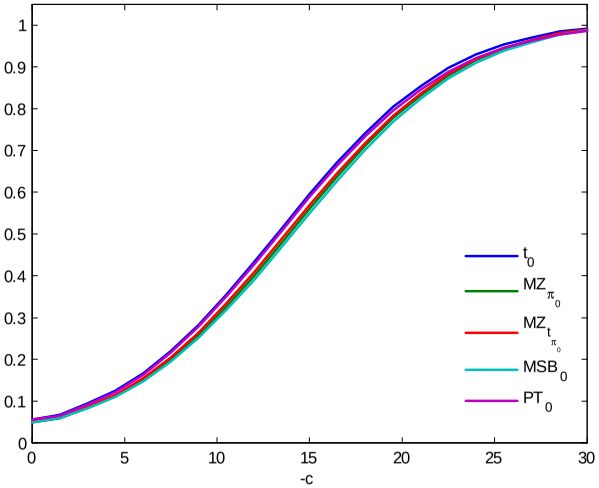

Figure S.2: Finite sample size-unadjusted power functions of harmonic frequency unit root tests (quarterly case, $S = 4$)

(a) local GLS de-meaned tests - $N = 50$

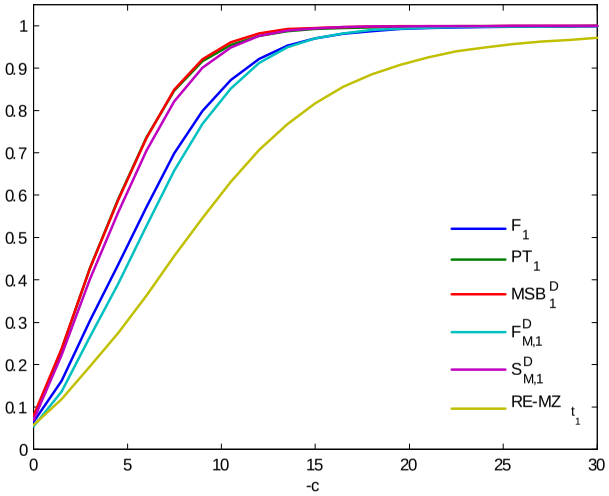

(b) local GLS de-meaned tests - $N = 100$

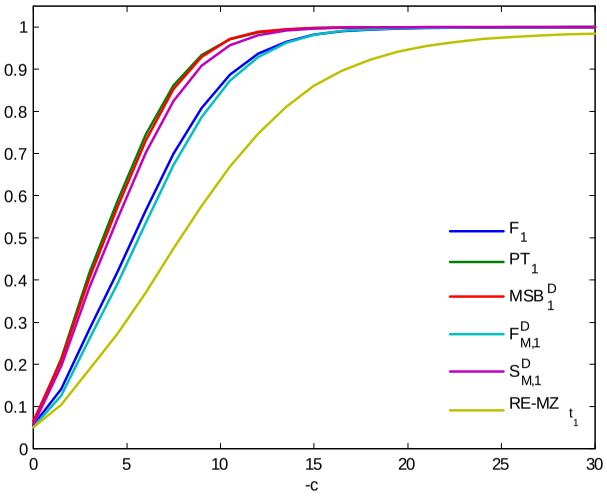

(c) local GLS de-trended tests - $N = 50$

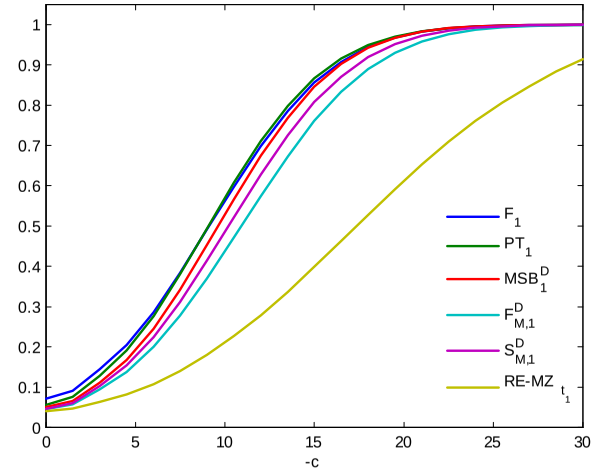

(d) local GLS de-trended tests - $N = 100$

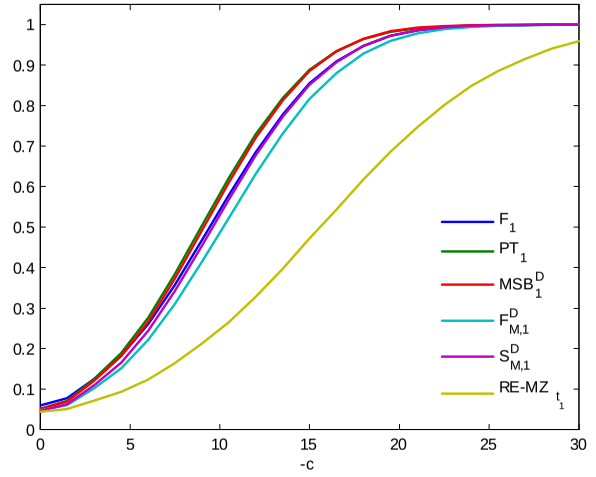

Figure S.3: Finite sample size-unadjusted power functions of joint seasonal frequency tests (quarterly case, $S = 4$)

(a) local GLS de-meaned tests - $N = 50$

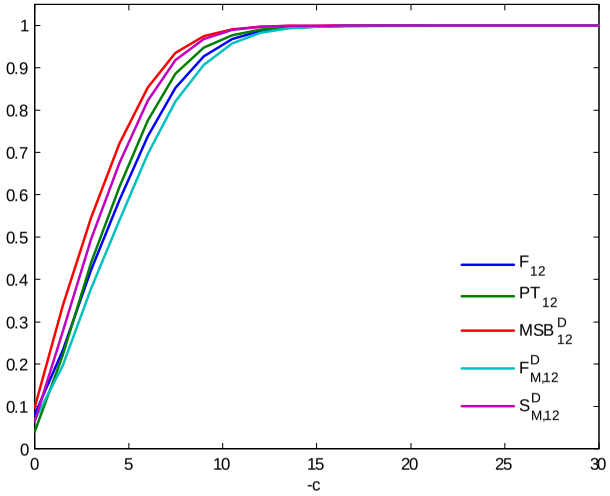

(b) local GLS de-meaned tests - $N = 100$

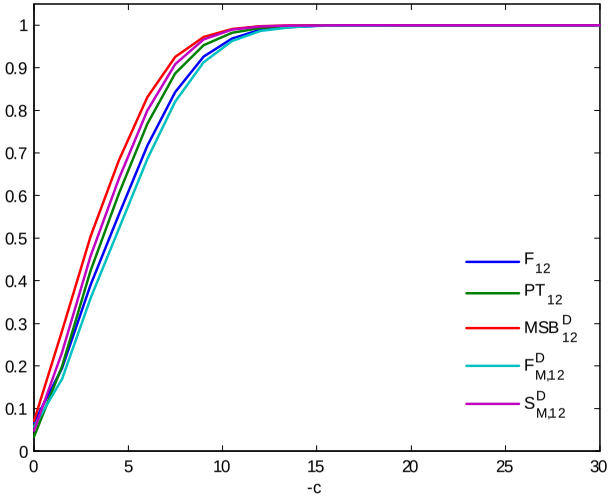

(c) local GLS de-trended tests - $N = 50$

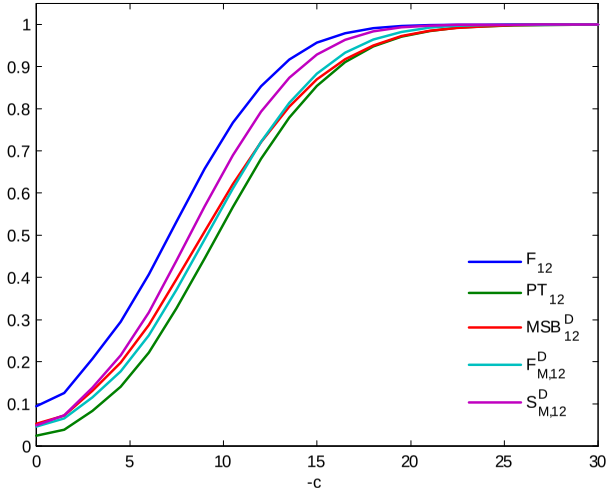

(d) local GLS de-trended tests - $N = 100$

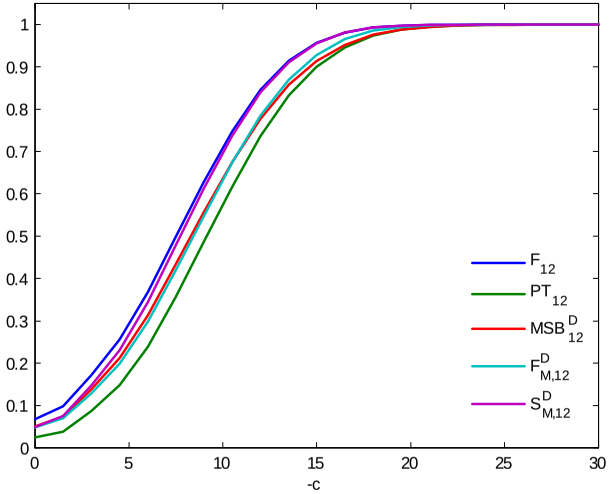

Figure S.4: Finite sample size-unadjusted power functions of joint zero and seasonal frequency tests (quarterly case, $S = 4$)

(a) local GLS de-meaned tests - $N = 50$

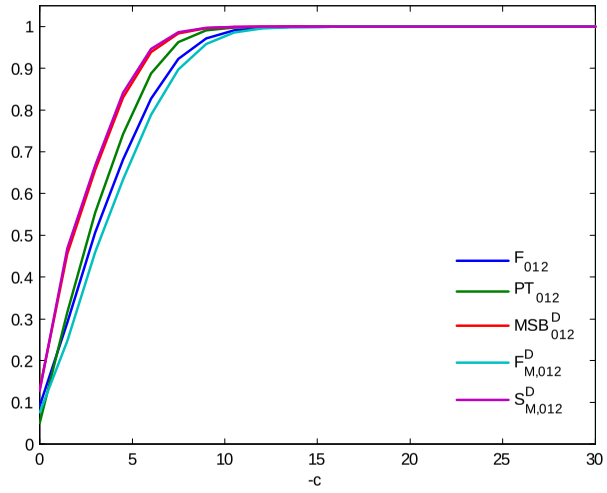

(b) local GLS de-meaned tests - $N = 100$

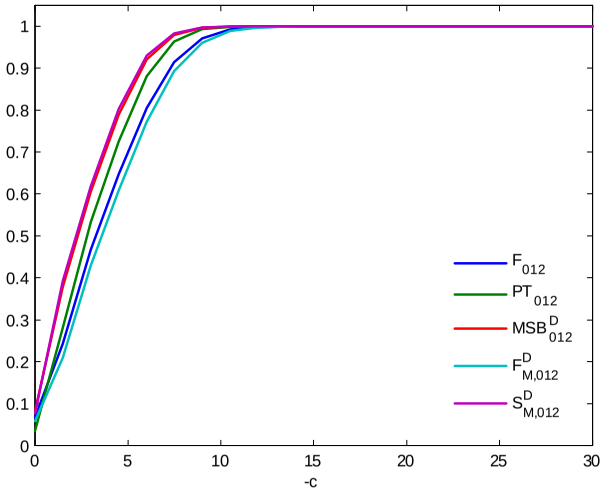

(c) local GLS de-trended tests - $N = 50$

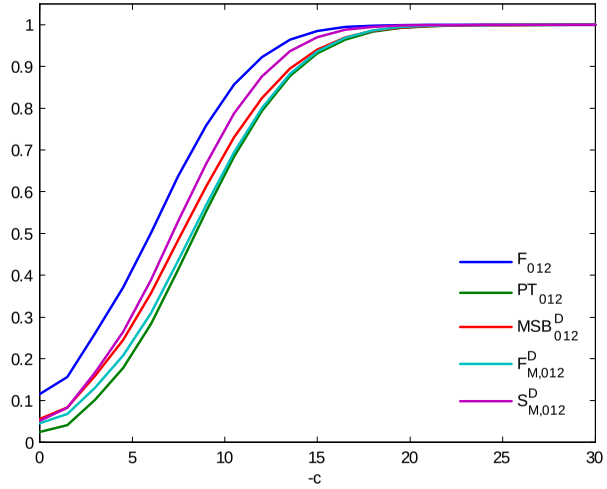

(d) local GLS de-trended tests - $N = 100$